

# COPINE III INTERACTS WITH ERBB2 AND PROMOTES TUMOR CELL MIGRATION

## Inauguraldissertation

zur Erlangung der Würde eines Doktors der Philosophie vorgelegt  
der Philosophisch-Naturwissenschaftlichen Fakultät der Universität Basel

von

**CONSTANZE KATHARINA HEINRICH**  
aus Esslingen am Neckar, Deutschland

Dissertationsleiter: Prof. Dr. Jan Hofsteenge  
Friedrich Miescher Institut für Biomedizinische Forschung

Basel, 2009

Originaldokument gespeichert auf dem Dokumentenserver der Universität Basel  
**edoc.unibas.ch**



Dieses Werk ist unter dem Vertrag „Creative Commons Namensnennung-Keine kommerzielle  
Nutzung-Keine Bearbeitung 2.5 Schweiz“ lizenziert. Die vollständige Lizenz kann unter  
**[creativecommons.org/licenses/by-nc-nd/2.5/ch](http://creativecommons.org/licenses/by-nc-nd/2.5/ch)**  
eingesehen werden.

Genehmigt von der Philosophisch-Naturwissenschaftlichen Fakultät  
auf Antrag von

Prof. Dr. Jan Hofsteenge

Prof. Dr. G. Christofori

Prof. Dr. Nancy E. Hynes

Basel, den 8. Dezember 2009

Prof. Dr. Eberhard Parlow  
Dekan



## Namensnennung-Keine kommerzielle Nutzung-Keine Bearbeitung 2.5 Schweiz

---

### Sie dürfen:



das Werk vervielfältigen, verbreiten und öffentlich zugänglich machen

### Zu den folgenden Bedingungen:



**Namensnennung.** Sie müssen den Namen des Autors/Rechteinhabers in der von ihm festgelegten Weise nennen (wodurch aber nicht der Eindruck entstehen darf, Sie oder die Nutzung des Werkes durch Sie würden entlohnt).



**Keine kommerzielle Nutzung.** Dieses Werk darf nicht für kommerzielle Zwecke verwendet werden.



**Keine Bearbeitung.** Dieses Werk darf nicht bearbeitet oder in anderer Weise verändert werden.

- Im Falle einer Verbreitung müssen Sie anderen die Lizenzbedingungen, unter welche dieses Werk fällt, mitteilen. Am Einfachsten ist es, einen Link auf diese Seite einzubinden.
- Jede der vorgenannten Bedingungen kann aufgehoben werden, sofern Sie die Einwilligung des Rechteinhabers dazu erhalten.
- Diese Lizenz lässt die Urheberpersönlichkeitsrechte unberührt.

#### Die gesetzlichen Schranken des Urheberrechts bleiben hiervon unberührt.

Die Commons Deed ist eine Zusammenfassung des Lizenzvertrags in allgemeinverständlicher Sprache: <http://creativecommons.org/licenses/by-nc-nd/2.5/ch/legalcode.de>

#### Haftungsausschluss:

Die Commons Deed ist kein Lizenzvertrag. Sie ist lediglich ein Referenztext, der den zugrundeliegenden Lizenzvertrag übersichtlich und in allgemeinverständlicher Sprache wiedergibt. Die Deed selbst entfaltet keine juristische Wirkung und erscheint im eigentlichen Lizenzvertrag nicht. Creative Commons ist keine Rechtsanwalts-gesellschaft und leistet keine Rechtsberatung. Die Weitergabe und Verlinkung des Commons Deeds führt zu keinem Mandatsverhältnis.



“I believe there exists, and I feel within me, an instinct for the truth, or knowledge or discovery, of something of the same nature as the instinct of virtue, and that our having such an instinct is reason enough for scientific researches without any practical results ever ensuing from them.”

Charles Darwin



## SUMMARY

Breast cancer is the most prevalent form of cancer in females: one of nine women develops breast cancer during her lifetime and it is predicted that one in 27 women will die as a result of this disease. Moreover, it is anticipated that with almost 30 % of females affected, breast cancer will be the most frequently diagnosed cancer in 2009 ([www.cancer.org](http://www.cancer.org)). Given these facts, much time and resources have been provided to research in the breast cancer area.

The ErbB2 receptor tyrosine kinase is one of the most-studied oncogenes in breast cancer as amplification and overexpression of the *ERBB2* gene is known to occur in up to 25 % of all affected patients and is correlated with a highly aggressive disease and poor patient prognosis. Our study focused on signaling molecules interacting with the C-terminal regulatory region of the ErbB2 receptor. We used T47D breast cancer cells metabolically labeled with SILAC to identify binding partners of the pTyr1248 site of ErbB2. Using a peptide affinity pull-down approach followed by quantitative mass spectrometry, we identified Copine III as a novel interaction partner of ErbB2-pTyr1248.

Copine III belongs to a family of Ca<sup>2+</sup>-dependent phospholipid binding proteins that is conserved from plants to humans. All copines carry two C2 domains followed by an A domain, similar to the von Willebrand A domain of integrins, in their C-terminus. Although Copine III is ubiquitously expressed, to date it has not been assigned a function downstream of ErbB2.

In this study we first analyzed the biochemical properties of Copine III and its interaction with ErbB2. We show that Copine III is a cytoplasmic protein that localizes to the nucleus and the plasma membrane in a Ca<sup>2+</sup>-dependent manner and upon stimulation of the cells with the ErbB ligand heregulin (HRG). We used FRET acceptor photobleaching to show that Copine III and ErbB2 not only co-localize in HRG-stimulated breast cancer cells, but also interact at the plasma membrane. This co-localization is blocked when the cells are treated with the ErbB2 inhibitor AEE788, implying that Copine III only interacts with phosphorylated active ErbB2.

The second goal of my studies was to place Copine III within a signaling pathway downstream of ErbB2. For this, we again used SILAC together with quantitative mass spectrometry and identified the scaffolding protein RACK1 as a binding partner of Copine III. We were able to show that Copine III, RACK1 and the adaptor molecule Shc form a complex with ErbB2 in HRG-stimulated cells. RACK1 has been implicated in focal-adhesion mediated cell migration and here we demonstrate that Copine III localizes to focal adhesions and is required for ErbB2-dependent cell migration. Moreover, knock-down of Copine III affects Src kinase activity and the subsequent phosphorylation of focal adhesion kinase, resulting in the observed defects in cellular migration. Thus Copine III is an important effector molecule in ErbB2-mediated cell migration.

Finally, we analyzed Copine III expression in the broader context of cancer, looking at carcinomas of the breast, prostate and ovary. In a set of 49 breast cancer tumor samples, 10 of the 11 cases with *ERBB2* amplification display elevated levels of Copine III. This connected well with the protein expression levels of Copine III in a panel of breast cancer cell lines that also correlated with ErbB2 amplification. In published ovarian and prostate transcriptome studies, Copine III mRNA levels are upregulated in cancer as compared to normal tissue. Based on these findings, we performed immunohistochemistry (IHC) stainings of Copine III on breast, prostate and ovarian tissue microarrays. While some Copine III staining was evident in normal breast, normal prostate and ovarian tissues have very low levels of Copine-III. Strikingly, tumors of all three types showed higher Copine III levels.

To summarize, we present Copine III here for the first time as an interaction partner of the ErbB2 receptor. Copine III interacts with ErbB2 in a  $\text{Ca}^{2+}$ - and HRG-dependent manner and is required for tumor cell migration. Furthermore, Copine III levels were found to be upregulated in tissue microarrays of breast, ovarian and prostate tumor tissue as compared to normal tissue. Together, these findings imply a biological function for Copine III in cancer progression and suggest that further studies into the functions of Copine III are merited.



---

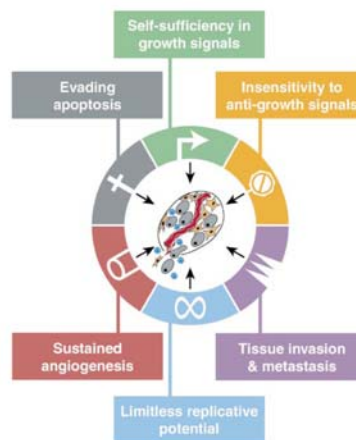
<b>SUMMARY</b> .....	<b>I</b>
<b>TABLE OF CONTENTS</b> .....	<b>III</b>
<b>1 INTRODUCTION</b> .....	<b>1</b>
1.1 Cell signaling and cancer .....	1
1.2 The ErbB family of RTKs.....	2
1.2.1 Evolution of the ErbB signaling network.....	3
1.3 The human ErbB receptor/ligand network.....	4
1.3.1 Ligand induced receptor activation.....	5
1.3.2 Signal transduction of ErbB receptors .....	9
1.3.3 Transactivation of ErbB receptors.....	12
1.3.4 Endocytosis, sorting and recycling of ErbBs .....	14
1.4 ErbB receptors in development and disease.....	15
1.5 ErbB receptors in cancer – aberrant signaling, treatment and resistance.....	16
1.5.1 ErbB2 in breast cancer.....	20
1.6 Copines – a conserved family of Ca <sup>2+</sup> -dependent, phospholipid binding proteins ..	23
1.6.1 General aspects, discovery, homology and conservation .....	23
1.6.2 Domain architecture.....	24
1.7 Biological roles of Copine family members.....	29
1.7.1 Copine in <i>Arabidopsis thaliana</i> .....	29
1.7.2 Copines in <i>Caenorhabditis elegans</i> .....	30
1.7.3 Copines in <i>Dictyostelium discoideum</i> .....	32
1.8 Human Copines .....	33
1.8.1 Phenotypes, biological roles.....	34
<b>2 RESEARCH OBJECTIVE</b> .....	<b>39</b>

<b>3</b>	<b>IDENTIFICATION OF COPINE III AS A BINDING PARTNER OF ERBB2</b> .....	<b>41</b>
3.1	Introduction .....	41
3.2	Materials and methods .....	49
3.3	Results .....	49
3.4	Discussion .....	53
<b>4</b>	<b><i>IN SILICO</i> ANALYSIS OF COPINE III</b> .....	<b>57</b>
<b>5</b>	<b>COPINE III INTERACTS WITH ERBB2 AND PROMOTES TUMOR CELL MIGRATION (IN PRESS)</b> .....	<b>63</b>
5.1	Abstract.....	64
5.2	Introduction .....	65
5.3	Materials and Methods .....	66
5.4	Results .....	71
5.5	Discussion .....	89
5.6	Acknowledgements .....	93
<b>6</b>	<b>COPINE III <i>IN VIVO</i></b> .....	<b>95</b>
6.1	Introduction .....	95
6.2	Materials and Methods .....	95
6.3	Results .....	98
6.4	Outlook .....	112
<b>7</b>	<b>DISCUSSION AND OUTLOOK</b> .....	<b>113</b>
<b>8</b>	<b>APPENDIX</b> .....	<b>123</b>
8.1	Abbreviations .....	123
8.2	List of figures and tables.....	124
<b>9</b>	<b>REFERENCES</b> .....	<b>127</b>
<b>10</b>	<b>ACKNOWLEDGEMENTS</b> .....	<b>137</b>
<b>11</b>	<b>CURRICULUM VITAE</b> .....	<b>139</b>

# 1 INTRODUCTION

## 1.1 Cell signaling and cancer

Each cell receives a plethora of external signals that it must integrate in order to initiate, maintain and attenuate cellular signaling pathways, thereby regulating such diverse processes as protein synthesis, cell growth, cell cycle progression and cell movement. Most cellular signaling pathways are involved in regulating several cellular functions, and in addition, can interact and cross-regulate other pathways thus generating a complex signaling network. Proper functioning of this network is essential for maintaining cell growth and homeostasis. Cancer cells are characterized by the acquisition of mutations leading to deregulated cell growth and homeostasis. In the past years it has become apparent that different types of cancer are characterized by the different mutations they acquire. Furthermore, the majority of cancers display disruption not only in one but several pathways, which results in the effects observed in cancer progression. The different alterations occurring in cancer can be grouped into six categories: self-sufficiency in growth signals, insensitivity to growth-inhibitory (antigrowth) signals, evasion of programmed cell death (apoptosis), limitless replicative potential, sustained angiogenesis, and tissue invasion and metastasis (Figure 1-1) (Hanahan and Weinberg, 2000).



(Hanahan and Weinberg, 2000)

### Figure 1-1 Acquired traits of cancer

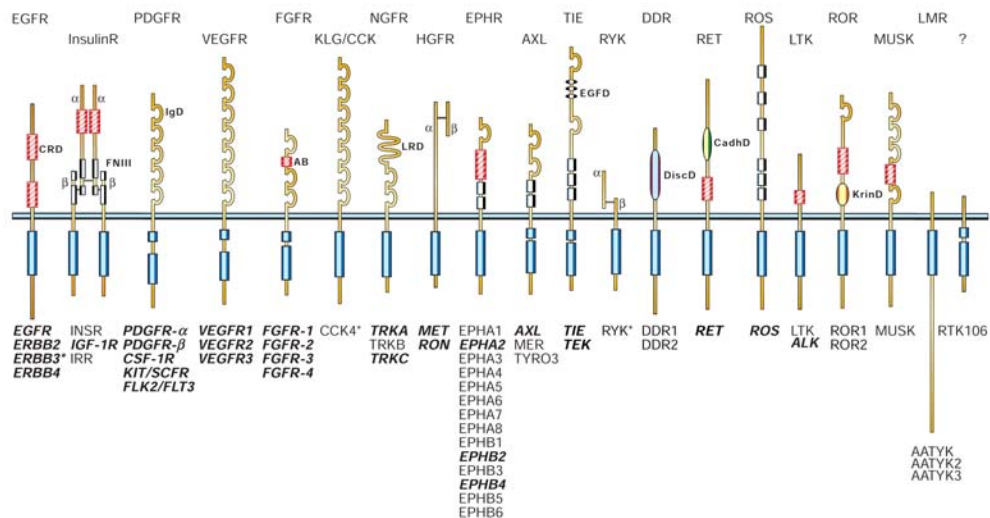
It was suggested that most, if not all, types of cancer have acquired the same set of capabilities during their development.

Three of these traits, namely growth signal autonomy, insensitivity to antigrowth signals and resistance to apoptosis, lead to an uncoupling of intracellular signaling from extracellular cues.

The proteins that receive these extracellular signals and convert them into information to guide intracellular responses are designated transmembrane receptors. Therefore, signaling pathways downstream of transmembrane receptors should be studied carefully in order to elucidate, which functional mutations give rise to specific cancer traits.

## 1.2 The ErbB family of RTKs

Certain classes of signaling proteins, such as molecules governing extracellular growth, differentiation and developmental signals are targeted much more frequently by oncogenic mutations than others. Good examples for this phenomenon are the receptor tyrosine kinases (RTKs), a subclass of transmembrane receptors carrying an intrinsic, ligand-stimulated kinase activity (Blume-Jensen and Hunter, 2001).



(Blume-Jensen and Hunter, 2001)

**Figure 1-2 Human receptor tyrosine kinases**

Depicted are the 20 families of human receptor tyrosine kinases. The prototypic receptor for each family is indicated above the receptor and the known members are listed below. EGFR, epidermal growth factor receptor; InsR, insulin receptor; PDGFR, platelet-derived growth factor receptor; VEGFR, vascular endothelial growth factor receptor; FGFR, fibroblast growth factor receptor; KLG/CCK, colon carcinoma kinase; NGFR, nerve growth factor receptor; HGFR, hepatocyte growth factor receptor, EphR, ephrin receptor; Axl, a Tyro3 PTK; TIE, tyrosine kinase receptor in endothelial cells; RYK, receptor related to tyrosine kinases; DDR, discoidin domain receptor; Ret, rearranged during transfection; ROS, RPTK expressed in some epithelial cell types; LTK, leukocyte tyrosine kinase; ROR, receptor orphan; MuSK, muscle-specific kinase; LMR, Lemur. Other abbreviations: AB, acidic box; CadhD, cadherin-like domain; CRD, cysteine-rich domain; DiscD, discoidin-like domain; EGFD, epidermal growth factor-like domain; FNIII, fibronectin type III-like domain; IgD, immunoglobulin-like domain; KrinD, kringle-like domain; LRD, leucine-rich domain. The symbols  $\alpha$  and  $\beta$  denote distinct subunits. Members in bold and italic type are implicated in human malignancies. An asterisk indicates lack of intrinsic kinase activity.

RTKs belong to a larger family consisting of > 90 genes encoding for protein tyrosine kinases in the human genome. Of these, 58 encode transmembrane RTKs, which are distributed among 20 subfamilies (Figure 1-2).

Subfamily I, also called the Epidermal Growth Factor (EGF/ErbB) family was originally named because of their homology to the erythroblastoma viral gene product v-erbB (Downward *et al.*, 1984). It encompasses four structurally related type I growth factor receptors: EGF receptor (ErbB1/HER1), ErbB2 (Neu/HER2), ErbB3 (HER3) and ErbB4 (HER4), as well as a number of soluble ligands, which bind to their cognate receptor (Yarden and Sliwkowski, 2001).

All ErbBs have a common extracellular ligand-binding domain, a single membrane-spanning region, a cytoplasmic kinase domain and a C-terminal regulatory domain (Holbro *et al.*, 2003b). Ligand binding induces receptor homo- and heterodimerization, which leads to the activation of their intrinsic kinase domain and auto- and transphosphorylation of specific tyrosine residues in their C-terminal intracellular domain (Schlessinger, 2000). These phosphorylated tyrosine residues act as docking sites for various adaptor molecules carrying Src-homology 2 (SH2) or phosphotyrosine-binding (PTB) domains, which then in turn initiate downstream signaling (Olayioye *et al.*, 2000).

Under normal physiological conditions the activity of ErbBs is controlled by the temporal and spatial expression of their ligands. Thus, ErbB receptor activity in a resting, non-transformed cell is tightly controlled. However, in transformed cells these receptors are often mutated, structurally altered or overexpressed, making them potent oncogenes. Over 30 RTKs have been implicated in human cancer, including ErbB2 and ErbB1, which are amplified, mutated or overexpressed in several prevalent cancers such as ovarian and non-small-cell lung cancers (Blume-Jensen and Hunter, 2001). Moreover, cancer patients, whose tumors have an alteration in either ErbB1 or ErbB2, tend to have a more aggressive disease associated with poor clinical outcome (Hynes and Stern, 1994).

### 1.2.1 Evolution of the ErbB signaling network

The ErbB family has developed from a single ligand/single receptor combination to a complex network of four receptors and multiple ligands throughout evolution.

Both the nematode *Caenorhabditis elegans* and the fruitfly *Drosophila melanogaster* have linear primordial versions of the ErbB signaling network, with one receptor and one ligand in *C. elegans* and one receptor and five ligands in *D. melanogaster* (Blume-Jensen and Hunter, 2001).

In *C. elegans* the ErbB receptor homolog LET-23 and its ligand LIN-3 have a known role in vulval development. Vulval development is substrate dependent. The gonadal precursor cell secretes

LIN-3, which is sensed by LET-23 expressed on the six vulva precursor cells (VPCs). Thus, LET-23 is involved in fate determination with regard to which VPC will differentiate into vulval tissue. This is underlined by the fact that loss-of-function of *let-23* leads to a vulvaless phenotype and overexpression of the receptor induces a multivulva phenotype (Aroian and Sternberg, 1991).

As in *C. elegans* the fruitfly *D. melanogaster* possesses a single ErbB2 homolog, DER, however, in contrast to *C. elegans*, it expresses five ligands: Spitz, Gurken, Keren, Vein and Argos. Receptor activation plays a role in successive cell fate determination events during oogenesis, embryogenesis, and the proliferation and differentiation of imaginal discs (Schweitzer and Shilo, 1997). The binding of Spitz, Gurken and Keren, all transforming growth factor  $\alpha$  (TGF $\alpha$ ) homologs, or Vein, a neuregulin-like ligand, leads to receptor activation. Contrary to this, Argos functions to inhibit DER activation by competing for binding to the other ligands. Recently, it was shown that Argos mediates inhibition by sequestering the other ligands (Klein *et al.*, 2004; Klein *et al.*, 2008).

It is intriguing that *D. melanogaster* has such an inhibitory ligand, since no inhibitory ligand has been discovered in higher vertebrates. In higher eukaryotes the ErbB signaling network evolved into a richly interactive, multilayered network, in which combinatorial expression and activation of components permits context-specific biological responses throughout development and adulthood (Yarden and Sliwkowski, 2001). The higher complexity of the system, consisting of four receptors and a multitude of ligands, confers tight regulatory control and therefore minimizes the need for inhibitory ligands.

### 1.3 The human ErbB receptor/ligand network

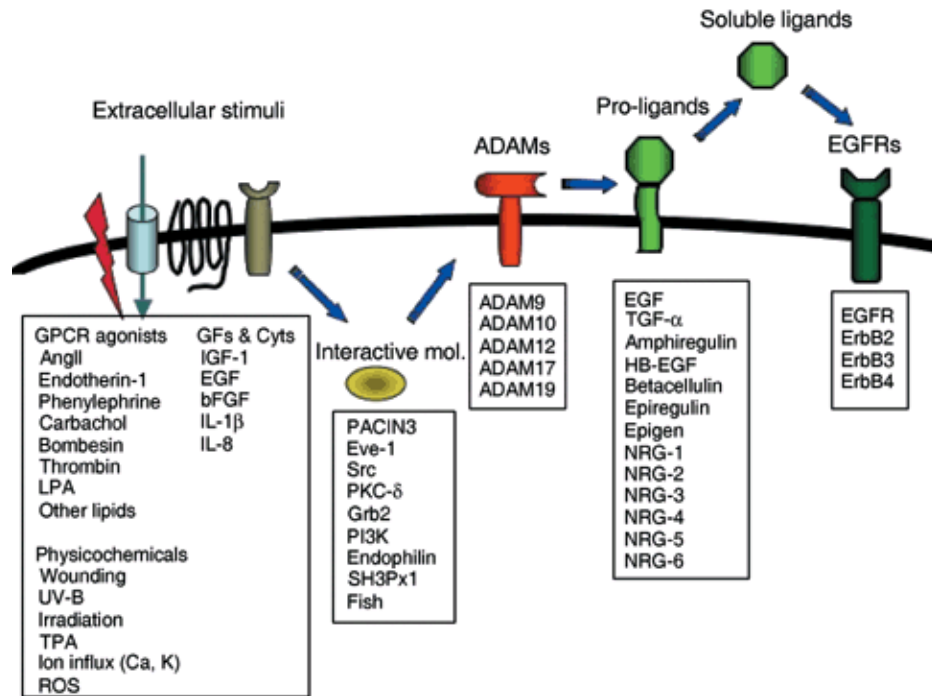
As previously mentioned, the ErbB receptor/ligand system evolved from a linear pathway in *C. elegans* into a complex signaling network in higher eukaryotes. The human ErbB receptor/ligand signaling network consists of four receptors, ErbB1, ErbB2, ErbB3 and ErbB4 and at least 12 ligands. One way of conferring context-specific responses of the cell to external stimuli is provided by the functional selectivity of the 11 ligands. Different ligands can stimulate divergent biological outcomes from the same receptor.

All of the identified ErbB ligands belong to the EGF family of peptide growth factors and are divided into three groups depending on their affinity for one or more receptors (Riese and Stern, 1998). The first group binds ErbB1 and includes EGF, transforming growth factor  $\alpha$  (TGF $\alpha$ ), amphiregulin (AR) and epigen (EPG). Ligands that bind both ErbB1 and ErbB4 comprise the second group, which contains betacellulin (BTC), heparin-binding EGF like growth factor (HB-EGF) and epiregulin (EPR). The third and final group consists of the neuregulins (NRGs), also

referred to as heregulins, which are again further subdivided into two groups: NRG-1 and NRG-2 that can bind to both ErbB1 and ErbB3; and NRG-3 and NRG-4 that are specific for ErbB4 (Olayioye *et al.*, 2000). Of note, none of these ligands binds ErbB2. Yet, despite having no ligand, the ErbB2 receptor is able to dimerize with all of the other receptors of the family and plays a pivotal role in cancer progression (Holbro *et al.*, 2003a). This aspect will be addressed in later sections.

### 1.3.1 Ligand induced receptor activation

Ligands can be produced both in an autocrine, where the cell produces its own growth factors, and paracrine manner, in which growth factors are released from surrounding cells. Autocrine ligands are produced as transmembrane proteins that are then cleaved by cell surface proteases to release the mature growth factor. The process by which the membrane-anchored forms (pro-forms) of the ligand are cleaved is called ectodomain shedding. The main enzymes performing this task are members of the family of zinc binding matrix metalloproteinases (MMPs) and the A disintegrin-like and metalloproteinase-containing (ADAM) family. Ectodomain shedding is a crucial step in controlling ligand availability and receptor activation (Higashiyama *et al.*, 2008). This is underlined by the fact that several members of the ADAMs family, including ADAM8, ADAM9, ADAM10, ADAM12, ADAM15, ADAM17, ADAM19, ADAM28, ADAMTS1, ADAMTS4 and ADAMTS5, have been associated with various types of cancer (breast, uterus, prostate, gastric, etc.) (Higashiyama *et al.*, 2008; Hynes and Schlang, 2006). ADAMs are activated by a variety of stimuli, like growth factor and cytokine signaling, or PKC activation, which induce ectodomain shedding (Figure 1-3).



(adapted from Higashiyama *et al.*, 2008)

### Figure 1-3 Activation of ADAMs, ectodomain-shedding of EGF ligands and receptor activation

Disintegrin and metalloprotease (ADAM) proteins are activated by various stimuli including wounding, ion influx, G-protein coupled receptor (GPCR) signaling, growth factor and cytokine signaling, protein kinase C (PKC) activation, and binding of cytoplasmic interactive proteins. EGFR ligand molecules are proteolytically cleaved by specific metalloprotease-activity of ADAMs, resulting in the production of soluble ligands and stimulation of EGFR in autocrine and paracrine manners. AngII, angiotensin II; Cyt, cytokines; GFs, growth factors; HB-EGF, Heparin-binding epidermal growth

factor carboxy-terminal fragment; LPA, lysophosphatidic acid; MAPK, mitogen-activated protein kinase; NRG, neuregulin; PI3K, phosphatidylinositol 3-kinase; PKC, protein kinase C; ROS, reactive oxygen species; TGF-α, transforming growth factor-α; TPA, 12-O-tetradecanoylphorbol-13-acetate.

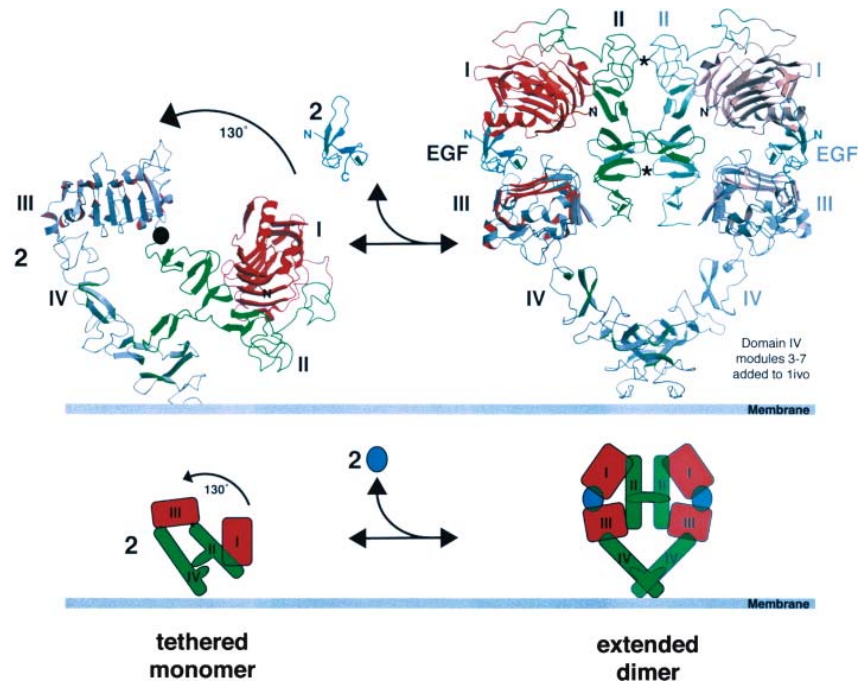
Each of the mature peptide growth factors is characterized by a consensus sequence of six spatially conserved cysteine residues that form three intramolecular disulfide bridges. This consensus sequence is known as the EGF motif and is crucial for binding to members of the ErbB family of RTKs. EGF ligands also contain additional structural motifs such as immunoglobulin-like domains, heparin-binding sites and glycosylation sites (Harris *et al.*, 2003). In addition to ectodomain shedding, juxtacrine stimulation of growth factors has been described in the case of uncleaved HB-EGF, which was able to stimulate ErbB1 in adjacent cells (Higashiyama *et al.*, 1995).

All four ErbB receptors are single-chain glycoproteins composed of an extracellular ligand-binding domain, a single transmembrane-spanning domain and a cytoplasmic domain containing the tyrosine kinase domain and a C-terminal regulatory region (Burgess *et al.*, 2003).



The extracellular domain is heavily glycosylated and is composed of four distinct protein domains: two homologous large (L) domains and two cysteine-rich (CR) domains, which occur in the order L1-CR1-L2-CR2 (Ward *et al.*, 1995). These domains can alternatively be named I-II-III-IV (Figure 1-4). Ligand binding occurs through domains I and III. Domain II contains the so-called dimerization arm, a prominent loop that reaches across the interface between two receptors to interact with its counterpart in the dimerization partner (Burgess *et al.*, 2003).

The ErbB receptors can exist in a closed inhibited or an open active conformation (Moasser, 2007). Crystal structures of ErbB1 (Ferguson *et al.*, 2003) and ErbB3 (Cho *et al.*, 2003) showed that these receptors form a “tethered” conformation, which is stabilized by an interaction of the two CR domains (II and IV) and restrains the dimerization arm of domain II and substantial domain rearrangement is required to switch between the closed and open conformation. A receptor in the tethered conformation cannot dimerize with another receptor. Moreover, the two ligand binding surfaces on domain I and III are too far apart for a single ligand to bind to both simultaneously (Burgess *et al.*, 2003) and so this tethered conformation confers only low ligand affinity. When a ligand does bind to the receptor, both domain I and III perform a  $\sim 130^\circ$  counterclockwise rotation around the x/y axis in addition to a  $\sim 20\text{\AA}$  translation along the z-axis. This rearrangement gives rise to an extended or open active conformation, in which the dimerization arm is exposed and able to form inter- rather than intramolecular interactions. Only the extended configuration of the receptor is capable of both high affinity ligand binding and efficient dimerization (Burgess *et al.*, 2003). ErbB2 plays a pivotal role in the family, because, unlike the other receptors, it does not exist in a tethered conformation, but is always found in the extended active conformation (Figure 1-4).



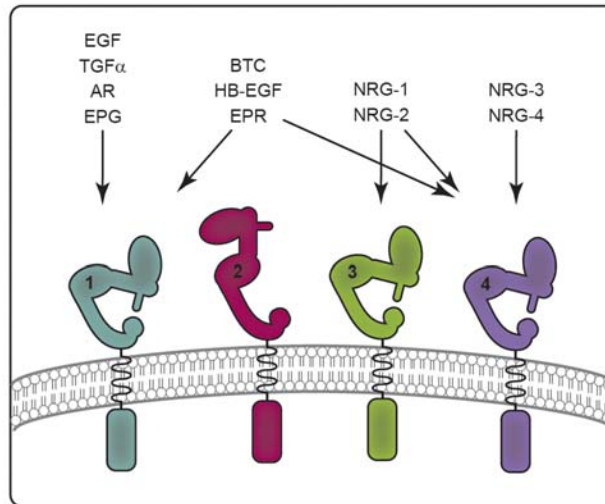
(adapted from Burgess *et al.*, 2003)

**Figure 1-4 Schematic illustration of ligand-induced conformational changes in sEGFR**

A transition between two sEGFR structures is shown in both ribbons and cartoon representation. The unactivated (tethered) sEGFR structure (Ferguson *et al.*, 2003) is shown on the left. A model of the EGF-induced dimer is shown on the right. This model uses the coordinates of (Ogiso *et al.*, 2002), which lacked 5 of the 7 disulfide-bonded modules of domain IV. The missing modules of domain IV have been added using the structure of unactivated sEGFR, and assuming that the domain III/IV relationship in sEGFR is unaltered upon ligand binding. L domains in the receptor (domains I and III) are colored red, and CR domains (domains II and IV) are green. Ligand is colored cyan. Domains I and III are distinguished from one another by the addition of gray to the outer surfaces of strands and helices. The two subunits in the dimer are distinguished by the fogging of the right-hand dimerization partner. Individual domains are labeled. The mutual “hooking” of the two domain II dimerization arms across the dimer interface can be observed in the center of the structure. The additional domain II contacts across the interface, at module 2 and module 6 are marked with asterisks. The speculated position of the plasma membrane is depicted as a gray bar. EGF binding is proposed to induce a 130° rotation of a rigid body containing domains I and II, about the axis represented by a filled black circle (at the domain II/III junction). This exposes the dimerization arm and allows dimerization of sEGFR, as depicted on the right.

Dimerization induces activation of the intracellular kinase domain and subsequent transphosphorylation of specific tyrosine residues in the C-terminal regulatory region. Dimerization partner selection appears to be a key determinant for the signaling activity of the ErbB receptors. They show a distinct hierarchical order for dimerization, preferring heterodimers over homodimers (Moasser, 2007). Under normal circumstances, neither ErbB2 nor ErbB3 homodimers support linear signaling as ErbB2 does not bind any ligand and ErbB3

has an impaired kinase domain. However, when overexpressed, ErbB2 can form potent homodimers, and is the preferred heterodimerization partner of the other receptors (Beerli and Hynes, 1996). These ErbB2-containing heterodimers are the most oncopotent dimers (Harari and Yarden, 2000).



(Hynes and MacDonald, 2009)

#### Figure 1-5 The human ErbB receptor/ligand family

There are four members of the ErbB family of RTKs, EGFR (1), ErbB2 (2), ErbB3 (3), and ErbB4 (4). Upon ligand binding the receptors undergo a conformational change allowing for the formation of homodimers and heterodimers. The receptors then become phosphorylated on tyrosine residues within their cytoplasmic kinase domain, initiating downstream signaling. Four groups of ErbB ligands have been described on the basis of their receptor specificity. The first group binds EGFR exclusively and includes EGF, TGF $\alpha$ , AR, and EPG. Members of the second group (BTC, HB-EGF, and EPR) exhibit dual specificity for EGFR and ErbB3. The neuregulins make up the third and fourth groups on the basis of their ability to bind both ErbB3 and ErbB4 (NRG-1 and NRG-2), or ErbB4 alone (NRG-3 and NRG-4). ErbB2 does not bind any of the ErbB ligands; however, its open conformation makes it the preferred dimerization partner for all of the other ErbB receptors.

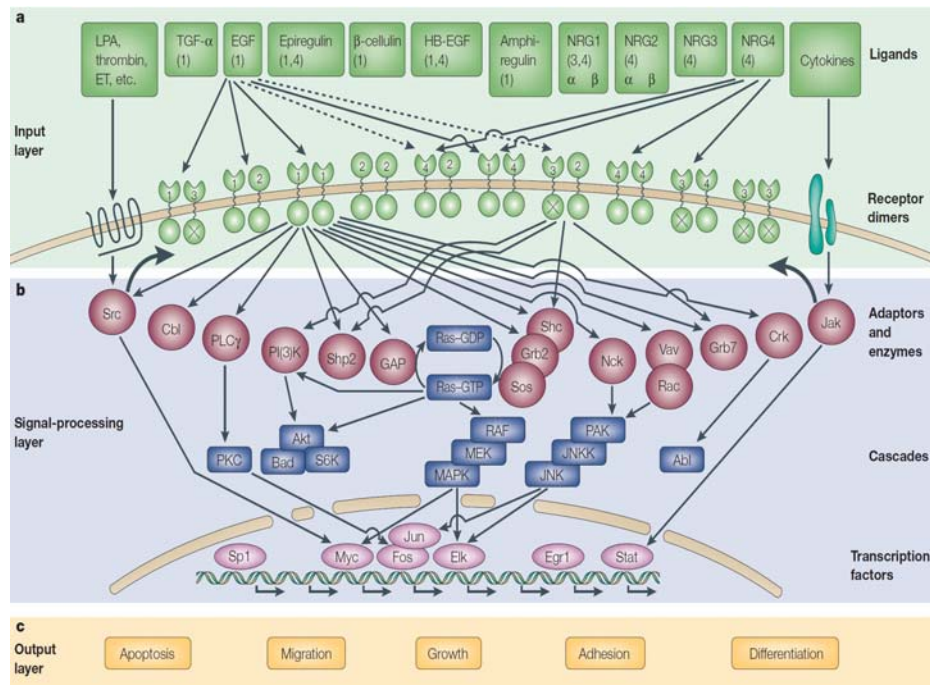
### 1.3.2 Signal transduction of ErbB receptors

ErbB ligands influence downstream signaling diversity by exhibiting differential binding affinities, signal strengths and duration, and receptor specificities. Temporally and spatially controlled ligand binding first induces homo- and heterodimerization of ErbB receptors, a process which results in activation of their intrinsic kinase domains and subsequent auto- and transphosphorylation of specific tyrosine residues at their C-terminal regulatory region. A model for the process of kinase activation following receptor dimerization has been proposed (Zhang *et al.*, 2006). It suggests that the ErbB1 kinase domain is intrinsically autoinhibited. Upon dimerization of two receptors, the C-lobe of one receptor's kinase domain allosterically

activates the kinase module of the other receptor by contacting its N-lobe. This interaction repositions the activation loop in a conformation which facilitates catalysis (Zhang *et al.*, 2006). The mechanism whereby ErbB2 is phosphorylated whilst partnered with the kinase inactive ErbB3 receptor remains poorly understood. However, one model predicts that activation of ErbB2 is possible due to an interaction between the C-lobe of ErbB3 and the N-lobe of ErbB2 (Zhang *et al.*, 2006).

Tyrosine phosphorylation (pTyr) of the receptors results in the formation of docking sites for adaptor proteins containing either a phosphotyrosine binding (PTB) or Src-homology 2 (SH2) domains, with which they bind to pTyr (Olayioye *et al.*, 2000). Each ErbB receptor displays a unique pattern of C-terminal autophosphorylation sites and thus recruits specific adapter proteins providing again means of selectivity and diversity for the system.

Several pathways crucial for cellular functioning are found to be activated downstream of the ErbB receptors. The mitogen-activated protein kinase (MAPK) pathway can be activated by all members of the ErbB family, via the adaptors Grb2 and Shc. A second important signaling pathway, most often selectively activated by ErbB3, is the phosphatidylinositol 3-kinase (PI3K) pathway. Though either ErbB3 or ErbB4 can bind directly to the p85 subunit of PI3K to induce signaling, ErbB1 has been shown to mediate activation of this pathway via its interaction with Grb2, which recruits Gab1 and thereby couples the receptor to the PI3K pathway (Hynes and Lane, 2005). Despite sharing some pathways, each receptor is also coupled to a distinct set of signaling proteins that allows them to activate discrete downstream targets (Yarden and Sliwkowski, 2001). For example, ErbB1 couples to the ubiquitin ligase Cbl, ErbB2 to PLC $\gamma$ , Grb2 and the Ras-specific GTPase-activating protein (Gap), and ErbB3 to Shc and Grb7 (Yarden and Sliwkowski, 2001).



(Yarden and Sliwkowski, 2001)

### Figure 1-6 The ErbB signaling network

a | Ligands and the ten dimeric receptor combinations comprise the input layer. Numbers in each ligand block indicate the respective high-affinity ErbB receptors. For simplicity, specificities of receptor binding are shown only for epidermal growth factor (EGF) and neuregulin 4 (NRG4). ErbB2 binds no ligand with high affinity, and ErbB3 homodimers are catalytically inactive (crossed kinase domains). Trans-regulation by G-protein-coupled receptors (such as those for lysophosphatidic acid (LPA), thrombin and endothelin (ET)), and cytokine receptors is shown by wide arrows. b | Signaling to the adaptor/enzyme layer is shown only for two receptor dimers: the weakly mitogenic ErbB1 homodimer, and the relatively potent ErbB2–ErbB3 heterodimer. Only some of the pathways and transcription factors are represented in this layer. c | How they are translated to specific types of output is poorly understood at present. (Abl, a proto-oncogenic tyrosine kinase whose targets are poorly understood; Akt, a serine/threonine kinase that phosphorylates the anti-apoptotic protein Bad and the ribosomal S6 kinase (S6K); GAP, GTPase activating protein; HB-EGF, heparin-binding EGF; Jak, janus kinase; PKC, protein kinase C; PLC $\gamma$ , phospholipase C; Shp2, Src homology domain-2-containing protein tyrosine phosphatase 2; Stat, signal transducer and activator of transcription; RAF–MEK–MAPK and PAK–JNKK–JNK, two cascades of serine/threonine kinases that regulate the activity of a number of transcription factors.)

Signaling cascades activating MAPK, protein kinase C (PKC) or the PI3K pathway translate signals directly into the nucleus. There, distinct transcriptional programs are initiated by transcription factors including not only some proto-oncogenes like fos, jun and myc, several of the STATS (signal transducers and activators of transcription) family members, but also a family of zinc-finger-containing transcription factors such as Sp1, Egr1 or the Ets family member GA-binding protein (GABP). In this way signaling through the ErbB receptors can induce a variety

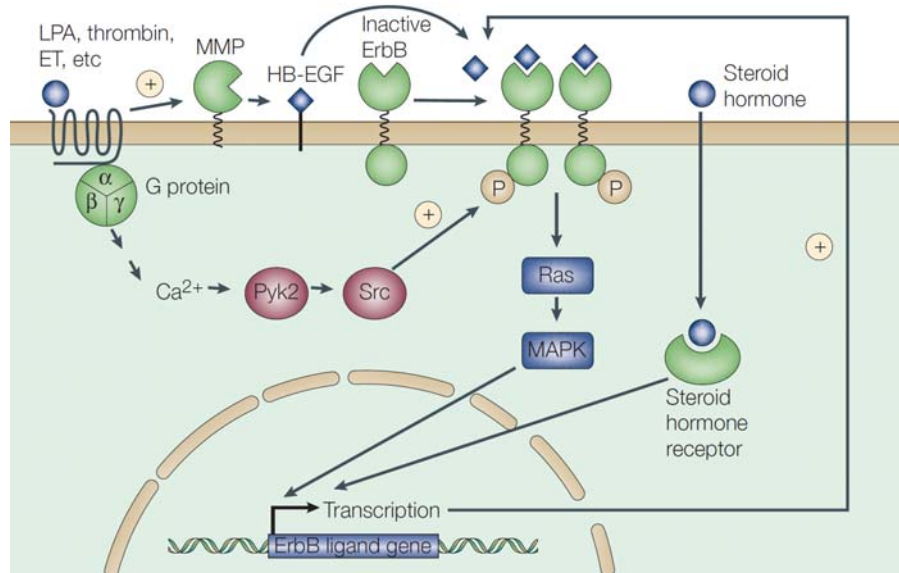
of cellular phenotypes such as cell division and migration, adhesion, differentiation and apoptosis (Figure 1-6).

In addition to multiple ligands, receptors and downstream effectors, the ErbB signaling network is made more complex still by combinatorial interactions with other receptor families and their downstream pathways. Thus, given the importance of these receptors for proper cell functioning, the kinetics of their signaling needs to be tightly controlled. In principal, this is controlled by ligand-mediated receptor endocytosis, a process whose kinetics also depends heavily on the receptor composition (Yarden and Sliwkowski, 2001).

### 1.3.3 Transactivation of ErbB receptors

Transactivation of the receptors by other signaling molecules can happen both outside of the cell by the production of soluble ligands, as well as inside the cell through receptor phosphorylation (Figure 1-7).

The production of soluble EGF ligands through ectodomain shedding by ADAMs was first shown following the activation of G-protein-coupled receptors (GPCRs). The process by which GPCR activation causes ErbB1 activation is termed ErbB1 transactivation (Hynes and Lane, 2005). More recently, other pathways capable of transactivating ErbB receptors through the production of extracellular ligands have been described: the binding of Wnt to its seven-pass membrane receptor frizzled leads to the transactivation of ErbB1 in a process similar to that of GPCRs (Civenni *et al.*, 2003; Schlange *et al.*, 2007). Furthermore, oestradiol (E2) binding to the plasma-membrane-associated oestrogen receptor (ER) has also been shown to transactivate ErbB1 (Razandi *et al.*, 2003). Since many GPCR agonists activate PKC and Src, these kinases might also play a role in ErbB transactivation (Hynes and Lane, 2005). It has been shown that PKC $\delta$  phosphorylates ADAM9, resulting in HB-EGF processing (Izumi *et al.*, 1998). The involvement of Src family members in ErbB transactivation through ectodomain shedding has not yet been shown. However, it is known that Src can phosphorylate ErbB1 intracellularly (Biscardi *et al.*, 1999). Moreover, other kinases and receptors have been shown to phosphorylate ErbB receptors: Janus tyrosine kinase 2 (Jak2) was shown to phosphorylate ErbB1 and ErbB2 once activated (Yamauchi *et al.*, 1997). Several studies have shown that integrins are capable of transactivating ErbB receptors:  $\alpha 6\beta 4$  integrin was shown to associate with ErbB2 at the cell surface and to regulate ErbB2 translation and ErbB1 transactivation *in vitro* (Yoon *et al.*, 2006). Even more compelling was the finding that  $\beta 4$  integrin also regulates ErbB2 signaling *in vivo*. A knockdown of  $\beta 4$  integrin suppresses mammary tumor onset and invasive growth of ErbB2-expressing tumors (Guo and Giancotti, 2004).



(Yarden and Sliwkowski, 2001)

**Figure 1-7 Crosstalk between the ErbB network and other signaling pathways**

G-protein-coupled receptors (GPCRs) such as those for lysophosphatidic acid (LPA), thrombin and endothelin (ET) can have positive effects on ErbB signaling through two mechanisms. First, through a poorly defined mechanism, they can activate matrix metalloproteinases (MMPs), which cleave membrane-tethered ErbB ligands (such as heparin binding EGF-like factor, HB-EGF), thereby freeing them to bind to ErbBs. Second, GPCRs indirectly activate Src (perhaps via PTyrk2), which phosphorylates the intracellular domains of ErbBs on tyrosine residues. Steroid hormones can have a positive effect on ErbB signaling by activating the transcription of genes encoding ErbB ligands. Finally, ErbB activation can activate a positive feedback loop through the Ras–MAPK (mitogen-activated protein kinase) pathway, which also activates transcription of ErbB ligand genes.

In summary, the ErbB receptor/ligand system is a complex signaling network that has become more complex and specialized throughout evolution, with divergent signaling inputs and outcomes. Control mechanisms are installed in both a temporal and spatial manner i.e. through the regulation of ligand expression. However, the ErbB2 signaling network does not function on its own, but receives activating and repressing signals from other pathways itself. It has been shown that signaling through ErbBs is frequently impaired in development and disease and thus this network has become a major target for therapy. However, considering the contribution of other signaling networks is crucial for designing targeted therapies.

### 1.3.4 Endocytosis, sorting and recycling of ErbBs

Endocytosis and thus degradation of the ErbB receptors is a major negative regulatory feedback mechanism that controls the intensity and duration of receptor signaling. This is mostly true for ErbB1, since endocytosis and degradation of ErbB2, ErbB3 and ErbB4 is much less efficient (Sorkin and Goh, 2009). Yet, ligand induced internalization of all the ErbB receptors can also lead to their sorting into endosomal complexes were they remain in active signaling complexes. Thus, depending on the context, endocytosis can be regarded as both a negative and a positive feedback loop of ErbB signaling (Sorkin and Goh, 2009). In the absence of activation, ErbB1 is constitutively internalized at a rate comparable to the rate of basal membrane recycling. After internalization, inactive ErbB receptors are mainly recycled back to the surface. Additionally, it was proposed to that both ErbB1 and ErbB2 can be translocated from the cell surface to the nucleus.

Activation of the receptor by ligand binding leads to an acceleration of receptor internalization. EGF-ErbB1 complexes are primarily internalized via clathrin coated pits. However, other mechanisms of ErbB1 internalization have been detected as well, including EGF-induced pinocytosis and internalization via the vesicular-tubular endocytosis compartment (Haigler *et al.*, 1979; Orth *et al.*, 2006). Studying the endocytosis of ErbB2 is difficult, since ErbB2 has no natural ligand. Despite this, it was found that in some cases overexpression of ErbB2 prevented ErbB1 internalization and, in others, re-routed ErbB1 from degradation to the recycling pathway. Yet, ErbB2 clearly has a lower potency to be ubiquitinated and targeted to the lysosome than ErbB1 (Sorkin and Goh, 2009).

Neuregulin induced internalization of ErbB3 and ErbB4 has been observed in many cell types, though their rates of degradation are much slower as compared to ErbB1. Trafficking of both receptors has been shown to be regulated by ubiquitination (Sorkin and Goh, 2009).

The mechanism of internalization of ErbB2, ErbB3 and ErbB4 is poorly understood and not well studied. Additional research, perhaps following up on initial observations from the studies on ErbB1 endocytosis, needs to be done to further our knowledge of this complex, but important, regulatory process.



## 1.4 ErbB receptors in development and disease

The ErbB network is a key developmental signaling pathway throughout evolution. Research using knockout and transgenic mice is helping to clarify the functions of individual ErbB receptors and specific ligands in mammalian development (Yarden and Sliwkowski, 2001).

Null mutations of ErbB1 are lethal prenatally or shortly postnatally and it was suggested that ErbB1 is required for the promotion of proliferation and differentiation of the epithelial component of skin, lung, pancreas and the gastrointestinal tract. Similarly, mice lacking the ErbB ligand TGF $\alpha$  show abnormal skin, hair and eye development. However, unlike ErbB1 knockout mice, which undergo massive apoptosis in cortical and thalamic brain regions, these mice show no brain abnormalities (Olayioye *et al.*, 2000; Yarden and Sliwkowski, 2001)

ErbB2 null mice die midgestation, a phenotype shared by ErbB4 knockout mice (Gassmann *et al.*, 1995, Olayioye, 2000 #7; Olayioye *et al.*, 2000). This is due to trabecular malformations of the heart, implying that ErbB2 and ErbB4 are essential for embryonic heart development. The important role of ErbB2 in the heart will be discussed further when discussing ErbB-targeted therapies.

Most ErbB3 knockout mice die by E13.5, displaying normal heart trabeculation, but defective valve formation. Moreover, these animals show a generalized neural crest defect and lack Schwann cell precursors (Olayioye *et al.*, 2000).

Since most ErbB receptor null mutations are lethal, it is difficult to study their role in adult development. In order to do this, conditional, organ-specific knockout mice have been generated. The most interesting organ, in which to study ErbB receptors in the adult, is the mammary gland as it undergoes most of its proliferation and differentiation postnatally (Olayioye *et al.*, 2000). All four ErbB receptors are expressed in cell type- and developmental stage-specific patterns (Schroeder and Lee, 1998). ErbB1 is expressed through all mammary gland developmental stages, and a mutation in the kinase domain leads to defective ductal growth. Similarly, ErbB2 is expressed throughout all developmental stages, yet dominant-negative (DN) ErbB2 mice display normal ductal growth. However, as with ErbB4 DN mice, these mice exhibit an impairment in lactation.

Collectively, these studies reveal the importance of the ErbB network during development, especially in the mammary gland. It is perhaps not surprising, given their requirement for proper cellular growth and differentiation that deregulation of the ErbB network in the mammary gland results in cancer.

## 1.5 ErbB receptors in cancer – aberrant signaling, treatment and resistance

The ErbB signaling network has been implicated in the development of many human cancers. In many cancer cell types the ErbB pathway becomes hyperactivated by a range of mechanisms such as kinase domain mutations, in-frame deletions, total deletion of the extracellular domain or ligand or receptor overproduction, all of which lead to a constitutive activation of the system (Hynes and MacDonald, 2009; Yarden and Sliwkowski, 2001). Receptor overexpression is either due to gene amplification, increased transcription or increased translation.

In-frame deletions in the extracellular domain of ErbB1, the most frequent being a deletion of the dimerization arm termed EGFR vIII, are often found in glioblastoma and lead to constitutive receptor activation and defective degradation (Jorissen *et al.*, 2003). Up to 20% of glioblastoma show ErbB1 rearrangements and up to 40% of glioma tumours overexpress the receptor (Citri and Yarden, 2006). Furthermore, overexpression of ErbB1 is seen in squamous cell carcinomas of head and neck (SCCHN), non-small cell lung cancers (NSCLC), ovarian and other tumors (Holbro and Hynes, 2004). However, receptor overexpression on its own is insufficient to induce its constitutive activation and in most primary cancers, co-expression of a ligand is seen (Holbro and Hynes, 2004). Both receptor overexpression and ligand co-expression in breast and ovarian cancers have been associated with poor patient prognosis (Citri and Yarden, 2006). Thus, the parallel analysis of both ErbB1 and its ligands provides a strong predictive tool for patient survival in several types of human cancer (reviewed in Nicholson *et al.*, 2001).

ErbB2 has been shown to be upregulated in many cancers due to gene amplification and overexpression, which leads to constitutive signaling. Overexpression of ErbB2 is seen in breast, lung, pancreas, colon, endometrium and ovarian cancers. Furthermore, in breast cancer, where 15-30% of all cases exhibit an overexpression, and in ovarian cancer, ErbB2 is considered to be a negative prognostic marker (Ross and Fletcher, 1998).

The catalytically inactive ErbB3 receptor is expressed in several cancer subtypes. However, there is no evidence to suggest that gene amplification or overexpression of ErbB3 plays a role in tumor progression. Rather, ErbB3 plays its pivotal role in cancer progression as the preferred dimerization partner of the other family members, especially ErbB2, and links to the pro-survival PI3K pathway. As with ErbB3, ErbB4 has been shown to be upregulated in different types of cancer, however, relatively little is known about the general or specific roles of ErbB4 in the development of human tumors.

Since the ErbB receptors have been shown to be aberrantly regulated in a wide range of human tumors, they are excellent targets for selective therapy (Hynes and Lane, 2005). Two

major therapeutic strategies to target ErbB receptors are currently in the final stages of drug development or are being used in the clinic, namely small molecule tyrosine kinase inhibitors (TKIs) and monoclonal antibodies targeting the extracellular domain of the receptors (Strome *et al.*, 2007) (Figure 1-8). TKIs usually bind to the ATP-binding pocket of the intracellular kinase domain thereby inhibiting kinase activity. In contrast to TKIs, targeted antibodies bind the extracellular domain of the receptor. Several mechanisms for their modes of action have been proposed, though why they are efficacious is not clearly understood. Several of these treatments, their proposed modes of action and their clinical status are discussed below.

Cetuximab or Erbitux, a chimeric monoclonal antibody (mAb), targets the extracellular domain of EGFR thereby preventing ligand binding, receptor activation and subsequent signal transduction. Furthermore, there is evidence to suggest that Cetuximab promotes receptor internalization (Baselga, 2001). It is approved for the treatment of colorectal cancer and clinical trials are ongoing to test its efficacy in the treatment of pancreatic cancer, SCCHN and NSCLC (Hynes and Lane, 2005).

Considering the phenotype observed in ErbB1 knockout mice, it is not surprising that the common side effects of ErbB1 targeted therapies include rash, acnetic skin reactions and diarrhea (Baselga *et al.*, 2002). Interestingly, cutaneous skin rash has been proposed as a surrogate marker of clinical benefit for many EGFR-targeted agents (Hynes and Lane, 2005).

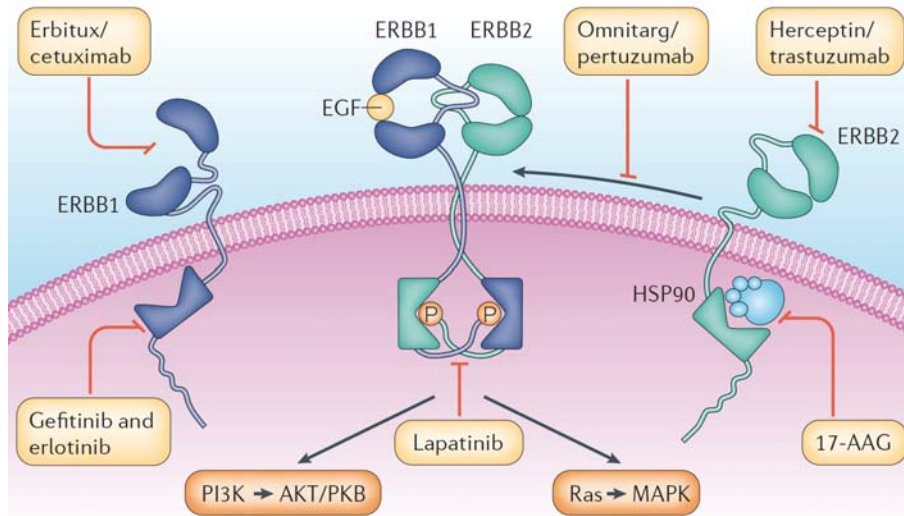
Trastuzumab (Herceptin) and Pertuzumab (Omnitarg) are both humanized mAbs targeting the ErbB2 receptor, however, their mode of action is different: Trastuzumab, which is used for the treatment of ErbB2 overexpressing breast cancer, binds domain IV of ErbB2 resulting in downregulation of ErbB2 levels and thus ErbB2 mediated signaling pathways. In addition, it blocks MMP-mediated ErbB2 ectodomain shedding, which would otherwise mediate constitutive signaling. It was observed in the clinic that some patients treated with Trastuzumab presented cardiac phenotypes, including cardiomyopathy, congestive heart failure and a decreased left vent ejection fraction (Hynes and Lane, 2005), most probably due to the important role of ErbB2 in the heart.

Pertuzumab on the other hand, binds domain II of ErbB2 thereby preventing ligand-induced receptor dimerization. This difference could explain why Pertuzumab is effective for the treatment of tumors expressing low levels of ErbB2, whereas Trastuzumab is not (Agus *et al.*, 2002). Clinical trials to test the efficacy of Pertuzumab in ovarian, breast, prostate and NSCLC cancer are ongoing.

It has been observed that only approximately one-third of all ErbB2-overexpressing breast cancer patients respond to Trastuzumab (reviewed in Hynes and Lane, 2005). This is an indication that many tumors acquire or have de novo resistance to Trastuzumab, an issue that

has been analyzed in several studies. Many of these provide evidence that modulation of other pathways compensates for the blockade of ErbB2, activating the PI3K pathway and contributing to resistance. For example, the Met receptor is rapidly upregulated in cells treated with Trastuzumab leading to activated PI3K signaling (Shattuck *et al.*, 2008) and activation of the insulin-like growth factor 1 receptor (IGF-IR) renders Trastuzumab-sensitive cells resistant to the antibody, an effect which was again linked to the PI3K pathways (Lu *et al.*, 2001, Lu, 2004 #857). More importantly, it was shown that activating mutations of *PIK3CA*, the gene encoding the PI3K p110 $\alpha$  catalytic subunit, as well as decreased expression of PTEN, the phosphatase that dephosphorylates PIP<sub>3</sub>, thus attenuating PI3K signaling, are very frequent in breast cancer, and serve as markers for poor response to Trastuzumab. Encouragingly, a recent study showed that this resistance can be overcome by the addition of selective PI3K inhibitors targeting the p110 subunits. *In vitro* studies proved that Trastuzumab together with GDC-0941, a selective p110 inhibitor, produces a synergistic effect and cell death is increased (Junttila *et al.*, 2009).

Recently, it was demonstrated that the mechanism underlying therapeutic resistance depends on the nature of the ErbB2/ErbB3 complexes at the cells surface. Trastuzumab destabilizes constitutive ligand-independent ErbB2/ErbB3 complexes, which exists due to ErbB2 overexpression, uncoupling ErbB3 from ErbB2 and thus blocking downstream PI3K signaling. However, these complexes are structurally distinct from the ligand-dependent Trastuzumab-insensitive ErbB2/ErbB3 complexes, which signal even in the absence of ErbB2 overexpression. Whether these different complexes also activate distinct downstream signaling pathways has not yet been resolved.



(Citri and Yarden, 2006)

### Figure 1-8 Targeting the ErbB signaling network in cancer

Several monoclonal antibodies as well as small-molecule tyrosine kinase inhibitors (TKIs) have been developed to target the ErbB signaling network in cancer. They include the antibodies Erbitux (Cetuximab) targeting EGFR for treatment of colorectal cancer, Trastuzumab (Herceptin) targeting ErbB2 for treatment of breast cancer and Pertuzumab (Omnitarg), which prevents ErbB2 from dimerizing with another receptor. Small molecule TKIs include two EGFR specific drugs, Gefitinib (Iressa) and Erlotinib (Tarceva), which are effective against tumors with hyperactive ERBB1 mutants and are used for the treatment of non-small-cell-lung cancers. Furthermore, the dual-specificity inhibitor Lapatinib targets both EGFR and ErbB2 and the HSP90 inhibitor 17-AAG (17-N-allylamino-17-demethoxygeldamycin) aims at the dissociation of HSP90 from the receptor thereby targeting the receptor for degradation.

Apart from monoclonal antibodies, small-molecule tyrosine kinase inhibitors (TKIs) have been, and are still, under development for the targeted treatment of cancer. Both Gefitinib (Iressa) and Erlotinib (Traceva) are TKIs targeting ErbB1 that have been approved for use in NSCLC after failure on other available treatments. Both have been shown to be effective against tumors that express catalytically hyperactive ErbB1 mutants. Even so, resistance to TKIs has also rapidly emerged as a significant clinical problem (Citri and Yarden, 2006). Similar to resistance to antibody therapies, tumors resistant to TKIs show an upregulation of other pathways or pathway components, leading to active signaling, mainly through the PI3K and MAPK pathway (Hynes and MacDonald, 2009). Compensatory signaling to PI3K via IGF-IR, as well as increased binding of the IRS-1 scaffold protein to the receptor, has been observed in Gefitinib-resistant NSCLC (Buck *et al.*, 2008; Guix *et al.*, 2008).

Altogether, it seems that the PI3K pathway plays an important role in tumors with ErbB receptor mutation (Hynes and MacDonald, 2009). Furthermore, although many targeted approaches are being tested and are already approved for the clinic, resistance to these therapies is inevitable. Future approaches to cancer treatment will have to involve the accurate prediction of which patients will benefit from a given treatment and to not only to develop

accurate predictors for the response to ErbB targeted therapies, but also to use combinations of known targeted therapies, like it was shown by the co-administration of Trastuzumab and the p110 $\alpha$  inhibitor GDC-0941 (Junttila *et al.*, 2009).

### 1.5.1 ErbB2 in breast cancer

ErbB2 is amplified in 15-30% of all breast cancers and serves as a prognostic indicator of poor outcome (Slamon *et al.*, 1987); (Ross and Fletcher, 1998). Although ErbB2 amplification is best studied in breast cancer, it has also been reported in other cancer types, including gastric, esophageal and endometrial cancers, where it is also associated with a poor prognosis. It has become increasingly apparent that ErbB2 plays a pivotal role within the family of ErbB receptors, as it is the preferred heterodimerization partner of all of the other receptors and when overexpressed, can become constitutively active. Thus it is not surprising that historically it has been the focus of attention for ErbB-directed targeted therapies. This chapter will focus on ErbB2 and its known functions in breast cancer.

In 1985 two independent studies, performed in human and mouse systems, described EGFR-related genes found to be amplified in breast cancer, namely *HER2* and *neu*, a gene homologous to the *v-ErbB* (avian erythroblastosis virus) viral oncogene. It was quickly reconciled that these two genes were in fact homologues of one another (King *et al.*, 1985; Schechter *et al.*, 1985; Schechter *et al.*, 1984; Slamon *et al.*, 1987). Although the nomenclature was initially complex, with *HER2* and *neu* used in the literature to refer to the human and rodent genes respectively, the field has slowly adopted the name ErbB2 for all species (Moasser, 2007).

The ErbB2 receptor is widely expressed in normal human organs and tissues, including the ovarian epithelium, endometrium, heart, lung, prostate, kidney, pancreas, and liver. It encodes a 185 kDa orphan receptor tyrosine kinase for which no direct ligand has been identified. The *ERBB2* oncogene is located on chromosome 17q12, a region frequently amplified in cancer. In breast cancer the amplified DNA fragment, or ErbB2 amplicon, covers a region of approximately 2Mb and includes 13 co-amplified genes, some or all of which may play a role in the phenotype and clinical characteristics of *ERBB2*-amplified tumors (Kauraniemi and Kallioniemi, 2006).

The role of ErbB2 within the cellular network remained largely unknown until 1988, when for the first time ErbB1 heterodimerization with ErbB2 was shown to induce its transactivation (Stern and Kamps, 1988). The ErbB2 receptor can mediate the lateral signal transduction of all ErbB receptors (Hynes and Lane, 2005). Therefore, normal activation of ErbB2 is highly

dependent on the expression of other family members, for which it acts as the preferred heterodimeric partner (Graus-Porta *et al.*, 1997). In fact, ErbB2 and ErbB3 have been established as obligate heterodimerization partners, since even chimeric kinase-active ErbB3 constructs fail to signal without hetero-partners suggesting that ErbB3 even lacks the ability to homodimerize (Moasser, 2007). In this context the main function of ErbB3 is to couple active ErbB2 to the PI3K pathway (Holbro *et al.*, 2003a). Conversely, overexpression and/or mutation of ErbB2 lead to its constitutive activation as well as spontaneous dimerization and stabilization of the homodimeric complex in a ligand-independent manner (Hynes and Stern, 1994).

It is indisputable that both the human *HER2* as well as the rodent *neu* have the ability to transform cells (reviewed in Moasser, 2007). The transforming potential of the *neu* oncogene is due to a point mutation in the transmembrane domain (V664E), which promotes receptor dimerization and kinase activity. Transgenic mouse models in which expression of the activated *neu* oncogene (*neuT*) is driven by the mouse mammary tumor virus promoter (MMTV-*neuT*) exhibit multifocal adenocarcinoma formation (Muller *et al.*, 1988). The MMTV-*neuT* model has become the workhorse for the study of ErbB2 tumorigenesis *in vivo* (Moasser, 2007), however, direct translation of the information gained using this model to the human disease may be limited, as in contrast to rodent ErbB2, overexpression of human ErbB2 appears to be sufficient for transformation. Although mutations in human HER2 have been identified, human breast cancer is most often characterized by an overexpression of wildtype ErbB2.

Amplification of ErbB2 appears to be an early event in human breast cancer as it is seen in nearly half of all *in situ* ductal carcinomas. Its status is also maintained during the transition to invasive disease, as well as in nodal and distal metastases (Park *et al.*, 2006). Human ErbB2 amplified breast cancers possess biological characteristics that distinguish them from other types of breast cancer. These include increased sensitivity to certain cytotoxic chemotherapeutic agents, resistance to endocrine therapies and an increased propensity to metastasize to the brain (Gabos *et al.*, 2006; Ross *et al.*, 2003).

As discussed previously, of the four ErbB family members, ErbB2 is the least susceptible to inactivation and when recruited into heterodimers, prolongs the signaling activity of its dimerization partner as well. Thus, ErbB2 overexpressing cells sustain downstream signaling significantly longer than those that exhibit low ErbB2 expression (Karunagaran *et al.*, 1996).

Five major ErbB2 autophosphorylation sites have been identified and mapped (Hazan *et al.*, 1990): Tyr1023/1028, Tyr1139/1144, Tyr1196/1201, Tyr1222/1227 and Tyr1248/1253 (human/rat) referred to herein as YA, YB, YC, YD and YE, respectively.

Mutation of any single pTyr site had minimal effect on the transformation potential of ErbB2 in focus formation assays, however despite this, it was shown that the YA site single add-back interferes with the transforming potential and is putatively a negative regulatory site, and sites YB through YE independently drive transformation monitored by colony formation in soft agar

(Dankort *et al.*, 1997). The transforming potential of YB, YD and YE single add-backs is susceptible to the Ras inhibitor Rap-1A, whereas the YC single add-back mutant transforming potential is resistant. This is due to the binding of Crk to phosphorylated YC, which recruits the C3G exchange factor that in turn can activate Erk kinases in a Ras-independent fashion, hence making the receptor signaling Ras-independent (Dankort *et al.*, 2001b).

Through its five phosphorylation sites the ErbB2 receptor links to a plethora of signaling pathways including PLC $\gamma$ , PI3K and MAPK. Indeed, the MAPK pathway effectors Grb2 and Shc have both been shown to bind to various autophosphorylation sites of ErbB2. Moreover, recently a novel factor, which binds to the pTyrD site of ErbB2 and was given the name Memo for Mediator of ErbB2-driven cell motility, was identified. Both Memo and PLC $\gamma$ , which also binds to pTyrC, have been shown to play a role in ErbB2-dependent cell migration (Marone *et al.*, 2004; Meira *et al.*, 2009).

Furthermore, it was demonstrated that the individual ErbB2 phosphorylation sites play distinct roles in tumorigenesis *in vivo*: Transgenic mice overexpressing the constitutively active Neu receptor carrying only a single phosphorylation site in the mammary gland develop metastatic mammary tumors when carrying the YB, YC, YD and YE sites, respectively. Out of these the YC-, YD-, and YE-derived tumors show similar pathologic and transcriptional features and both the YC and YE tumors activate the MAPK and the PI3K pathway. Furthermore, it was observed that YE-derived tumors show a decreased expression of MMPs (Schade *et al.*, 2007). In contrast to that, both Neu-YB and-YD overexpressing lines developed lung metastases, however, the YB lines at a significantly higher rate.

In summary, numerous studies have shown that the ErbB2 receptor is a key signaling molecule in both the development as well as the spread of breast cancer. ErbB2 amplification and/or overexpression have clearly become prognostic factors for this type of cancer. However, there are still pieces missing in understanding the full picture of ErbB2 in pathogenesis. A key question remains the downstream signaling of the receptor in cancer, neither have all ErbB2 adaptor proteins been characterized, nor was their spatial and temporal binding and its effect on signaling determined, yet.

Therefore, we set out to identify known or novel binding partners of ErbB2, especially of the phosphorylated YE site, and link them to a cancer phenotype. In the course of our studies we identified human Copine III as a binding partner of pTyr1248 of ErbB2. These findings and the experiments leading to them will be explained in the results part. However, prior to this, the Copines, a family of Ca<sup>2+</sup>-dependent phospholipid binding proteins, will be introduced.



## 1.6 Copines – a conserved family of Ca<sup>2+</sup>-dependent, phospholipid binding proteins

### 1.6.1 General aspects, discovery, homology and conservation

In search for Ca<sup>2+</sup>-dependent, phospholipid-binding proteins that might be involved in membrane trafficking in the ciliate protozoa *Dictyostelium discoideum* the group of Carl Creutz discovered a novel protein, which they named Copine. Its name arises from its property to bind the membrane like a friend (Copine = french noun for friend). This Paramecium protein was shown to bind phosphatidylserine (PS), but not phosphatidylcholine dependent on Ca<sup>2+</sup>, but not Mg<sup>2+</sup>. Furthermore, the group also found and cloned a human Copine homolog and showed that this human Copine also possesses the ability to bind to phospholipids (Creutz *et al.*, 1998). Thus, the authors for the first time, presented the Copines as a novel family of Ca<sup>2+</sup>-dependent, phospholipid binding proteins, which might be involved in membrane trafficking (Creutz *et al.*, 1998).

Since their first discovery multiple copine homologs have been identified and studied in various organisms such as *A. thaliana*, *D. discoideum*, *C. elegans* and *H. sapiens*. Similar to other gene families, the number of copines genes increased throughout evolution: *A. thaliana* has 3 copine genes, whereas there are 6 in *D. discoideum* and, up to now, 9 have been identified in *H. sapiens*. No copine gene has been found in yeast. The Copines show a high degree of sequence conservation between different species: Copine I shares 40, 40 and 33% sequence identity with copines from *C.elegans*, *A. thaliana* and *P. tetraurelia*, respectively. The widespread distribution of copines throughout different kingdoms as well as their high degree of conservation implies that copines may play an important role in eukaryotic biology (Tomsig and Creutz, 2002).

### 1.6.2 Domain architecture

All copines share the same domain architecture: they contain two N-terminal C2 domains (C2A and C2B) followed by an von Willebrand A or A domain towards the C-terminus.

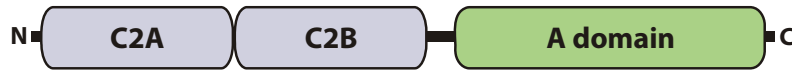
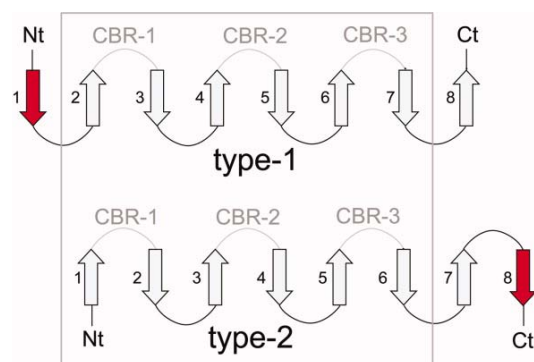


**Figure 1-9 Domain architecture of Copine family members**

All Copine family members share the same domain architecture: Two C2-domains, named C2A and C2B followed by a von Willebrand A-like or A domain towards the C-terminus.

#### C2 domains

C2 domains are  $\text{Ca}^{2+}$ -dependent, phospholipid binding domains found in a growing number of membrane binding proteins involved in various cellular signaling pathways such as membrane trafficking, generation of lipid messengers, activation of GTPases and protein phosphorylation. C2 domains are characterized by adopting an eight-stranded antiparallel  $\beta$ -sandwich and are classified into two distinct topologies, which differ slightly in structural position and connectivity of the  $\beta$ -strands: the first strand of topology I occupies the same structural position as the eighth  $\beta$ -strand of topology II (Figure 1-10) (Nalefski and Falke, 1996). Proteins, which contain only one C2 domain, such as protein kinase C (PKC), or phospholipase C (PLC), usually fall into the type II topology and proteins carrying two C2 domain, like synaptotagmin or rabphilin, into the type I topology.



(Jimenez and Davletov, 2007)

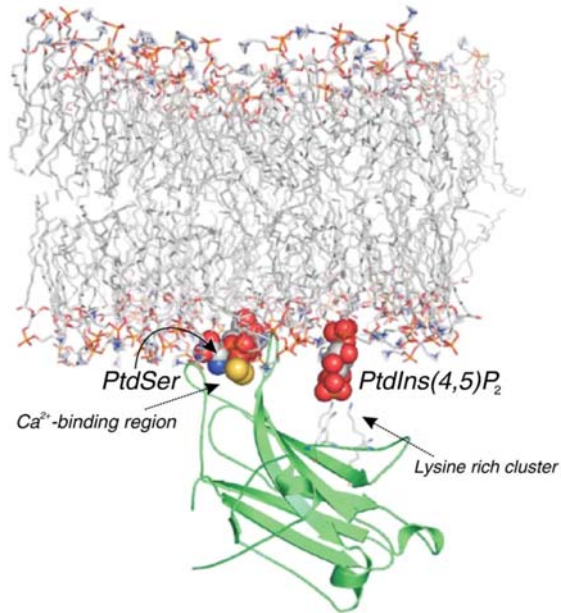
### Figure 1-10 Two structurally different topologies of C2 domains

Schematic representation of the  $\beta$  sandwich structure encompassing eight  $\beta$  strands that are aligned in two C2 domain topologies, type I and type II. Strand 1 of topology I corresponds to strand 8 in topology II (both highlighted in red). Both of these strands are structurally equivalent but permuted in the linear sequence. The Calcium binding loop or regions (CBRs) are also shown and lie within the conserved six-stranded core (boxed).

C2 domains bind  $\text{Ca}^{2+}$  through conserved aspartate residues in the loops connecting the  $\beta$ -strands. However, these  $\text{Ca}^{2+}$ -binding sites are not conserved in all C2 domains and hence not all C2 domains are  $\text{Ca}^{2+}$ -dependent. In the family of protein kinase C the diversity of  $\text{Ca}^{2+}$ -dependency of C2 domains is illustrated: the family is divided into different subgroups: conventional, novel and atypical PKCs: conventional or classical PKCs (PKC $\alpha$ ,  $\beta$ I,  $\beta$ II,  $\gamma$ ) carry a C2 domain that is  $\text{Ca}^{2+}$ - and diacylglycerol (DAG)-dependent for protein activity, whereas the C2 domain of novel PKCs (PKC $\delta$ ,  $\epsilon$ ,  $\theta$ ) is  $\text{Ca}^{2+}$ -independent and only activated by DAG. For completeness it has to be mentioned that the family contains a third group, the atypical PKCs (PKC $\zeta$ ,  $\lambda$ /I) that do not contain a C2 domain (Kheifets and Mochly-Rosen, 2007).

Lipid selectivity is variable among the family of C2 domain containing proteins, yet, most C2 domains bind phosphatidylserine (PS) with high affinity (Cho and Stahelin, 2006). Although not all C2 domains are  $\text{Ca}^{2+}$ -dependent, for those which do bind  $\text{Ca}^{2+}$  a temporal specificity of membrane binding is achieved by transient increases of intracellular  $\text{Ca}^{2+}$ . The membrane binding region of these C2 domains is often acidic in the absence of  $\text{Ca}^{2+}$ .  $\text{Ca}^{2+}$ -binding confers positive charges to this region thereby changing its electrostatic potential, making it able to bind negatively charged lipids. Additionally, the bound  $\text{Ca}^{2+}$ -ions, usually two to three per binding region, form a "bridge" between the C2 domain and PS (Lemmon, 2008). Some C2 domains can simultaneously engage multiple membrane components with both their  $\text{Ca}^{2+}$ -binding loops and the cationic  $\beta$ -groove (Cho and Stahelin, 2006). This has been modeled for the C2 domain of PKC $\alpha$ , which binds PS in a  $\text{Ca}^{2+}$ -dependent manner and simultaneously binds

phosphatidylinositol4,5diphosphate (PtdIns(4,5)P<sub>2</sub>) through a Lysine-rich cluster located on the β3 and β4 strands (Figure 1-11) (Guerrero-Valero *et al.*, 2007).



(Guerrero-Valero *et al.*, 2007)

**Figure 1-11 Model of the membrane docked C2 domain of PKCα**

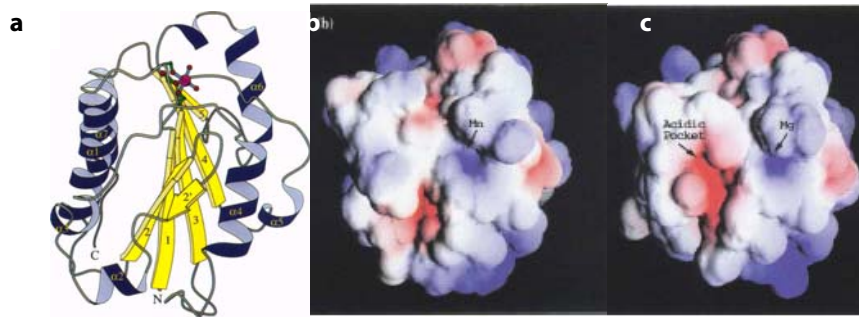
Structural representation of the PKCα C2 domain modeled to a membrane. The membrane is represented as a stick model with carbon in grey, nitrogen in blue and oxygen in red. The overall structure of the C2 domain of PKCα is represented as a cartoon model in green (PDB 1DSY). The four Lys residues located in the Lysine-rich cluster are represented by a stick model with carbon in grey and nitrogen in blue. The headgroup of the two interacting phospholipids, phosphatidylserine (PtdSer) and PtdIns(4,5)P<sub>2</sub> are represented as spheres, Calcium ions as yellow spheres. The C2 domain that binds one PS molecule through its Ca<sup>2+</sup>-binding region and one PtdIns(4,5)P<sub>2</sub> molecule through its Lysine-rich cluster.

Von Willebrand A-like or A domain

The analysis of *P. tetraurelia* Copine1 showed that this copine carried a domain related to the von Willebrand A (VWA) or the Integrin A/I domain. Later on, this domain was found to be conserved in all copine family members. VWA domains are most widely distributed phylogenetically: they can be found in all sequenced eukaryotic genomes (Whittaker and Hynes, 2002). The VWA domain is present in many cell adhesion or extracellular matrix proteins, such as collagens and is most often found in integrins. Most proteins carry the VWA domain extracellularly. Only recently a group of intracellular VWA domain-containing proteins was discovered. Interestingly, these intracellular VWA domain-carrying proteins can be found in all eukaryotes, in contrast to extracellular VWA domains, which are only found in metazoa.

Intracellular VWA domains are involved in fundamental cellular processes such as DNA repair and transcription and include the Rpn10-26S proteasome regulatory subunit (*C. elegans*), the TFIIHp44 multi protein complex transcription factor (*A. thaliana*), the Ku70/80 DNA helicase family (*H. sapiens*), the family of ATPases associated with diverse cellular activities (*D. melanogaster*), Sec-23 (*S. cerevisiae*), the uncharacterized protein Q9VPY0 (*H. sapiens*) and Copines. This, as well as the fact that VWA domains are absent from bacterial genomes, suggests that intracellular VWA domains are the most ancient VWA domains (Whittaker and Hynes, 2002).

The first structure of a VWA domain was solved in 1995 (the A domain of  $\alpha\text{M}\beta\text{2}$  integrin (CD11b/CD18, CR3)) (Lee *et al.*, 1995b). The domain adopts a classic alpha/beta Rossmann fold, a hydrophobic core of  $\beta$ -sheets surrounded by seven  $\alpha$  helices, and contains an unusual metal ion coordination site at its surface (Figure 1-12). It has been suggested that this site represents a general metal ion-dependent adhesion site (MIDAS) for binding protein ligands (Lee *et al.*, 1995b). The integrin VWA domain plays a major role in ligand binding and undergoes conformational changes in response to receptor activation (Lee *et al.*, 1995a). Furthermore, it was proposed from structural analyses of integrin VWA domains bound to different metal ions, that binding of  $\text{Mn}^{2+}$  to the VWA domain MIDAS motif renders the protein inactive ("unliganded"), whereas  $\text{Mg}^{2+}$  binding represents the active conformation ("liganded") (Figure 1-12) (Lee *et al.*, 1995a). It was suggested that this influences the ligand binding properties of integrins: the  $\text{Mn}^{2+}$ -bound state is more stable without a ligand, whereas the  $\text{Mg}^{2+}$ -bound form has a high affinity for ligand binding. These findings confirmed the common feature seen in VWA domains, which seem to be ligand/protein binding and involvement in multi-protein complexes.



(adapted from Lee *et al.*, 1995a; Qu and Leahy, 1995)

**Figure 1-12 Structure of an integrin A domain**

a) the integrin CD11a A domain adopts a Rossmann fold with a hydrophobic core of  $\beta$ -sheets encompassed by  $\alpha$ -helices and contains a metal affinity metal ion-dependent adhesion site (MIDAS) here shown with a bound  $Mg^{2+}$  ion.

b) and c) Solvent accessible surface of the  $Mn^{2+}$  and the  $Mg^{2+}$  bound A domain. Negatively charged regions are shown in red, positive in blue.  $Mg^{2+}$ -binding allows acidic residues to be exposed to the surface, which increase the hydrophobicity and thus ligand binding.

The A domain of human Copine I shows a distant relationship to the VWA domain with the highest homology in the C-terminal 2/3 of the domain (Creutz *et al.*, 1998). The MIDAS motif and especially the residues involved in  $Mg^{2+}$  and  $Mn^{2+}$  binding are conserved and it was shown that human Copine I binds both  $Mg^{2+}$  and  $Mn^{2+}$  (Tomsig and Creutz, 2000). Evidence from yeast-two hybrid (YTH) screens supports the idea that also Copine A domains are involved in protein-protein binding: The purified A domains of human Copine I, II and IV bind various substrates such as protein phosphatase 5, myc binding protein, apoptosis linker-gene 2 or  $\beta$ -actin (Tomsig *et al.*, 2003). For the majority of these proteins the copines bound to regions predicted to form a coiled-coil and a consensus sequence was determined as a predictor for novel copine targets (Tomsig *et al.*, 2003). The potential binders identified are involved in many divergent cellular processes such as protein phosphorylation, transcription, or ubiquitination. Furthermore, it was shown that Copines and their associated proteins can be recruited to immobilized lipids *in vitro* in a  $Ca^{2+}$ -dependent manner. These findings led to the hypothesis that a function of Copines is to recruit target proteins to the plasma membrane or intracellular membrane that contain acidic lipids. However, due to the divergence of copine-associated proteins identified, the biological function of each Copine, although highly homologous, appears to be very specific.

## 1.7 Biological roles of Copine family members

Since the discovery of the copine proteins in 1998 the question about their biological function has remained intriguing. The widespread distribution of copine family members, as well as their high degree of conservation suggests that copines might have an important biological function. The presence of C2 domains and the A domain led to the hypothesis that the function of copines involves  $\text{Ca}^{2+}$ -dependent phospholipid binding and protein-protein interactions. Copine family members have been studied to different degrees in various organisms and in particular the work in *A. thaliana*, *C. elegans* and *D. discoideum* has yielded valuable insights. Biochemically, human Copine I is by far the most extensively studied protein of the family and recently the function of human copines has also been addressed. These results on biological roles of copine are summarized in the following section.

### 1.7.1 Copine in *Arabidopsis thaliana*

In *A. thaliana* mutants of the two copine genes BON1 and CPN1 were analyzed (Hua *et al.*, 2001; Jambunathan *et al.*, 2001). These genes were analyzed in different studies and were found to exhibit different phenotypes, however, they are both orthologues of human Copine III and therefore, in fact, the same gene.

Plants are anchored organisms and therefore need to regulate homeostasis in response to environmental factors. Usually *Arabidopsis* sustain a relatively constant size at a variety of temperatures. Deletion of the BONZAI1 (BON1) gene gives rise to miniature plants at 22°C, whereas the growth is normal at 28°C (Hua *et al.*, 2001). Additionally, it was shown that the expression of BON1 RNA is high in young, growing plants and downregulated with increasing temperature, thus BON1 might have a direct role in regulating cell expansion and cell division at lower temperatures. One known mechanism in plants for the adaptation to temperature changes is adjusting their membrane composition, in particular their lipid content, in order to remain fluid even at low temperatures. Yet, BON1 null mutants do not show a significant difference in overall lipid composition to wild type plants. Furthermore, purified BON1 protein was shown to possess  $\text{Ca}^{2+}$ -dependent activity and to be associated with PS *in vitro*. From these observations the authors conclude that BON1 is important in plant homeostasis possibly by either catalyzing membrane fusion or preserving membrane function at low temperatures (Hua *et al.*, 2001).

CPN1 mutants were shown to have multiple phenotypes in response to humidity changes. They show an aberrant regulation of cell death as well as morphological abnormalities.

Furthermore, these mutants have an increased susceptibility to infection by *Pseudomonas syringae* and *Peronospora parasitica* by repression of a disease resistance gene (R gene). BON1 or CPN1 RNA levels are increased under low humidity conditions and the expression is decreased with increasing humidity. Therefore, CPN1 might be a regulator of plant responses to humidity and the effects on disease resistance are indirect or CPN1 might be a direct regulator of *Arabidopsis* defense responses (Jambunathan *et al.*, 2001).

Following these studies, more copine family members were discovered in *Arabidopsis* (BON1-3). BON1 and BON2 share 82% sequence identity and 91% similarity, whereas BON3 is more distantly related and shares 62% identity and 75% similarity with BON1. The Ca<sup>2+</sup>-binding aspartates are conserved in both C2 domains of all three proteins. Single loss-of-function mutants of BON2 and BON3 display a wild-type (wt) phenotype, in contrast to the BON1 mutant that, when analyzed in the same experiment, showed again a growth phenotype. However, BON3, but not BON2 was found to rescue the BON1 growth phenotype. Furthermore, BON2/BON3 double mutants do not show any phenotype, whereas the other double mutants (BON1/BON2 and BON1/BON3) show an even more severe phenotype than BON1 single mutants and are seedling-lethal at 22°C. Triple mutants show a severe seedling-lethal phenotype at 22°C and 28°C.

These studies show that the *Arabidopsis* copine family members have both distinct and overlapping functions and BON1 seems to play a dominant role among the three proteins, exhibiting growth defects and precocious cell death under low temperature or low humidity conditions (Yang *et al.*, 2006).

### 1.7.2 Copines in *Caenorhabditis elegans*

Several putative members of the copine family have been identified in the nematode *Caenorhabditis elegans*. Most of these genes were classed as copine family members based on their homology to human copines (cpna1 to cpna5). However, only the function of two family members has been studied in some detail: GEM-4 and T28F3.1.

The gonad of *C. elegans* is derived from four postembryonic blast cells that initiate divisions several hours after the larva hatches from the egg. These divisions require the activity of GON-2, a predicted cation channel that is likely to mediate Ca<sup>2+</sup> and Mg<sup>2+</sup> influx. *Gem-4* encodes a Ca<sup>2+</sup>-dependent PS binding protein that is highly similar to three human proteins, copine I, copine III, and KIAA1599 (40% identity over 590 residues). *Gem-4* (*gon-2* extragenic modifier) mutation results in suppression of loss-of-function alleles of *gon-2*. *Gem-4* antagonizes *gon-2* in gonadal development. Both *gem-4* mutants as well as *gem-4*(RNAi) efficiently suppress the



*gon-2* phenotype. It is speculated that this is mediated by a direct interaction of the two proteins, since both proteins are predicted to localize to the plasma membrane. Another possibility is that the two proteins act in parallel functioning pathways.

The expression of GFP-GEM-4 is brightest at the plasma membrane and in some cases a punctuate staining is detectable in the cytoplasm, which could be due to an association of GEM-4 with vesicular structures. Yet, the localization of GEM-4 to the plasma membrane is not dependent on *gon-2* function, which could implicate that GEM-4 localization to the membrane is not Ca<sup>2+</sup>- dependent. In a wild-type background *gem-4* mutants do not show an apparent phenotype (Church and Lambie, 2003).

T28F3.1 also encodes a putative calcium-dependent phospholipid binding protein of the copine family, sharing a high degree of homology with human Copine V. It was identified in a screen for proteins associated with the levamisole sensitive nicotinic acetylcholin receptor (nAChR). nAChRs are pentameric, ligand-gated ion channels of which the levamisole-sensitive receptor is the best studied. They mediate excitatory neurotransmission in neurons and muscles. A good read-out for the function of the levamisole nAChR is nicotine resistance in a paralysis assay, since its depletion causes nicotine resistance. T28F3.1(RNAi) and T28F3.1 mutants showed moderate resistance to nicotine as well as moderate levamisole resistance (a specific nAChR agonist). Moreover, T28F3.1 mutants showed reduced synaptic nAChR expression.

T28F3.1 is expressed in many cell types including neurons in the head and tail as well as in body muscle. Importantly, it localizes to plasma membranes and co-localizes with nAChR.

This study implies that T28F3.1 specifically affects cell surface expression of the levamisole nAChRs and could therefore be a general membrane organizer (Gottschalk *et al.*, 2005).

In another study, T28F3.1 was found to be required for sperm migration towards a polyunsaturated fatty acid (PUFA)-based signal exuded by oocytes. In search for genes encoding proteins synthesizing PUFA-derived signal, T28F3.1 was identified as one of 35 target genes. T28F3.1(RNAi) hermaphrodites are infertile, both through aberrant loss of their own sperm and through failure of males to effectively inseminate them due to defects in directional sperm motility. Thus, T28F3.1 is involved in directional cell migration by somehow influencing PUFA-derived signals from the oocytes (Kubagawa *et al.*, 2006).

### 1.7.3 Copines in *Dictyostelium discoideum*

*Dictyostelium discoideum* lives as a single-celled amoeba, is very motile and possesses phagocytic cells, processing organelles and membrane trafficking pathways similar to mammalian cells. These features make *Dictyostelium* an ideal model organism to study copine function.

The *Dictyostelium* genome contains six copine genes encoding copine proteins named CpnA to CpnF. They share between 26% (CpnA and CpnF) and 80% (CpnB and CpnE) sequence homology. All six copines are expressed throughout *D. discoideum* development showing an upregulation at one or two developmental stages. Only CpnF shows a decreasing RNA expression level throughout development (Damer *et al.*, 2005).

The best-studied copine protein in *Dictyostelium* is CpnA. The recombinant C2A domain of CpnA binds lipids in a Ca<sup>2+</sup>-dependent manner and endogenous CpnA was found to be associated with *Dictyostelium* membranes in the presence of Ca<sup>2+</sup>. Furthermore, GFP-CpnA localized to the cytoplasm of vegetative cells, but was shown to transiently translocate to the plasma membrane in an oscillating manner as a result of peaks in intracellular Ca<sup>2+</sup> concentrations. Moreover, GFP-CpnA localized to contractile vacuoles, endosomal organelles and phagosomes (Damer *et al.*, 2005).

Knock-out strains for *cpnA* (*cpnA*<sup>-</sup>) show only mild phenotypes: they exhibit a normal growth rate with few multinucleated cells, suggesting a defect in cytokinesis. Additionally, they are delayed or arrested in finger state development. When placed under starvation conditions *Dictyostelium* cells undergo cell differentiation and morphogenesis to form multicellular structures: after 14 – 16h of starvation the cells have accumulated and form a finger-like structure (finger state) and at 19 – 20h, during the final stage of development, the cells terminally differentiate into spore or stalk cell. The requirement for CpnA in fruiting body formation correlated with increased *CpnA* gene expression during development.

In line with previous findings that CpnA localized to contractile vacuoles, it was discovered that *cpnA*<sup>-</sup> cells exhibited unusually large contractile vacuoles when put into H<sub>2</sub>O. However, no effect on the growth rate of *cpnA*<sup>-</sup> cells in H<sub>2</sub>O was observed, nor swelling or bursting of *cpnA*<sup>-</sup> cells, as well as no upregulation of any of the *Cpn* genes upon osmotic pressure (Damer *et al.*, 2007).

The hypothesis for the major function of copines in *D. discoideum* is similar to that in *A. thaliana* and *C. elegans* (Gem-4): the phenotypes seen in the CpnA, such as the defective cytokinesis or the delayed or arrested finger state development mutants could originate from changes in membrane properties or defective membrane trafficking.

Interestingly, in a proteomics study performed to identify proteins involved in mouse embryo development, Copine I was identified as being upregulated during embryonic day E8.5 – 10.5. During this time, major developmental events occur, including axonal rotation, formation of differentiated somites, extensive remodeling of the heart with onset of regular contractions and formation of the neural tube. Thus, this is the first indication that a copine family member plays a role in mouse development (Greene *et al.*, 2002).

The temporal expression of Copine family members as well as studies in *Dictyostelium* (CpnA) and mouse (Copine I) imply that they play a role during development.

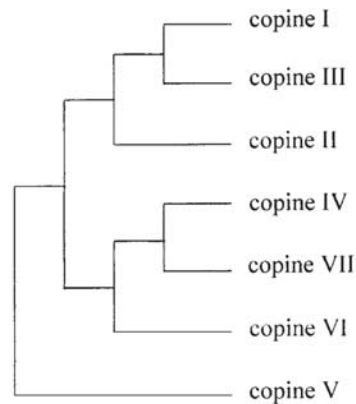
In summary, the studies of copine family members in *Arabidopsis*, *C. elegans* and *Dictyostelium* show that they have distinct roles. The observed mutant phenotypes could be classified as rather “mild”, occurring only under special environmental conditions (temperature or humidity in *Arabidopsis* or osmotic pressure in *Dictyostelium*). In most of the cases it was speculated that the role of copines lies in signal transduction from the membrane, membrane trafficking or that copines are general membrane organizers.

This is underscored by the fact that they all are Ca<sup>2+</sup>-dependent (when tested) membrane binding proteins.

## 1.8 Human Copines

Nine genes belonging to the copine family have been identified in *H. sapiens*. Human copines are a relatively novel family of proteins, with the first discovery of copine I in 1998 (Creutz *et al.*, 1998). Much of what we now know about human copines emerged from *in vitro* studies, but increasingly *in vivo* functions are being assigned to members of the human copine family.

Human copines are highly homologous: copine I shares 60, 78, 53 and 56 % homology to copines II to V, respectively (Figure 1-13). Copines I, II and III are expressed ubiquitously, the others being tissue specific. Copine IV is only expressed in the brain, heart and prostate, whereas the expression of Copine VI is restricted to the brain and it is therefore also referred to as N-copine (neuronal-copine).



(Tomsig and Creutz, 2002)

**Figure 1-13 Dendrogram showing the relationship of seven human Copines**

Multiple sequence alignment of seven human copine proteins. Copine I and Copine III share the highest sequence homology (78%), whereas Copine I shared 60%, 53 and 58% sequence homology with Copines II, IV and V.

### 1.8.1 Phenotypes, biological roles

Copine VI or N-Copine has been studied to some extent. It was shown that N-Copine expression is truly restricted to the brain and that it is expressed throughout development with a drastic increase of expression after birth. Further studies demonstrated that N-Copine mRNA is expressed exclusively in neurons of the hippocampus and in the main and accessory olfactory bulb. These are brain areas, where various forms of synaptic plasticity and memory formation occur. There N-Copine is found mainly in the cell bodies and dendrites in the neurons.

Moreover, N-Copine was shown to exhibit  $\text{Ca}^{2+}$ -dependent phospholipid binding similar to other family members. Thus, the function of N-Copine, although not known yet, seems to differ from other neuronal proteins carrying two C2 domains and might be to act as a  $\text{Ca}^{2+}$  sensor in a postsynaptic event (Nakayama *et al.*, 1999a; Nakayama *et al.*, 1999b; Nakayama *et al.*, 1998).

The best studied among the human copines is Copine I. The group of Carl Creutz, who was the first to identify copines, published several articles focusing on the biochemistry of copine I. Already in their early studies they showed that copine I binds PS in a  $\text{Ca}^{2+}$ -dependent, but  $\text{Mg}^{2+}$ -independent manner (Creutz *et al.*, 1998). They also showed that  $\text{Ca}^{2+}$  changes the aggregation state of Copine I. Addition of  $\text{Ca}^{2+}$  to purified monomeric copine induces copine aggregation into multimers as observed by measuring dynamic light scattering. According to

these measurements aggregates of 17 copine molecules can exist in the presence of  $\text{Ca}^{2+}$ . Moreover, the aggregation was reversible by the addition of EDTA.

Copine I binds to PS containing lipid vesicles as well as to those containing phosphoinositides (PI), phosphoglycerides (PG) and phosphatidic acid (PA). Copine binding to PA is  $\text{Ca}^{2+}$ -independent, and its affinity for PI is less than for the other phospholipids.

Furthermore, the biochemical analysis of copine 1 also showed that it can bind both  $\text{Mn}^{2+}$  and  $\text{Mg}^{2+}$  suggesting that the conserved MIDAS motif within the A domain is functional (Tomsig and Creutz, 2000).

These biochemical studies confirmed that human copines exhibited the same features (e.g.  $\text{Ca}^{2+}$ -dependent phospholipid binding) as other copines family members. Yet, the question about a function of human copines still remained unanswered. Therefore putative binding partners of purified recombinant A domains of human Copines I, II and IV were used as baits in a yeast-two-hybrid assay with the aim to find the function or functional pathways copines are involved in. It was found that copine A domains can bind a variety of proteins involved in different cellular processes such as protein phosphorylation (MEK1), transcriptional regulation (Myc binding proteins) or regulators of ubiquitination (E2-230K). A common structural feature was a sequence predicted to fold into a coiled-coil domain: E... R..R.L.E..EQ.RK.LELR..KQR... EL.QLD.E.E. This has been designated as the Copine-binding motif. Furthermore, it was demonstrated that full length copines can recruit their binding partner to immobilized lipids in a  $\text{Ca}^{2+}$ -dependent manner. Importantly, the purified A domain alone is not enough to recruit proteins to lipid bilayers.

This was the first evidence that Copines might have a transporter function, between the cytoplasm and the plasma membrane and so regulate signaling processes at the membrane (Tomsig and Creutz, 2000; Tomsig *et al.*, 2003).

Since two of the identified binding partners of Copine I were proteins regulating NF $\kappa$ B activity and Copine I was shown to possess a cis- $\kappa$ B-binding element in the promoter region (Tomsig *et al.*, 2003), two follow-up studies analyzed the effect of Copine I on NF $\kappa$ B. In the first study the purified A domain of Copine I was used as a dominant negative construct based on the assumption that it binds to putative target proteins. Using this construct it was shown that Copine I regulates TNF $\alpha$ -induced NF $\kappa$ B activation. Moreover,  $\text{Ca}^{2+}$  acts in synergy with TNF $\alpha$  and the effect of  $\text{Ca}^{2+}$  on NF $\kappa$ B activation was also blocked by the Copine A domain. Furthermore, a feedback loop was found between TNF $\alpha$  and Copine I, where stimulation with TNF $\alpha$  increases Copine I expression levels significantly (Tomsig *et al.*, 2004).

These findings were revised in a later publication on Copine I and its role in the NF $\kappa$ B pathway: it was illustrated that copine I represses NF $\kappa$ B-mediated transcription by recruiting a mediator,

which endoproteolytically cleaves the p65 subunit. The authors claimed that the different results to their previous study, which showed that Copine I activated NFκB, was due to the fact, that in this first study, a GFP-tagged Copine was used, that was excluded from the nucleus. Since the phenotype that is reported in the later publication occurs mainly in the nucleus this would explain why the results seem contradictory.

In the later study it was shown that Copine I represses NFκB activation at a common point in the cytokine pathway, since the cells could be stimulated with different cytokines and the result on NFκB activity was the same. In the inverse experiment, the KD of Copine I increased NFκB activity. The authors could show that Copine I binds to the N-terminus of p65 and initiates the endoproteolytic cleavage of p65. Moreover, Copine I was found to cleave other Rel family members such as p50, p52, RelB and cRel.

Copine I cleaves p65 at its DNA binding domain and in that way inhibits p65 binding to DNA and therefore represses NFκB activity. It is important to note that the authors specifically stated that Copine I has not been shown to possess endoproteolytic activity itself, but rather recruits another protein with enzymatic activity. Even more convincing for this hypothesis is the fact that immunopurified Copine I was not able to stimulate proteolysis of p65. (Ramsey *et al.*, 2008)

Another family member that has been studied to some extent is Copine III. In primary rat hippocampal cultures loss of Copine III reduces dendritic protrusions and causes a collapse of the dendritic tree during synapse formation. Furthermore, Copine III was shown to interact with Copine VI and the actin-modulating small-GTPases Rac1 and Pak1 *in vitro* (M. Galic, Inauguraldissertation 2006; Biozentrum Basel).

In another study, it has been claimed that Copine III is a phosphoprotein that possesses kinase activity. This evidence is based on studies in which partially purified Copine III was used. It phosphorylated myelin basic protein *in vitro* and in an in-gel kinase assay a band with the size of Copine III was detected. Copine III carries no known kinase motif and it is therefore very plausible that this kinase activity resulted from a co-purified enzyme, rather than from Copine III itself (Caudell *et al.*, 2000). No evidence for kinase activity or ATP-binding has been found for any other Copine either (Tomsig and Creutz, 2002)

Thus, the collective biochemical results on Copine I and Copine III suggest that these proteins could function by interacting with specific enzymes, possibly through their A domains. However, the functional consequences of such associations yet remain unclear. To bridge the gap between the intriguing biological and biochemical properties of this protein family, functional studies are needed to place its members in a cellular context.

Human Copines have not been studied extensively since their discovery in 1998. There are some good biochemical studies, especially on Copine I, but apart from that the number of publications on human Copines is limited. This is probably due to the fact that no real function has been assigned to any human Copine family member so far. Two publications argue for a function for Copine I and Copine III, yet, as illustrated above, the evidence that these are indeed the functions of Copines and not rather those of associated proteins is weak. In summary, in addition to the biochemical data available for human Copines, functional data needs to be obtained to place this interesting family of proteins into a cellular context.





## 2 RESEARCH OBJECTIVE

It is a matter of fact that the ErbB2 receptor plays a pivotal role in the initiation and progression of breast cancer. Up to 30% of all breast cancers show an ErbB2 overexpression, a property correlated with poor prognosis for these patients. Therefore, it is of uttermost importance to study signaling pathways initiated by ErbB2 in more detail.

Recently, Memo (Mediator of ErbB2-mediated cell motility) was identified as a novel ErbB2 interacting protein and was shown to be important for ErbB2-mediated cell motility, a trait important in cancer metastasis. This illustrates that there are still “blind spots” in our knowledge of the ErbB2 signaling cascade. Therefore, a better understanding of these pathway could provide more specific targets for the treatment of cancer.

In line with these previous findings we set out:

- (I) To identify novel interacting proteins of the phosphorylated Tyr1248 (YE) site of the ErbB2 receptor

We addressed this question using a combination of SILAC (stable isotope labeling of amino acids in cell culture), a peptide affinity pull-down and quantitative mass spectrometry.

- (II) To place the ErbB2-binding protein into the signaling pathways downstream of the receptor and find an associated cancer phenotype

This aim was addressed using RNAi in culture cells, which were subjected to assays determining cancerous traits such as proliferation, anchorage-independent growth or migration.



## 3 IDENTIFICATION OF COPINE III AS A BINDING PARTNER OF ERBB2

### 3.1 Introduction

Members of the ErbB family of receptors are expressed in multiple tissues and play a crucial role in initiating diverse signaling cascades. Out of these receptors, ErbB plays a pivotal role, since it is the preferred heterodimerization partner of the other receptors. Signal transduction through ErbB2 is mediated by tyrosine phosphorylation on specific residues in the C-terminal regulatory region of the receptor, which leads to the binding of specific adapter proteins and the initiation of signaling cascades. As mentioned before, the five major pTyr sites of ErbB2 receptor have been mapped and several interacting proteins to each site have been identified since. In the area of high throughput genomics and proteomics studies have aimed at identifying a whole “interactome” of putative binding partners of the ErbB family of receptors (Jones *et al.*, 2006; Schulze *et al.*, 2005). These studies have, without doubt, elucidated the variety of signaling molecules able to bind to the receptors and they have greatly deepened our understanding of ErbB signaling. However, although these studies aimed at identifying protein-protein interactions at the resolution of a single tyrosine phosphorylation site, the question about the temporal and spatial binding of each adaptor protein to the receptor and hence its impact on downstream signaling remains unanswered. Therefore, the aim of our study was to use state-of-the-art quantitative mass spectrometry at the resolution of a single modification to identify binding partners of a single pTyr site of ErbB2 and, furthermore, to place this identified protein within a pathway and thus a function downstream of ErbB2. For our analysis we chose pTyr1248, because, although some binding partners to this site have already been identified (Dankort *et al.*, 2001a; Jones *et al.*, 2006; Schulze *et al.*, 2005), a link between a specific binder and a signaling effect downstream of ErbB2 has not been shown yet. In order to identify interaction partners of specific pTyr residues of the ErbB2 receptor we used a combination of SILAC (stable isotope labeling by amino acids in cell culture) (Ong *et al.*, 2003) together with a peptide affinity pull-down purification (Schulze *et al.*, 2005), followed by quantitative mass spectrometry. It has been shown previously in the lab that the use of synthetic peptides mimicking the C-terminal region of ErbB2, including a specific pTyr residue, can be used as baits to identify binding proteins of the receptor *in vitro* (Marone *et al.*, 2004). Furthermore, at the time of our experiments, the use of quantitative mass spectrometry emerged as a major topic in proteomic studies, allowing for a robust and highly sensitive determination of binding partners.

#### *Quantitative mass spectrometry*

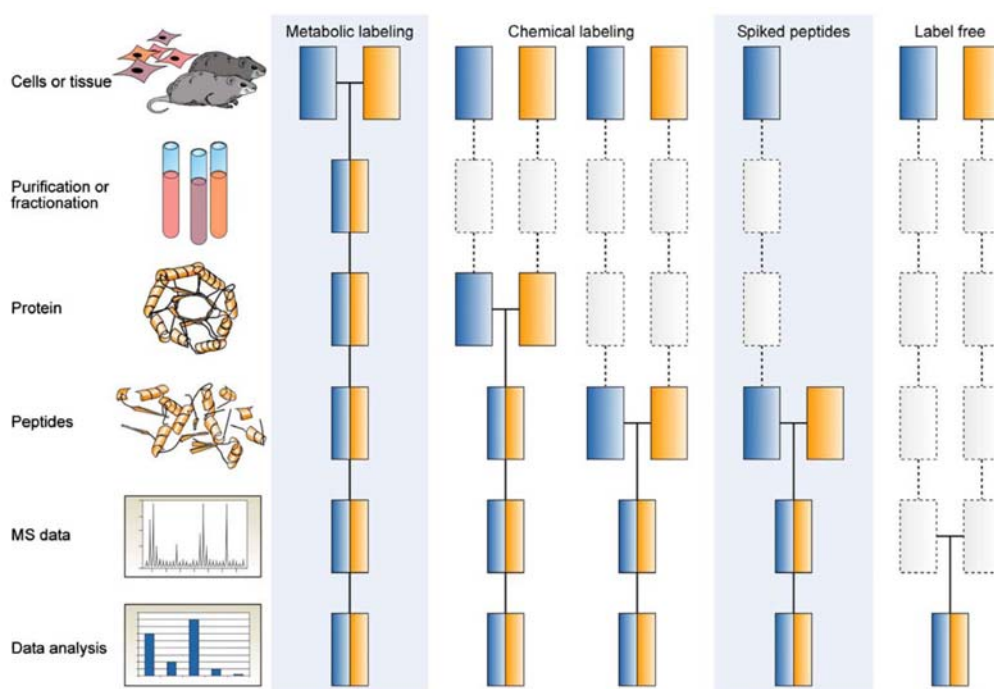
Quantitative mass spectrometry has emerged as a highly accurate, sensitive and reliable technique to measure relative and absolute amounts of given proteins within a complex mixture. Several techniques for quantitation by mass spectrometry have been established: Most of these techniques employ differential stable isotope labeling to create a specific mass tag, which can be recognized by the mass spectrometer. Special mass tags can be introduced into proteins or peptides metabolically, by chemical means, enzymatically or provided by spiking with synthetic peptide standards (Bantscheff *et al.*, 2007) (Figure 3-1). Stable isotope labeling was introduced as a tool in protein analysis by MS in 1999 by three independent groups (Gygi *et al.*, 1999; Oda *et al.*, 1999; Pasa-Tolic, 1999) and has since then been widely accepted, modified and advanced in the field. The earliest possible point for introducing a stable isotope tag into proteins is by metabolically labeling proteins during cell growth and division. Metabolic labeling has been performed in cell culture, which is used widely in the field, and in whole animals (Wu *et al.*, 2004), a method that has been shown to work, but still remains difficult and is far from being standardized. Metabolic labeling in the form of SILAC was introduced in 2002 (Ong *et al.*, 2002). In the most common implementation of this method the medium used for culturing cells contains  $^{13}\text{C}_6$ -Arginine and  $^{13}\text{C}_6$ -Lysine ensuring that all tryptic peptides carry at least one labeled amino acid resulting in a constant mass increment over their non-labeled counterpart (Bantscheff *et al.*, 2007). First the peptides and proteins are identified followed by a relative quantification by comparing the intensities of isotope clusters of the intact peptide in the survey spectrum.

Another way of labeling, which happens later on in the experiment, is done by post-biosynthetic labeling of proteins and peptides either by chemical or enzymatic derivatization *in vitro*. Enzymatic labeling can be performed either during proteolytic digestion or as a second independent enzymatic step afterwards. In principal, every reactive amino acid side chain can be used to chemically incorporate isotope-coded mass tags, however, in practice, mostly Lysine and cysteine side chains are used for this purpose (Bantscheff *et al.*, 2007). One specific application of this category uses the isotope-coded affinity tag (ICAT) reagents (Gygi *et al.*, 1999), where cysteine residues are specifically derivatized with a reagent that not only introduces zero or eight deuterium atoms, but also a biotin group for affinity purification. Since the initial description of ICAT, several variations of this method have emerged to improve e.g. the recovery of labeled peptides (Hansen *et al.*, 2003). One drawback of ICAT is certainly the fact that this method is not suitable to quantify proteins containing few or none cysteine residues and it is of limited use to analyze post-translational modifications and splice variants.

A prominent example of another group of labeling reagents, which targets the peptide N-terminus and the epsilon amino group of lysine residues, are the isotope tags for relative and

absolute quantification (iTRAQ). The iTRAQ reagents are a set of isobaric reagents which are amine specific and allow for the identification and quantitation of up to eight different samples simultaneously. They are designed as an isobaric tag consisting of a charged reporter group, a peptide reactive group, and a neutral balance portion to maintain an overall mass of 145. Isobaric, by definition, implies that any two or more species have the same atomic mass but different atomic arrangements (Zieske, 2006). Currently, there are two mainly reagents used: 4-plex and 8-plex, which can be used to label all peptides, in theory, from different samples/treatments.

However, in contrast to metabolic labeling techniques, with both ICAT and iTRAQ the labeling occurs at a later step in the experimental protocol, meaning that samples with different treatments/conditions need to be handled in parallel for longer and thus this increases the likelihood of errors in the quantification (Figure 3-1).



(Bantscheff *et al.*, 2007)

**Figure 3-1 Common quantitative mass spectrometry workflows**

Boxes in blue and yellow represent two experimental conditions. Horizontal lines indicate when samples are combined. Dashed lines indicate points at which experimental variation and thus quantification errors can occur.

The use of isotope-labeled synthetic standards for use in absolute quantification is becoming more and more broadly applied using a technique called AQUA (absolute quantification of proteins). In a simple set-up the addition of a known quantity of a stable isotope-labeled

peptide to a protein digest and subsequent comparison of the intensity of the mass spectrometric signal to that of the endogenous peptides can yield absolute quantification of protein amounts. Since the amount of sample and spiked peptides must be similar, and most of the times the amount of peptides from each endogenous protein varies with its expression level (protein abundance) and digestibility, which may differ greatly in-between samples, "guessing" the right amount of peptide to be spiked in, is a major drawback of this method

Another technique for quantification, not involving stable isotope tags, is label-free quantification, which aims at correlating the mass spectrometric signal of intact polypeptides or the number of peptide sequencing events with the relative or absolute protein quantity directly (Bantscheff *et al.*, 2007)(Figure 3-1). Currently, there are two widely used, but fundamentally different techniques for label-free quantitation: measuring and comparing the spectrometric signal intensity of peptide precursor ions belonging to a particular protein or counting and comparing the number of fragment spectra identifying peptides of a given protein. Label-free approaches are certainly the least accurate among the mass spectrometric quantification techniques when considering the overall experimental process, because all the systematic and non-systematic variations between experiments are reflected in the obtained data (Bantscheff *et al.*, 2007).

Although each of the discussed methods has drawbacks depending on the question addressed and the accuracy required, each has its specific virtues as well. In summary, the ability of mass spectrometry to identify and, increasingly precisely quantify thousands of proteins from complex samples can be expected to impact broadly on biology and medicine (Aebersold and Mann, 2003).

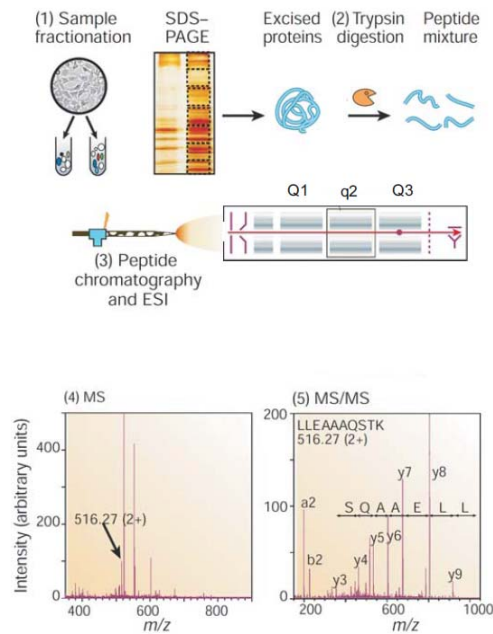
*General aspects of mass spectrometers and protein identification on the 4000QTrap*

Mass spectrometers consist of a few simple modules: an ionization mechanism; a section to separate, select and fragment peptides (analyzer); and a detector (de Hoog and Mann, 2004). In general, mass spectrometers are named or classified by the type of ionization mechanism and analyzer they contain (e.g. MALDI-TOF or ESI-Quad).

By definition, a mass spectrometer consists of an ion source, a mass analyzer that measures the mass-to-charge ratio ( $m/z$ ) of the ionized analytes, and a detector that registers the number of ions at each  $m/z$  value. Electrospray ionization (ESI) and matrix-assisted laser desorption/ionization (MALDI) are the two most commonly used techniques to volatilize and ionize proteins or peptides for mass spectrometric analysis (Aebersold and Mann, 2003). In contrast to MALDI, which ionizes samples out of a dry matrix using laser pulses, ESI ionizes the analytes out of solutions. Therefore, ESI-MS is mostly coupled to a liquid chromatography system (LC) and, due to the pre-separation step, used for the analysis of complex samples. MALDI-MS is routinely used to measure relatively simple mixtures, however, recent advantages allow also for MALDI-MS to be coupled (off-line) to a chromatography system and thus to analyze far more complex samples.

For our quantitative analysis we used nano-LC-ESI-MS/MS using a triple quadrupole mass spectrometer (4000QTrap, from Applied Biosystems).

In a triple quadrupole instrument the linear set-up of the modules is: Q1, a quadrupole, followed by q2, which can be used as either an ion trap or a collision cell and Q3, another quadrupole (Figure 3-2). In a standard experiment the samples are treated and/or prefractionated to reduce the complexity. Afterwards the proteins are separated by SDS PAGE, individual bands are cut and proteins are digested for mass spectrometry. The resulting peptide mixture is then separated in the LC system that is directly coupled to the mass spectrometer. The amino acids sequences of the individual peptides can be deduced and thus proteins in the mixture can be identified (Figure 3-2)



(Aebersold and Mann, 2003)

**Figure 3-2 Generic mass spectrometry-based proteomics experiment**

The proteins to be analyzed are isolated from cell lysate or tissues by biochemical fractionation or affinity selection (1). This often includes a final step of one-dimensional gel electrophoresis, and defines the 'sub-proteome' to be analyzed. Proteins are degraded enzymatically to peptides, usually by trypsin, leading to peptides with C-terminally protonated amino acids, providing an advantage in subsequent peptide sequencing (2). The peptides are separated by one or more steps of high-pressure liquid chromatography in very fine capillaries and eluted into an electrospray ion source where they are nebulized in small, highly charged droplets. (3) After evaporation, multiply protonated peptides enter the mass spectrometer and a mass spectrum of the peptides eluting at this time point is taken (MS; spectrum, or 'normal mass spectrum') (4). The computer generates a prioritized list of these peptides for fragmentation and a series of tandem mass spectrometric or 'MS/MS' experiments ensues (5).

In our set-up proteins were metabolically labeled with Lysine and Arginine residues containing stable isotopes (SILAC) leading to mass shift of 6 and 10Da, respectively, between the labeled amino acids and their non-labeled counterparts. By definition these peptides behave similarly in LC-MS and are therefore eluted and analyzed at the same time.

Tandem mass spectrometry was used (MS/MS) and the peptides were analyzed in the following way: first an overall elution chromatogram of all peptides eluting from the LC system was monitored (total ion chromatogram - TIC). At any timepoint the *m/z* value of the eluted ions is monitored. This yields a low resolution survey scan. The ion with the most intense *m/z* ratio in this spectrum is further analyzed. First a survey scan is performed, from which the ionization state of the ion can be deduced (MS1). Next, the selected ion is further fragmented in q2 and all resulting fragments are analyzed in Q3 and measured by the detector (MS/MS). This enhanced



product ion (EPI) scan is used in a database search. In principal the EPI spectrum is searched against a database (Mascot database) of known spectra and thus the peptide sequence is elucidated. Furthermore, peptides identified from the same protein are grouped and thus proteins are identified (Figure 3-3).

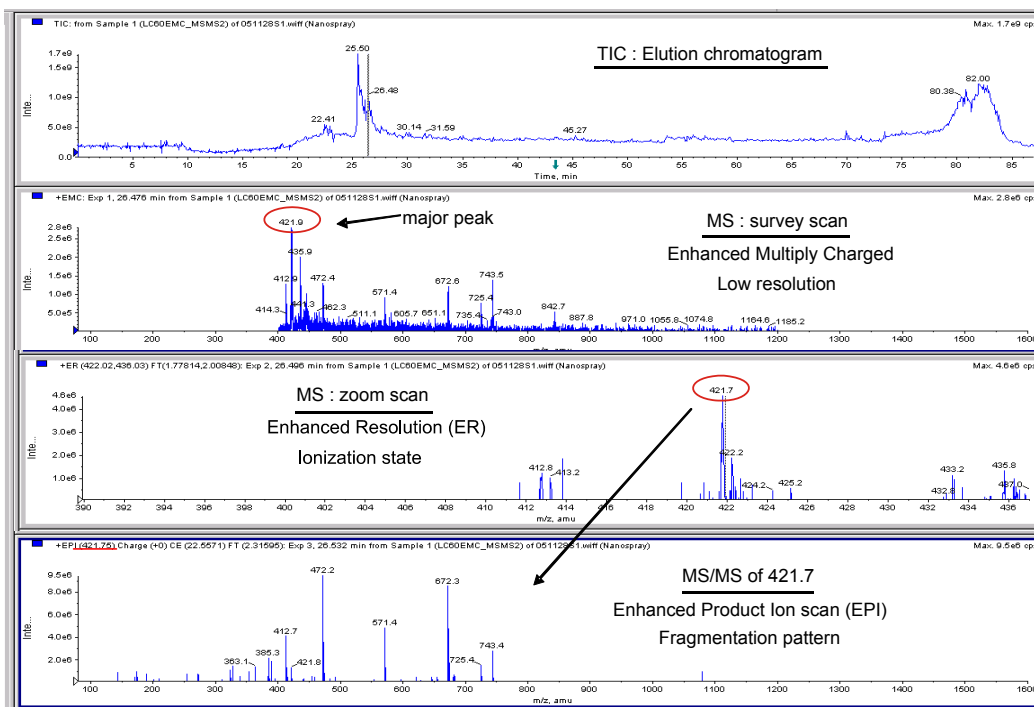


**Figure 3-3 Peptide and Protein identification on the 4000QTrap**

All eluted peptides are ionized in the source and monitored in a first elution chromatogram (TIC). A more detailed low resolution scan identifies the ion with the most intense  $m/z$  at the specific timepoint. This ion is then selected for further analysis: first, in an enhanced resolution scan, the charge of the ion is determined. Next, it is fragmented in  $q_2$  and the resulting fragments are analyzed in  $Q_3$  and measured in the detector. From this fragmentation pattern the peptide sequence can be deduced using database search. Hence peptides and proteins are identified. The 4000QTrap is a cycling instrument; many ions are selected, fragmented and analyzed at a given timepoint. Each ion is only selected twice within a timeframe of 1 minute, which allows also the analysis of less intense ions.

Each ion can only be selected for MS/MS fragmentation twice within a timeframe of 1 minute (by default setting). Thus also less intense ions are selected for fragmentation making the analysis more sensitive and comprehensive. After the identification run, the identified peptide sequences are searched versus the UniProt data base (version 6.4) restricted to *homo sapiens* using Mascot (version 2.1, Matrix Science, London, UK) and the proteins they belong to are identified. The proteins that have been reliably identified (with at least 2 peptides and a protein score  $\geq 20$ ) are selected and their identified peptides chosen for quantification in a second run in the multiple reaction monitoring (MRM) mode.

#### *Multiple reaction monitoring - MRM*

In principle, multiple reaction monitoring describes a method, which allows for the monitoring of many transitions in a cycling fashion. A transition is defined as the combination of a precursor ion and one of its fragment ions. Using MRM, relative amounts of peptides and hence proteins can be quantified, by measuring the intensity of a given transition over time during the chromatographic elution. The term "multiple" implies that many such transitions can be measured sequentially in one experiment. The relative amounts of each peptide are calculated from the area under the peak resulting from the measurement.

To extract the required peptide information for quantification (precursor ion mass, fragment ion mass, retention time, etc.) from Mascot we use a program called MRM buddy (developed at the FMI in Basel, Switzerland. The MRM buddy interface allows the user to select peptides for quantification. The user can decide, whether peptides are suitable for quantification or rather not, depending on their modification and amino acid composition and charge state.

MRM buddy contains a function so that it automatically calculates the labeled or endogenous counterpart for any measured peptide, in case this has not been measured during the identification run. MRM buddy then generates a list of transitions to be quantified, which can be directly used in setting up the MRM run on the 4000QTrap. In the second run, the MRM run, these selected transitions are then monitored over time during the chromatographic elution.

After the analysis of the sample in the MRM mode, the peak areas for each measured transition have to be integrated manually. Then MRM buddy incorporates the measured areas for each peptide into the previously established transition list and calculates peptide ratios (e.g. labeled over endogenous AA). It also takes into account the correction factor for the purity of the stable isotope labeled amino acids and a factor for normalization. From the resulting peptide ratios overall protein ratios are calculated. Therefore, each protein needs to be quantified by at least 3 peptides.

In such an experiment, the user has to make sure, not only to quantify proteins that are interesting in the experiment, but also proteins that are known to be unchanged by the kind of treatment or purification performed. These proteins will yield a quantification ratio around one and thus make it easier to determine proteins, whose ratio is significantly decreased or increased in the sample. All protein ratios are plotted and, assuming normal distribution, a cut-off is determined at  $\pm 2\sigma$  from the mean. In this way proteins, which are regulated (e.g. by some treatment prior to the MS experiment) can be identified through the quantification of their relative amounts within the sample.

## 3.2 Materials and methods

A description of the Materials and Methods used in these experiments is found in section 4.3.

## 3.3 Results

### *Metabolic labeling of T47D breast cancer cells using SILAC*

In order to identify proteins that specifically bind to pTyr1248 of the ErbB2 receptor we used a combination of a peptide affinity pull-down and SILAC, followed by quantitative mass spectrometry. For SILAC, one set of T47D cell was kept in normal growth medium with endogenous non-labeled amino acids. The other set was cultured in SILAC medium for at least five passages. This medium contained 400x excess of  $^{13}\text{C}_6^{14}\text{N}_4$ - Lysine (Lys6) and  $^{13}\text{C}_6^{15}\text{N}_4$ - Arginine (Arg10). The cells were lysed and the percentage of incorporation of the isotopically labeled amino acids was monitored by MALDI-TOF MS. We found an incorporation of  $\geq 90$ -95 % after five passages. Additionally, we monitored the T47D breast cancer cells grown in SILAC medium and compared their growth and morphology to the cells grown in parallel in normal medium. We could not detect any obvious differences in cell proliferation rate or the morphology of the cells due to the metabolic labeling with Lysine and Arginine. Therefore, these cells were used for the pull-down experiments.

### *Peptide affinity purification, protein identification and quantification by MRM*

Peptides mimicking the C-terminal regulatory region of ErbB2 were synthesized with an N-terminal desthiobiotin group connected by an SGSG linker to a 15mer peptide sequence with the specific tyrosine residue in the middle (desthiobiotin-SGSGPTAENPEYLGLDVPV-NH<sub>2</sub>). Peptides were synthesized as pairs of a non-phosphorylated and a tyrosine phosphorylated version. Desthiobiotin was used as affinity tag, and biotin, as the specific eluant.

The peptides were bound to streptavidin attached to magnetic beads and incubated with equal amounts of cell extract from HRG-stimulated non-labeled and labeled T47D cells (Figure 3-4). After binding the beads were washed to remove unbound proteins, then the peptides and their bound proteins were eluted using biotin or by boiling the samples in SDS buffer. The eluted proteins were separated by SDS-PAGE and digested with trypsin. Trypsin cleaves after Lysine and Arginine residues ensuring that all resulting peptides are labeled except the very C-terminal one. The eluted proteins were analyzed by the two-step MS method described above. We were especially interested in peptides that were enriched by the affinity purification as indicated by an increased intensity for the isotopically labeled form (Figure 3-4).

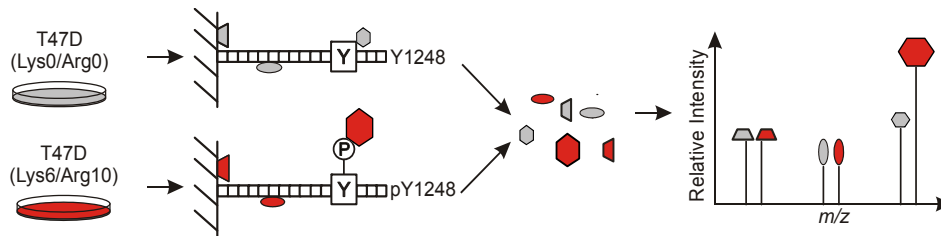


**Figure 3-4 Identification of binding partners of pTyr1248 of ErbB2**

T47D breast cancer cells were either grown in normal medium (grey) or in medium containing stable isotope labeled Lysine and Arginine (red). The cells were starved overnight and stimulated with 1 nM HRG for 20min. Then the cells were lysed and equal amount of whole cell extract (WCE) were incubated with the respective peptide linked to magnetic beads. After binding the beads were washed and the peptides and bound proteins were eluted using biotin. The proteins were separated by SDS PAGE, digested by trypsin and identified by MS. Quantification was done by multiple reaction monitoring. Peptides with a higher intensity of the labeled peptide were of interest, because they should be derived from protein binding specifically to pTyr1248.

Figure 3-5 shows an example of an MRM run from one sample of a pull-down experiment. The chromatographic traces of all transitions monitored are shown in the upperpanel. Since all individual transitions are monitored over time their traces occur as curves, of which the area can be taken for quantitation analysis. The chromatographic traces from peptide pairs (e.g. Arg0 or Arg10 labeled) are overlaying curves since both peptides behave similar during the chromatography and the MS. The two lower panels of Figure 3-5 depict transitions for 2 peptide pairs that are either non-regulated (left) or show an increased intensity for the labeled peptide (right). This means that the peptide pair on the left bound to the Tyr1248 and pTyr1248 peptides equally well, whereas the peptide on the right bound to the pTyr1248 with a much higher affinity that to the Tyr1248 peptide. Presumably, this peptide belongs to a protein that specifically binds to the phosphorylated Tyr1248 site. However, it is important to note, that from each protein at least 3 peptides with a Mascot peptide score  $\geq 20$  need to be quantified to draw any reliable conclusion about the binding preference of the protein. Therefore, an observed regulation of a single peptide pair does not necessarily lead to the right conclusion.

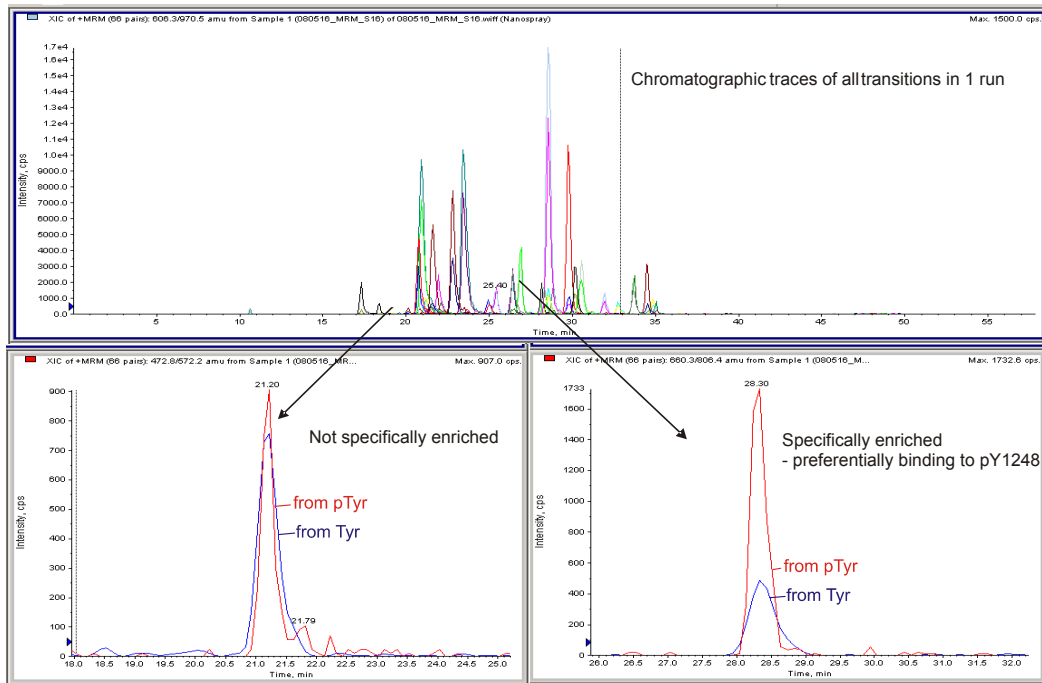


**Figure 3-5 Example of an MRM run for one sample**

All chromatographic traces from one MRM experiment are shown in the top column; transitions of peptide pairs that have been monitored are shown as overlaying curves. The lower panels show two examples of transitions of peptide pairs that can be used for quantification. On the left side the area under both peak, from the non-labeled and the labeled peptide, are about equal, meaning that this peptide was binding to both Tyr1248 and pTyr1248 with the same affinity. On the right side the area under the curve for the labeled peptide is much larger than that of the non-labeled peptide suggesting that this peptide preferentially bound to pTyr1248.

For each of the monitored transitions a peak integration needs to be performed (Figure 3-6). This can be done automatically using Analyst1.4 peak integrator. However, it is advisable to check all integrations manually and to correct them if necessary. The integrated peak areas can then be exported into Excel, from which they can be either imported into MRMBuddy or analyzed manually.

### 3. Identification of Copine III as a binding partner of ErbB2

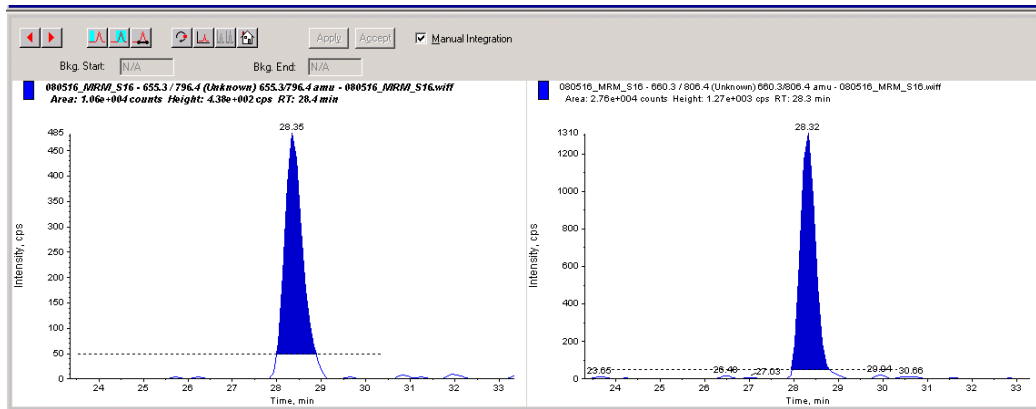


**Figure 3-6 Peak integration in Analyst 1.4**

For each peptide pair measured during the MRM run peak integration has to be done using Analyst peak integrator. The peak areas are integrated manually to avoid false integration. All integrated areas are calculated by Analyst and can be exported into Excel.

For one pull-down experiment we usually cut the SDS gel into 24 pieces that were all analyzed individually. For all proteins in one samples the chosen transitions were monitored, the peaks integrated and the ratios (labeled AA/ endogenous AA) were calculated. Then all these data were pooled for all 24 samples and overall proteins ratios were calculated. These ratios were then grouped and plotted for the frequency of their occurrence (Figure 3-7). Since we also quantified many proteins of which we were assuming that they bound to both the Tyr1248 and the pTyr1248 peptide in the same ratio we expected to find most of the protein ratios around 1. This was indeed true as seen in the example shown in Figure 3-7. Additionally, the distribution of all protein ratios adopted a normal distribution. This assures a more reliable distinction between background and specific binding proteins.

Therefore, we determined the mean of this curve and set the cut-off for specific binding at  $\pm 2\sigma$  from the mean. Since we were mainly interested in proteins binding specifically to the phosphorylated Tyr1248 site we only considered proteins with a ratio  $\geq 1.5$ . In this first experiment we found several proteins falling into this category (Figure 3-7).

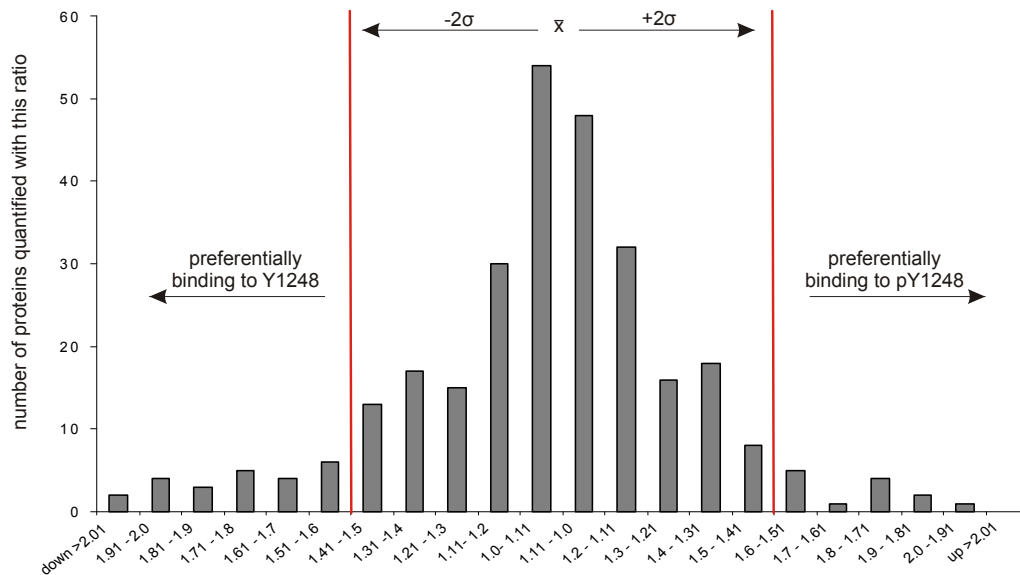


**Figure 3-7 Distribution of all quantified protein ratios from one experiment**

From the quantification ratios for each peptide pair to overall ratios for the identified proteins were calculated. These ratios were grouped as above and plotted versus the number of proteins falling in this group. As expected, the distribution assumes a Gaussian or normal distribution with most of the ratios around 1. This means that the majority of the protein quantified bind to Tyr1248 and pTyr1248 with the same affinity. We set the cut of for significant binders at  $\pm 2\sigma$  from the mean (red line). All proteins above this cut-off are of potential interest since they bind pTyr1248 preferentially.

The complete experiment was repeated three times with fresh cell extracts to verify specific binders.

In this way, we identified Copine III as a specific binding partner of pTyr1248 of the ErbB2 receptor. In the above experiment, the first full pull-down experiment performed, we identified Copine III with 4 peptides. 3 of these were taken for quantification and yielded an overall protein ratio (Arg10 over Arg0 and/or Lys6 over Lys0) of 1.76, thereby being clearly above the cut-off. In two other full experiments we quantified Copine III with ratios of 1.76 (5 peptides identified, 4 quantified) and 1.78 (9 peptides identified, 6 quantified) confirming that, at least *in vitro*, Copine III interacts with pTyr1248 of the ErbB2 receptor.

### 3.4 Discussion

We could show, by using a combination of a peptide affinity pull-down and quantitative mass spectrometry, that Copine III is a putative interaction partner of the ErbB2 receptor. Using set of non-phosphorylated and phosphorylated peptides mimicking different areas of the C-terminal regulatory domain of ErbB2 (Tyr1196/pTyr1196 and Tyr1248/pTyr1248), we were also able to show that Copine III binds specifically to pTyr1248 of the receptor.

Although we used a previously published method for the peptide affinity pull-down, some optimization had to be done to achieve optimal binding. Prior to the full scale experiments the binding capacity of the magnetic beads used was tested with the Tyr and pTyr-peptides. Using a titration approach and by monitoring the amount of bound peptide by HPLC, we determined the individual binding capacity for each peptide on the beads. In this way, we wanted to minimize background protein binding by occupying all binding spaces on the beads with peptide.

Nevertheless, we still observed a large amount of background proteins eluting from the beads. Since we were using streptavidin beads we tried solutions like binding the dethiobiotinylated peptide to the beads and then incubating the beads with biotin to block empty streptavidin binding sites. Yet, this did not markedly decrease the amount of background proteins bound and eluted from the beads. Therefore, the sample was far too complex to be run on the MS from solution and had to be pre-separated by SDS PAGE. Even though the MS approach used is a highly sensitive approach, we had to start out with relatively large amounts of input protein samples and beads. A reason for this could have been that after binding the sample was separated by SDS PAGE and peptides were eluted from the gel pieces, a technique, which is known to cause a large decrease in sensitivity.

We identified up to 300 proteins in one experiment, showing on the one hand the amount of background binding in the experiment and, on the other hand, the sensitivity of the mass spectrometry approach. Although the background proteins result in poor signal to noise ratios, their identification was also desired in order to clearly distinguish specific and non-specific binders. In different experiments we always found more than one protein binding specifically to the pTyr1248-containing peptide. However, Copine III was the only one found in all full scale experiments. This, and the fact that the ratios obtained for Copine III binding to pTyr1248 in all experiments are very similar, made us confident to have identified a true interaction partner of the receptor.

One curious observation of our mass spectrometry experiments was the absence of Shc amongst the identified. Shc has been shown to bind pTyr1248 *in vitro* using the same peptide affinity pull-down approach (Schulze *et al.*, 2005). In western blots done in parallel to the MS identification, we detected Shc in the elution fraction. This is rather curious, since MS is much more sensitive in terms of amounts of proteins than western blotting. One explanation for this phenomenon could be that in our studies a different type of mass spectrometer was used than in the other study, in which Shc was identified. We used a nano-LC-ESI-triple quadrupole



instrument, whereas Schulze *et al.* worked on an ESI-quadrupole TOF hybrid mass spectrometer and on a LTQ-FT (ion trap Fourier transform ultra hybrid MS).

In a quadrupole TOF hybrid mass spectrometer the final quadrupole is replaced by a time-of-flight device. Therefore, this hybrid MS contains two mass analyzers, which provides a much higher mass accuracy in the measurements than in instruments with only one kind of mass analyzer. Similarly, Fourier transform ion cyclotron resonance (FTICR) mass spectrometers have a very high resolution and mass accuracy. FTICR-MS is useful for dealing with complex mixtures since the resolution allows the signals of two ions of similar  $m/z$  to be detected as distinct ions. Therefore, it might be possible that Shc was not detected using our triple quadrupole instrument, because the ions it produced were overlaid by other ions at the same  $m/z$  ratio that were measured with a higher intensity. We tried to circumvent this by specifically monitoring Shc peptide transitions in the MRM run. However, since Shc had not been identified in any identification run, the transitions used from the MRM run were produced *in silico*. This could be a reason why also in such a directed MRM experiment we did not identify Shc in the sample.

Even though it would have been a good internal control to identify Shc with the pTyr1248 peptide in the MS approach, we are still very confident that Copine III is indeed binding to pY1248 of ErbB2 specifically. To further confirm this data, we were able to show this interaction by other means and we also found a functional link between these two proteins (section 3.3).



## 4 IN SILICO ANALYSIS OF COPINE III

After the identification of Copine III as a putative binding partner of the ErbB2 receptor, we searched the literature for publications on Copine III. We found that it belongs to a recently identified family of proteins, on which not many studies have been published. We therefore started to investigate Copine III using bioinformatic tools. This was done in order to gain information about Copine III from the *in silico* analyses to help us to place it within a framework of proteins or a specific network.

First we performed sequence alignments of all human Copines identified to date. This alignment showed that the human Copines are indeed a highly conserved family of proteins. Overall, there are two stretches, one being the N-terminus and the other being the C-terminus, that are not as conserved as the rest of the sequence. Copine V has an insertion of 19 amino acids (AAs) that is not seen in any of the other sequences (Figure 4-1).

In order to retrieve more information about Copine III we analyzed its domain structure in more detail. From the literature it was known that all Copines carry two C2 domains (C2A and C2B) and a Copine-specific A domain (Creutz *et al.*, 1998). We performed sequence alignments of Copine III with other proteins carrying a C2 domain, mainly of the PKCs and synaptotagmin family of proteins. Furthermore, 3D modeling of the putative regions forming each domain was performed to define the borders of the domains. A similar analysis was done for the A domain by aligning and modeling it to an integrin A domain. According to these results the domain architecture of human Copine III was determined as follows: C2A: 7 – 104, C2B: 143 – 270, A domain: 375 – 498 (Figure 4-1).

.

4. In silico analysis of Copine III

```

Copine-4 MK--KMSNIYE SAANTLGI FNSPCITKVE LRVACKGI SDRDALSKPDP -CVILKM-QSHG 56
Copine-7 MS--AGS--ERGAATPGGLPAPCAS KVELRLSCRHLLDRDP LTKSDP -SVALLQ-QAQQ 54
Copine-6 MSDPEMGWVPE PPTMTLG-----ASRVELRVSCHGLLDRDTLTKPHF -CVLKLK-LYSDE 52
Copine-1 -----MAHCVTLVQLSISCDHLLDKDI GSKSDPLCVLFLQD-VGGG 39
Copine-3 -----MAAQCVTKVALNVSANLLDKDI GSKSDPLCVLFLN-TSQQ 40
Copine-2 --MAHIPSGGAPAA GAAPMGPOYCVCKVELSVSQNLDRDVTSKSDPFCVLFTE-NNG- 56
Copine-5 --ME-QPEDMASLSEFDSLAGSIPATKVEITVSCRNLLDKDMFSKSDPLCVMYTQGMENK 57
Copine-8 --MDSRYNSTAGIGDLNQLSAAIPATRVESVSCRNLLDRDVTFSKSDPICVLYVQGVGNK 58
Copine-9 -----MSLGGASER-----SVPATKIEITVSCRNLLDLTFSKSDPMVLYTQSRASQ 48
          : : : : : * * * : * . * * *

Copine-4 QWFEVDRTEVIRTCINPVYSKLFVDFYFEEVQR LRFVHDIS-SNHNGLEADFLGGME 115
Copine-7 QWVQGRTEVVRSSLHPVFSKVFVDFYFEEVQR LRFVYDTHGSPGFSCQEDDFLGGME 114
Copine-6 QWVEVERTEVLRSCSSPVFSRVLALEYFEEKQLQPHVFDAB-DGATSPRNDTFLGSTE 111
Copine-1 SWAELGRTERVRNCSSEPFESKTLQLEYRFEVTVQKLRFGIYDID-NKTPELRDDDFLGGAE 98
Copine-3 QWVEVERTERIKNCLNPFQSKTFIDYFEEVQKLFQGVYDID-NKTIELSDDFLGECE 99
Copine-2 RWI EYDR TETA INNLNPAF SKK FVLDYH FEEVQK LK FALFDQD -KSMRLDEHDFLGGQFS 115
Copine-5 QWR EFGRT EVIDNTL NPDV RKFVLDYF FEEKQL RFDLYD V -SKSPDL SKHDFLGGQAF 116
Copine-8 EWR EFGRT EVIDNTL NPDV RKFVLDYF FEEENLR FDLYD V -SKSPNL SKHDFLGGQAF 117
Copine-9 EWR EFGRT EVIDNTL NPDV RKFVLDYF FEEKQL RFDVYVND -SKTNISKPKDFLGGQAF 107
          * : * * * . * : : : : * * : * * : : * * *

Copine-4 CTLGQIVSQRKLSKS-LLKHGN-----TAGK--SSITVIAEELSGND 154
Copine-7 CTLGQIVAQKVKTRPLLKFG-----NAGK--STITVIAEDISGND 154
Copine-6 CTLGQIVSQTQVTKPLLLKNG-----TAGK--STITVIAEVSQGN 151
Copine-1 CSLGQIVSSQVLTPLMLKPKG-----PAGR--GTITVSAQELK-DN 137
Copine-3 CTLGQIVSSKLTLPVLMKTGR-----PAGK--GSITISABEIK-DN 138
Copine-2 CSLGQIVSSKLTIPVLLNDK-----PAGK--GLITIAQELK-DN 154
Copine-5 CTLGQIVGSPGSRLEKPLTI GAFSINSR TGKMPMPAVSNGGVPKCGCTIILSAAELSNCR 176
Copine-8 CTLGQIVGSGSRLEKPIVG-----IPGKCGTIIILTAELSNCR 157
Copine-9 LALGQVIGGQSRVERTLTG-----VPGKCGTIIILTAELSNCR 147
          : * * : : : : * : * * : * : * : * : *

Copine-4 DYVHLAFNARKLDDKDFFSKSDPFLEIFRMNDATQQLVHRTVEVMNLSPAWKFVKVSV 214
Copine-7 GYVHLSFRARKLDDKDFFSKSDPFLELYRVNDQGLQLVYRTEVVKNNLNVPWEAFKVS 214
Copine-6 DYVQLTFRAYKLDNKDFFSKSDPFMEIYKTNEQSDQLVWRTVEVKNLNLPSEPPRLSL 211
Copine-1 RVVIMEVEARNLDDKDFLGGSDPFLEFFRQ-GDGKHLVYRSEV IKNLNLPWKRF SVVP 196
Copine-3 RVVILFEMEARKLDDKDFFSKSDPFLEFHKQTS DGNWLMVHRTVEVKNLNLPVWRPFKISL 198
Copine-2 RVI TILSLAGRRLDKKDFFSKSDPFLEFYKPGD DGNWLMVHRTVEV IKYTLDVWKPFTPL 214
Copine-5 DVAIMQFCANKLDDKDFFSKSDPFVLYR SNE DGTFTICHKTEVMKNTLNVPVQFTSIPV 236
Copine-8 DAVIMQFCANKLDDKDFFSKSDPFVLYR SNE DGSFTICHKTEVMKNTLNVPVQAFKISV 217
Copine-9 DIATMQLCANKLDDKDFFSKSDPFVLYR SNE DGTFTICHKTEVMKNTLNVPVQFP SIFV 207
          : : : * * * * * : : : * : * * * : * * * : * : *

Copine-4 NSLCSGDPDRRLKCI VWDWDSNGKHDFIGEFTSTFKEMRG-----AMEGKQVQWECINP 268
Copine-7 SSLCSCEETPLKCLVWDYDSRKHDFIGEFTSTFKEMQK-----AFEEGQAWDCVNP 268
Copine-6 HSLCS CDVHRPLKFLVYDYSSGKHDFIGEFTSTFQEMQEG-----TANPGQEMQWDCINP 267
Copine-1 QHFCGPNPSTPIQVQCSDYSDGSHDLIGTFHTSLAQLQAV-----PAEFCIHP 246
Copine-3 NSLCYGDMDKTIKVECYDYDNDGSHDLIGTFHTMTKLEASRS-----PVEFCINE 252
Copine-2 VSLCDGDMKPIQVMCYDYDNDGSHDFIGFTS VMSQCEARDSV-----PLEFCINE 268
Copine-5 RALCNGDYDRTIKVEYDWRDGSDFIGFTSYRELSRG-----QSQFNIEYVWNP 289
Copine-8 RALCNGDYDRTIKVEYDWRDGSDFIGFTSYRELSRG-----QSQFNIEYVWNP 270
Copine-9 RALCNGDYDRTVKIDVYDWRDGSDFIGFTSYRELSKA-----QNQFTVYEVLPN 260
          : * : : : * * * * * : : : : : : :

Copine-4 KYKAKKKNYKSGTVILNLCKIKMHSLFDYIMGGCQIQFTVAIDFTASNGDPRNSCSLH 328
Copine-7 KYKQKRRSYKNSGVVLA DLKFRVYSLFDYIMGGCQIHFVTAIDFTASNGDPRNSCSLH 328
Copine-6 KYRDKKKNYKSGTVVLAQC TVEKVHTFLDYIMGGCQISFTVAIDFTASNGDPRSSQSLH 327
Copine-1 EKQKQKSYKNSGTIRVKICRVETYSFLDYIMGGCQINF TVGVDF TGSNGDPRSPDSLH 306
Copine-3 KKRQKQKSYKNSGTVSVKQCEITVECTFLDYIMGGCQLNF TVGVDF TGSNGDPRSPDSLH 312
Copine-2 KKQRKKNYKSGTIIILRSCKINRDYSLFDYILGGCQLMFTVIGIDFTASNGNPLDSSLH 328
Copine-5 KKKMKKKYVNSGTVTLISFAVES ECTFLDYIKGGTQINF TVAIDFTASNGNPSQSTSLH 349
Copine-8 KKKGKKKYTNISGTVTLISFLVETEVSLFDYIKGGTQINF TVAIDFTASNGNPAQPTSLH 330
Copine-9 RKKCKKKKYVNSGTVTLISF SVDS EFTFVDYIKGGTQLNF TVAIDFTASNGNPLQPTSLH 320
          : : * : * * * : : : * * * * * : * * * * * : * * * * *

Copine-4 YIHPYQPNY LKALVAVGEI CQDYDSDKMFPALFGFARIPPEYTVSHDFAINFNEDNPEC 388
Copine-7 YINPYQPNY LKALVAVGEI CQDYDSDKRFSALFGFARIPKVEVSHDFAINFNEDDEC 388
Copine-6 CLSPRQPNHYLQALRAVGGICQDYDSDKRFPALFGFARIPNPFVSHDFAINFNEDPEC 387
Copine-1 YLSPGTVNEYLMALWSVGSVVDYDSDKLFPALFGFARIPPDWQVSHFALNPNPNYC 366
Copine-3 YINPNGTNEYLSAIWAVGQIQDYDSDKMFPALFGFARIPPDWQVSHFEPNPNPNYC 372
Copine-2 YINPNGTNEYLSAIWAVGQIQDYDSDKMFPALFGFARIPPDWQVSHFALNPNPNPC 388
Copine-5 YMNPYQLNAYLALAVGGEIQHYDSDKMFPALFGFARIPPDGRVSHFALNPNPNPC 409
Copine-8 YMNPYQLNAYGMALAVGGEIQDYDSDKMFPALFGFARIPPDGRVSHFALNPNPNPC 390
Copine-9 YMNPYQLSAYAMALAVGGEIQDYDSDKLFPALFGFARIPPEGRVSHFALNPNPNPC 380
          : * . * * : * * : * * * * * * * * * * * * * * * * * *

```

Copine-4	YIHPYQPNEYLKALVAVGEICQDYSDSKMFP AFGFGARIPPEYTVSHDFAINFNEDNPEC	388
Copine-7	YINPYQPNEYLKALVSVGEICQDYSDKRFSAFGFGARIPPKYEVSHDFAINFNPEDEDEC	388
Copine-6	CLSPRPQPNHYLQALRAVGGICQDYSDKRFPAFGFGARIPPNFVSHDFAINFNDFENPEC	387
Copine-1	YLSPTGVNEYLMALWSVSGSVVQDYSDKLFPAFGFGAQVPPDWQVSHDFALNFPNSNPYC	366
Copine-3	YISPNGVNEYLTALWSVGLVIQDYDADKMFPAFGFGAQIPQWQVSHDFPMNFPNSNPYC	372
Copine-2	YINPMGTNEYLSAIWAVGQIIQDYSDSKMFPALGFGAQLEPPDWKVSHEFALNFPNTNPF	388
Copine-5	YMSPYQLNAYALALTAVGEIIQHYSKDKMFPALGFGAKLPPDGRVSHDFPLNGNQENPSC	409
Copine-8	YMNPYQLNAYGMALKAVGEIVQDYSDSKMFPALGFGAKLPPDGRISHEFALNGNPQNPF	390
Copine-9	YMSPYQLSAYAMALKAVGEIIQDYSDKLFPAFGFGAKLPPDGRISHQFPPLNNNDEDPNC	380
	: * . * * : : * * : * * * * * : * * * * * : * * * * * : * * * * * : *	
Copine-4	AGIQGVVEAYQSCLPKQLYGPNTAPIIQKVAKSASEETNTKEASQYFILLITLDGVIT	448
Copine-7	EGIQGVVEAYQNCLPRVQLYGPNTVAPIISKVARVAAAEESTGKASQYFILLITLDGVVT	448
Copine-6	EEISGVIASYRRCLPQIQLYGPNTVAPIINRVAEPAQREQSTGQATKYSVLLVLTLDGVVS	447
Copine-1	AGIQGIVDAYRQALPQVRLYGPNTFAPIIINHVARFAAQAAHQGTASQYFMLLLITDGAVT	426
Copine-3	NGIQGIVEAYRSCLPQIKLYGPNTFSPIIINHVARFAAAATQQQTASQYFVLLITDGVIT	432
Copine-2	SGVDGIAQAYSACLPHIRFYGPNTFSPIVNHVARFAAAATQQQTATQYFILLITDGVIS	448
Copine-5	CGIDGILEAYHRSRRTVQLYGPNTFAPVVTTHVARNAAVQ---DGSQYVLLITDGVIS	466
Copine-8	DGIEGVMEAYRSLKSVQLYGPNTFAPVINHVARYASSVK---DGSQYVLLITDGVIS	447
Copine-9	AGIEGVLESYFQSLRTVQLYGPNTFAPVINQVARAAAKIS---DGSQYVLLITDGVIS	437
	: * : * . * * : : * * * * * : * * * * * : * * * * * : * * * * * : *	
Copine-4	DMADTREAIVHASHLPMSVIVGVGNADFSDMQMLDGDGILRSPKGEVPLRDIQFVVPF	508
Copine-7	DMADTREAIVRSRLPMSIIVGVGNADFTDMQVLDGDGVLRSRGEPAALRDIQFVVPF	508
Copine-6	DMAETRTAIVRSRLPMSIIVGVGNADFSMDRLDGDGILRCPRGVPAALRDIQFVVPF	507
Copine-1	DVEATREAVVRSNLPMSVIVGVGGADF EAMEQLDADGGPLHTRSGQAAARDIQFVVPY	486
Copine-3	DLDETRQAIIVNASRLPMSIIVGVGGADF SAMEFLDGDGGSQRSLPGEVAALRDIQFVVPF	492
Copine-2	DMEETRHAVVQA SKLPMSIIVGVGNADFAAMEFLDGDGRMLRSHLGEAAARDIQFVVPF	508
Copine-5	DMAQTKEAIVNAKLPMSIIVGVGAEFDAMVELDGD-VRVSSRGLAERDIQFVVPF	525
Copine-8	DMAQTKEAIVNASLPMSIIVGVGAEFDAMVELDGD-VRVSSRGLAERDIQFVVPF	506
Copine-9	DMTQTKEAIVSASLPMSIIVGVGPAEF EAMEELDGD-VRVSSRGRYAERDIQFVVPF	494
	* : * : * * : *	
Copine-4	RNFKH-----A SPAALAKSVLAEVNPQVVDYYNGKGIKPKCS-----SEMYESS	552
Copine-7	RELKN-----A SPAALAKCVLAEVPKQVVEYYSHRGLPPRLG-----VPAGEAS	553
Copine-6	RDFKD-----A APSALAKCVLAEVPRQVVEYYASQGISPGAPR-----PCTLATT	552
Copine-1	RRFQN-----A PRELAQTVLAEVPTQLVSYFRAQGWAPLKL-----PPSAKDP	531
Copine-3	RQFQN-----A PKEALAQCVLAEIPQVQVGFNTY-----KLL-----PP--KNP	530
Copine-2	REFRN-----A AKETLAKAVLAEIPQVQVYFHKHN-----L-----PPTNSEP	547
Copine-5	RDYVDRTGNHVL SMARLARDVLAEPDQLVSYMKAQGI RPRPPAAPHTSPSQSPARTPP	585
Copine-8	RDYIDRSGNHIL SMARLAKDVLAEIPQFLSYMRARGIKFSPAP-----PPYTPP	556
Copine-9	-----CCSLGTSVV-----	503
	* . * :	
Copine-4	RTLAP---	557
Copine-7	PGCTP---	558
Copine-6	PSPSP---	557
Copine-1	AQAPQA--	537
Copine-3	ATKQKQ-	537
Copine-2	A-----	548
Copine-5	ASPLHTI	593
Copine-8	THVLQTI	564
Copine-9	-----	

**Figure 4-1 Sequence alignment of nine human Copine proteins**

The amino acid sequences from nine human Copine proteins were extracted from the SwissProt database and aligned using ClustalW. Domains, as characterized by sequence alignments and modeling, were annotated as follows: grey – C2A, blue – C2B, light red – Lysine-rich cluster and green – A domain. The domain borders were set for human Copine III. Stars denote amino acids conserved in all proteins, points those that are conserved in all but one sequence and colons those that are conserved in tall but two of the aligned sequences.

Moreover, the AA sequence of both C2 domains hints to a secondary structure, in which the  $\beta$ -strands fold occurs in an order as seen in other type II C2 domains, which was already claimed (Creutz *et al.*, 1998). This is an intriguing result, since in other proteins that carry two C2 domains, like annexins or synaptotagmin, these domains fall into the type I topology.

Furthermore, our sequence alignment demonstrated that the six aspartate residues, which have been shown to confer  $\text{Ca}^{2+}$ -binding in other proteins, are conserved throughout the

Copine family (Figure 4-2). This result strongly suggests that the Copines will exhibit  $Ca^{2+}$ -dependent functions in the cell.

When further analyzing the alignments we found that all copine family members have a 5-6 AA stretch rich in lysine residues, which we, therefore, termed "Lysine-rich motif". This motif is found at the C-terminus of the C2B domain. Interestingly, it has been hypothesized, since other C2 domain containing proteins also carry such a motif, that it helps targeting the protein to the membrane by binding to  $PIP_2$  (Guerrero-Valero *et al.*, 2007).

Moreover, we found that all copines have a conserved MIDAS (metal ion-dependent adhesion site) motif in their A domain (Figure 4-3).

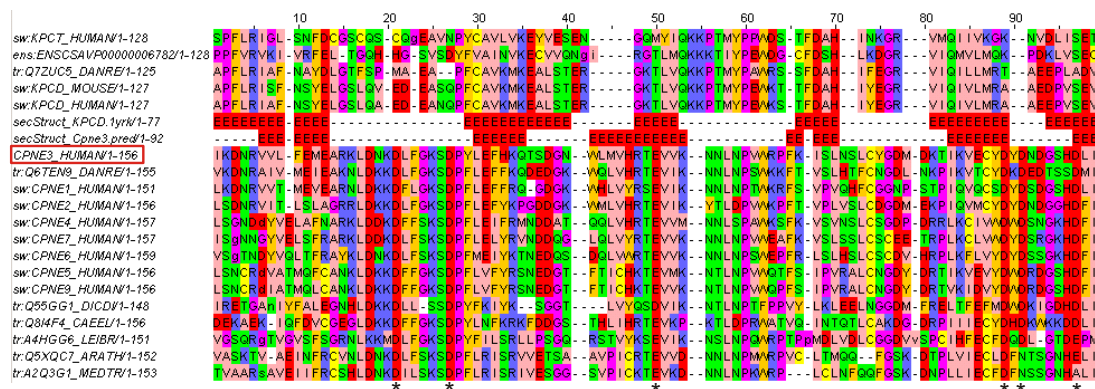


**Figure 4-2 Alignment of the Copine III C2B domain to C2 domains of PKCδ and other Copines**

Residues 1-156 of human Copine III were aligned to the C2 domains of other human Copines and those of PKCδ. Five aspartate residues were conserved in all Copines (marked with an asterisk) and a probably required for  $Ca^{2+}$ -binding. The alignment was performed using HHPred (M. Rebhan, FMI)

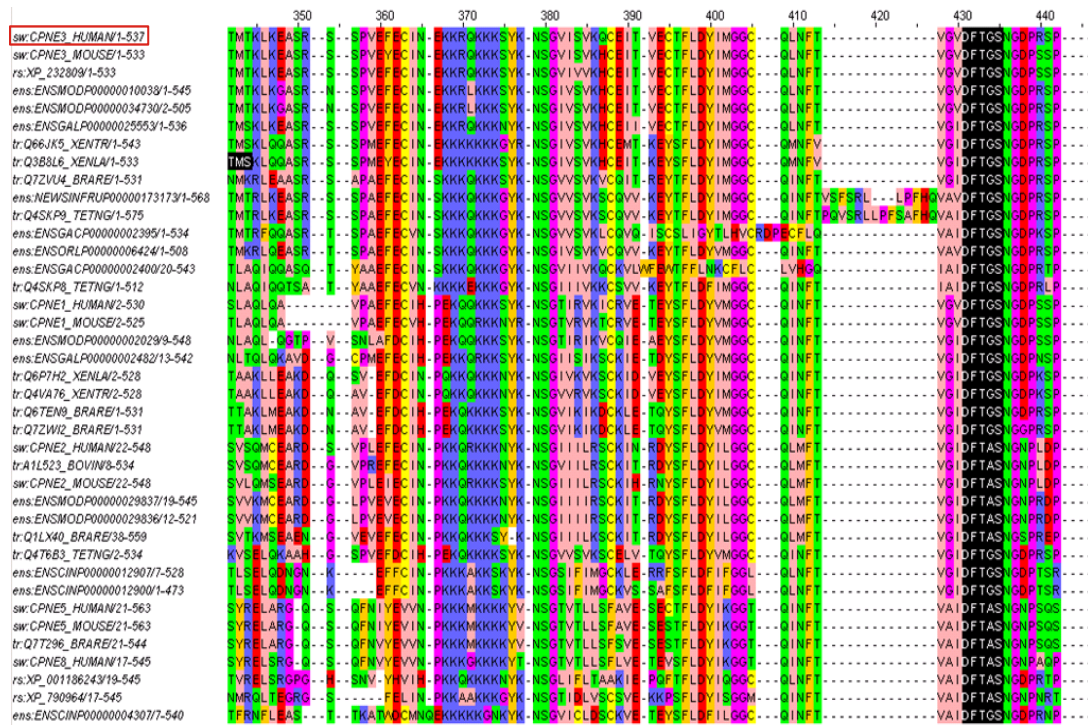


**Figure 4-3 Alignment of Copine III to other Copine family members**

Residues 1 – 573 of human Copine III were aligned to AA sequences of Copine family members from different species. A Lysine-rich cluster, which is conserved throughout the whole family, is depicted in blue with a black bar underneath. Moreover, all Copine family members carry a conserved MIDAS motif, denoted in black, within their A domain. The alignment was performed using HHPred (M. Rebhan, FMI)

Therefore, these *in silico* analyses of human Copine III support the hypothesis that it exhibits  $\text{Ca}^{2+}$ -dependent phospholipid binding activity within the cell. Furthermore, since it shows the conserve MIDAS motif it probably binds  $\text{Mg}^{2+}$  and/or  $\text{Mn}^{2+}$ , which might influence its interaction properties (e.g. membrane binding)





## 5 COPINE III INTERACTS WITH ERBB2 AND PROMOTES TUMOR CELL MIGRATION (IN PRESS)

Constanze Heinrich<sup>1</sup>, Claudia Keller<sup>1</sup>, Anne Boulay<sup>1</sup>, Manuela Vecchi<sup>2</sup>, Marco Bianchi<sup>2</sup>, Ragna Sack<sup>1</sup>, Susanne Lienhard<sup>1</sup>, Stephan Duss<sup>1</sup>, Jan Hofsteenge<sup>1</sup> and Nancy E. Hynes<sup>1\*</sup>

<sup>1</sup>Friedrich Miescher Institute for Biomedical Research (FMI), Maulbeerstr. 66, Basel, Switzerland

<sup>2</sup>IFOM, The FIRC Institute for Molecular Oncology Foundation, Via Adamello 16, 20139, Milan, Italy

\* corresponding author:

Nancy E. Hynes  
Friedrich Miescher Institute for Biomedical Research  
Maulbeerstrasse 66  
WRO-10.66.2.06  
CH-4058 Basel  
Switzerland  
Telephone: +41 (61) 697-8107  
Fax: +41 (61) 697-3976  
Email: [nancy.hynes@fmi.ch](mailto:nancy.hynes@fmi.ch)

JH and NEH are joint senior authors

Running title: Copine III and ErbB2 mediated migration

## 5.1 Abstract

ErbB2 amplification and overexpression in breast cancer correlates with aggressive disease and poor prognosis. To find novel ErbB2 interacting proteins, we employed SILAC followed by peptide affinity pull-downs and identified specific binders using relative quantification by mass spectrometry. Copine III, a member of a Ca<sup>2+</sup>-dependent phospholipid binding protein family, was identified as binding to phosphorylated Tyr1248 of ErbB2. In breast cancer cells, Copine III requires Ca<sup>2+</sup> for binding to the plasma membrane, where it interacts with ErbB2 upon receptor stimulation, an interaction that is dependent on receptor activity. Copine III also binds RACK1 (receptor of activated C kinase 1) and co-localizes with phosphorylated focal adhesion kinase at the leading edge of migrating cells. Importantly, knockdown of Copine III in T47D breast cancer cells causes a decrease in Src kinase activation and ErbB2-dependent wound healing. Our data suggest that Copine III is a novel player in the regulation of ErbB2-dependent cancer cell motility. In primary breast tumors, high CPNE3 RNA levels significantly correlate with *ERBB2* amplification. Moreover, in an *in situ* tissue microarray analysis, we detected differential protein expression of Copine III in normal versus breast, prostate and ovarian tumors suggesting a more general role for Copine III in carcinogenesis.

**Keywords:** quantitative mass spectrometry, ErbB2, HRG, Copine III, FRET acceptor photobleaching, cell migration

## 5.2 Introduction

The ErbB2/Her-2/Neu receptor belongs to the type I receptor tyrosine kinase (RTK) family also including EGFR, ErbB3 and ErbB4 (Schlessinger, 2000). Alterations in EGFR or ErbB2 promoting constitutive receptor activation have been implicated in development of many human cancers. Patients whose tumors show ErbB receptor alterations tend to have an aggressive disease and poor prognosis (Slamon *et al.*, 1987); (Holbro and Hynes, 2004; Hynes and Lane, 2005; Ross and Fletcher, 1998). Upon binding of EGF-related ligands to ErbBs, receptor homo- and heterodimers form, leading to kinase activation and phosphorylation of specific tyrosine residues in the cytoplasmic tail (Hazan *et al.*, 1990; Hynes and Lane, 2005.). ErbB2 has no ligand, but is the favored dimerization partner of the other family members (Graus-Porta *et al.*, 1997). ErbB3, although able to bind ligands, has impaired kinase activity. ErbB2 is the preferred heterodimerization partner of ErbB3, thereby coupling ErbB2 to the PI3K pathway (Holbro *et al.*, 2003a). ErbB2, via activation of signaling pathways including Erk and PI3K/Akt mediates numerous cellular processes important for tumorigenesis including proliferation, survival and migration, (Citri and Yarden, 2006; Keely *et al.*, 1997; Klemke *et al.*, 1997; Schlessinger, 2000; Yarden and Sliwkowski, 2001).

The five major tyrosine phosphorylation sites, Tyr1023/1028, Tyr1139/1144, Tyr1196/1201, Tyr1222/1227 and Tyr1248/1253 (human/rat) and their role in ErbB2 signaling has been studied by various means. Tyr1028 couples to a pathway implicated in negative regulation of NeuT transforming potential, whereas the four other sites have a potentiating effect. Tyr1144, Tyr1201 and Tyr1227 signal through the Ras/Erk pathway by binding Grb2, Crk and Shc (Akiyama *et al.*, 1991; Dankort *et al.*, 2001b; Dankort *et al.*, 1997), which also binds Tyr1253 (Schulze *et al.*, 2005). The role of pTyr residues has also been examined in migration assays. In T47D breast tumor cells, Tyr1196 and Tyr1222 have each been linked to ErbB2-mediated cell migration via PLC $\gamma$  and Memo, respectively (Marone *et al.*, 2004; Meira *et al.*, 2009)

We set out to identify novel binding proteins for Tyr1248 and to link them to an ErbB2-mediated phenotype. Using a pTyr1248 encompassing peptide in an affinity pull-down approach followed by relative quantification by mass spectrometry, we identified Copine III, which belongs to a family of Ca<sup>2+</sup>-dependent phospholipid binding proteins first found in the ciliate protozoan *Paramecium tetraurelia*. Copines are conserved from plants to humans, where nine CPNE genes have been identified (CPNE I - IX) (Tomsig and Creutz, 2002). All copines possess two N-terminal C2 domains (C2Ds) followed by a von Willebrand A-like or A domain.

C2Ds were originally identified in conventional protein kinase C isoforms and have been found in a growing number of eukaryotic proteins (Nalefski and Falke, 1996). The copine A domain, while similar to the extracellular A domain of integrins, is cytoplasmic and thought to mediate protein-protein interactions (Tomsig and Creutz, 2002).

Although widely expressed throughout the eukaryotes, indeed, most cells express multiple copines, relatively little is known about their specific roles. Interestingly, Copine III was shown to be up-regulated in tumor cells in response to ErbB2 overexpression (Gharbi *et al.*, 2002; White *et al.*, 2004). We examined the role of Copine III downstream of ErbB2 receptor signaling and show here that Copine III is a Ca<sup>2+</sup>-dependent, phospholipid-binding protein that interacts with activated ErbB2 at the plasma membrane of tumor cells. Moreover, we identified the focal adhesion (FA) associated scaffold protein RACK1 as a Copine III binding partner. Importantly, we show that Copine III is required for ErbB2-dependent cell migration.

### 5.3 Materials and Methods

#### *Antibodies and Reagents*

Recombinant heregulin  $\beta$ -1 (HRG) was purchased from R&D Systems (Minneapolis, MN, USA) and solubilized in PBS + 0.1% BSA.

The following antibodies were used: The serum for the polyclonal antibody against a 17- amino acid peptide of Copine III was provided by Elisabeth A. Grimm (MD Anderson, Houston, TX, USA) (Caudell *et al.*, 2000). The monoclonal Copine III antibody was generated against the recombinant C2B domain of human Copine III (AA132 to 278) (for antibody specificity see supplementary figure 1). This antibody was used for all immunofluorescence (IF) studies. For ErbB2, the 21N polyclonal antiserum was used in western blot analysis (Hynes *et al.*, 1989). A polyclonal antibody (sc-284) purchased from Santa Cruz (Santa Cruz, CA) was used in IF studies. For pY1248-ErbB2 the 06-229 antibody from Upstate (Millipore, Billerica, MA) was used in both WB and IF.

Other antibodies used in western blot analyses included rabbit anti-GAPDH (ab9385) and rabbit anti-Calnexin (ab10286) from Abcam (Cambridge, CA, USA), rabbit anti-p42/44 Erk (#9102), rabbit anti-phosphorylated p42/44 Erk (#9101), rabbit anti-Akt (#9272), rabbit anti-phosphorylated Akt (#9271), rabbit anti-phosphorylated pY925 FAK (#3284) all from Cell Signaling (Danvers, MA, USA), the anti-mouse Src (0-5184) antibody from Upstate, the rabbit anti-phosphorylated Src (44-660G), the rabbit anti-phosphorylated pY861FAK (07-832) and the rabbit anti-phosphorylated pY397FAK (44-624G) were from Biosource (Invitrogen) and rabbit

anti-FAK (sc-932) from Santa Cruz (Santa Cruz Biotechnology Inc., Santa Cruz, USA). The rabbit anti Copine-I antibody (10126-2-AP) was from PTGLabs (Chicago, IL). PTyr was detected with the 4G10 monoclonal antibody (a gift from Juergen Mestan, NIBR, Basel, Switzerland). For the transferrin receptor, cells were stained with the Ber-T9 antibody (sc-19675) from Santa Cruz.

The following secondary antibodies were used: An alexa488-conjugated goat anti-mouse antibody, an alexa568-conjugated goat anti-rabbit antibody (both Molecular Probes, Eugene, OR, USA) and a Cy3-conjugated donkey anti-rabbit antibody (Jackson ImmunoResearch Laboratories, Inc., West Grove, PA, USA)

DMSO was purchased from Sigma, Ionomycin from Calbiochem (Merck, Germany). The small molecule inhibitor AEE788 is a Novartis compound (Basel, Switzerland) (Traxler *et al.*, 2004).

#### *Cell Culture*

T47D and SKBr3 breast tumor cells were cultured in Dulbecco's modified Eagle's medium supplemented with 10% fetal bovine serum (FBS) (GIBCO Invitrogen, Basel, Switzerland) and 2 mM glutamine at 37 °C, 5 % CO<sub>2</sub>.

#### *SILAC*

Cells were cultured in medium without arginine (Arg) and lysine (Lys), which was supplemented with a 400-fold excess of <sup>12</sup>C<sub>6</sub><sup>14</sup>N<sub>4</sub> (Arg0) or <sup>13</sup>C<sub>6</sub><sup>15</sup>N<sub>4</sub> (Arg10) and <sup>12</sup>C<sub>6</sub><sup>14</sup>N<sub>2</sub> (Lys0) or <sup>13</sup>C<sub>6</sub><sup>14</sup>N<sub>2</sub> (Lys6) (Sigma and Cambridge Isotope Laboratories, Andover, MA, USA). Cells were cultured for at least 5 passages. The level of incorporation was measured by MALDI mass spectrometry (Ultraflex II, Bruker, Bremen, Germany).

#### *Peptide synthesis and affinity pull-down*

Peptides were synthesized as 15mers carrying an N-terminal desthiobiotin group followed by a four amino acid linker (Ward *et al.*, 1996) by JPT Peptide Technologies GmbH (Berlin, Germany) in the non-phosphorylated and Tyr-phosphorylated form (sequence: desthiobiotin-SGSGPTAENPEYLGLDVPV-NH<sub>2</sub>)

For affinity pull-downs, 2 mg Dynabeads MyOne Streptavidin C1 (Invitrogen) were incubated with 150 pmol peptide for 30 min at room temperature (RT). Heregulin β-1 (HRG) stimulated T47D cells were lysed in 50 mM Tris-HCl pH 7.5, 150 mM sodium chloride, 1 % (v/v) Nonident P-40, protease inhibitors (Complete Tablets, Roche), and 1 mM sodium orthovanadate. 12 mg of protein lysate were added and incubated for 4 hours at 4 °C, afterwards beads were washed and samples pooled (see Figure 1a). Proteins were eluted in biotin for 30 min at 30 °C or in SDS buffer at 95 °C for 10 min, subjected to SDS-polyacrylamide gel electrophoresis (SDS PAGE) and visualized using the Colloidal Blue Staining Kit (Invitrogen).

#### *Mass Spectrometry and Quantification*

The Coomassie stained bands were processed by reduction and alkylation of the cysteines followed by tryptic digestion. Peptides were analyzed by nano-HPLC (Agilent 1100 nanoLC system, Agilent Technologies, Santa Clara, USA) coupled to a 4000QTRAP mass spectrometer (Applied Biosystems, Foster City, USA). Peptides were identified searching UniProt data base (version 6.4) restricted to *Homo sapiens* using Mascot (version 2.1, Matrix Science, London, UK)(Perkins *et al.*, 1999).

For relative quantification, the required peptide information (e.g. *m/z* values of the precursor and fragment ions, retention time) was extracted from the Mascot dta file using “MRM buddy” (unpublished, developed at the FMI, Basel, Switzerland by Alessandro di Cara and Reto Portman). Proteins identified with  $\geq 2$  peptides and with a Mascot protein score  $\geq 20$  were quantified. For quantification, samples were re-injected and analyzed in the multiple reaction monitoring (MRM) mode. Relative quantification was performed by comparing the peak areas that were extracted using Analyst Classic in Analyst 1.4.1.

#### *Quantification correction and normalization*

Ratios (heavy/light) of peak areas for each individual light and heavy form of each peptide were calculated using Excel. Individual peptide ratios were corrected for the purity (given by the manufacturer) and incorporation (measured) of the labeled isotopes. From the corrected and normalized peptide ratios overall protein ratios were determined. Assuming a normal distribution we determined the mean of all protein ratios and set the cut-off for specific binding proteins at  $2\sigma$  below and above the mean.

#### *Immunofluorescence microscopy*

Preparation of cells was performed as described previously (Meira *et al.*, 2009). Images were recorded with an Axioskop Zeiss Microscope coupled to a Sony 3 CDD camera. For inhibitor studies, cultures were starved overnight, then preincubated 1.5 h with 0.5  $\mu\text{M}$  AEE788 (DMSO for controls) then 1 nM HRG (PBS for controls) was added for 20 min. Cells were fixed and stained as described (Meira *et al.*, 2009).

#### *Subcellular fractionation*

The cells were washed and detached by scraping in PBS, then homogenized and fractionated following the Membrane Preparation by Homogenization protocol from Current Protocols in Cell Biology online (Unit 7.10, support protocol 1; Wiley Interscience, John Wiley & Sons Inc, Malden, MA). All buffers were supplemented with either 10  $\mu\text{M}$   $\text{CaCl}_2$  or 1 mM EGTA. Equal

volumes of each fraction were used for subsequent SDS-PAGE and western blotting with specific antibodies.

#### *Preparation of cell lysates, IP and immunoblotting*

For assaying the effect of stimulation, cells were starved in DMEM + 0.1 % FBS overnight and subsequently stimulated with 10 ng ml<sup>-1</sup> HRG for 20 minutes, unless indicated otherwise. Control cells were treated with PBS + 0.1 % BSA for the same time. Whole cell extracts (WCEs) were prepared in lysis buffer (50 mM HEPES, pH 7.4, 150 mM NaCl, 1 % Triton X-100, 1x complete EDTA-free, 1 mM sodium orthovanadate) and total protein content was determined using the Bradford Protein Assay (Bio-Rad, Hercules, CA, USA). Immunoprecipitations (IPs) were performed as described previously (Meira *et al.*, 2009)

#### *FRET acceptor photobleaching*

SKBr3 cells were grown on glass coverslips (BD Biosciences, San Diego, CA) coated with 25 µg ml<sup>-1</sup> rat-tail Collagen I (Roche Diagnostics, Indianapolis, IN) and stimulated 20 min with 1 nM HRG as described (Meira *et al.*, 2009), except that slides were mounted using Mowiol (Calbiochem, EMD Chemicals, Gibbstown, NJ). Copine III was visualized using a secondary anti-mouse Alexa488-conjugated antibody. ErbB2 and transferrin receptor were visualized using a secondary anti-rabbit Cy3-conjugated antibody. Acceptor photobleaching was used to assess FRET efficiency on a Zeiss LSM510 confocal microscope equipped with a 63x/1.4 oil immersion objective. Alexa488 was excited with a 488nm laser line, emission measured with a BP505-530 filter. Cy3 was excited with a 543nm laser line, emission measured with a LP560 filter. For each measure Cy3 bleaching had to be over 90 % and FRET efficiency (E) was calculated after background subtraction and Alexa488 bleaching correction as follows:  $E = (I_D - I_{DA}) / I_D$ , where  $I_D$  and  $I_{DA}$  are Alexa488 intensities in the bleached region after and before photobleaching of Cy3, respectively. For each condition, 4 to 10 cells were assessed.

#### *Copine III knockdown*

Transient: Copine III siRNA was obtained from Qiagen (Germantown, MD). Cells were transfected in OptiMEM medium with the HiPerfect Transfection reagent (Qiagen) according to the protocol, using 2 µM siRNA. Successful KD was obtained using the following siRNA sequences: Optimal down-regulation occurred 96 h post transfection with the following siRNA sequences: siRNA1 5'-CCAGUUAUCUGUAAUCAA-3', siRNA2 5'-GGCAAUCUUCCAAGUAA-3'. LacZ: 5'-GCGGCGCCGAAUUUACC-3'.

Stable: Bacterial glycerol stocks of pLKO.1-puro vectors containing different shRNA sequences targeting Copine III were purchased from Sigma (MISSION shRNA library, TCRN\_NM\_003905).

Infections were done as described in Section III: Lentiviral Infection Protocol from the RNAi Consortium (Cambridge, MA). Copine III knock-down (KD) was confirmed by western blotting. The shLacZ vector was produced by cloning the 5'-CCGGGCGGCTGCCG GAATTTACCTTCTCGAGGGTAAATTCGGCAGCCGCTTTTAATT-3' sequence into the pLKO.1-puro plasmid. Bacterial glycerol stocks of pLKO.1-puro vectors containing different shRNA sequences targeting Copine III were purchased from Sigma (MISSION shRNA library, TCRN\_NM\_003905). Successful knockdown was achieved with: shRNA1: 5'-CCGGCCCTACTGCAATGGAATCCAACCTCGAGTTGGATTCCA TTGCAGTAGGGTTTTT-3', shRNA2: 5'-CCGGGCACAGAAAGGATTAAGAATTC TCGAGAATTCTTAATCCTTTCTGTGCTTTTT-3'.

HEK293 packaging cells were transiently transfected with polyethylenimine (PEI) (Polysciences Inc.) at a PEI:DNA ratio of 4:1. PEI was added to DNA diluted in serum-free media (8 µg pLKO.1-puro backbone with shLacZ or shCopine III, 0.4 µg HDM-tat16, 0.4 µg HDM-HgPM2, 0.4 µg pRC-CMV-Rall and 0.8 µg HDM-VSV-G), vortexed and incubated at RT for 15 min. The PEI/DNA mix was added to the cells and incubated for 16h at 37°C, at which point the media was changed. Media containing viruses was collected 72h post-transfection, filter sterilized, aliquoted and stored at -80 °C.

T47D and SKBr3 cells were infected by incubation in media containing 8µg/mL polybrene (Sigma) and 600 µl of viral supernatant for 24 h at 37 °C. The media was then changed and the cells were incubated another 24 h at 37 °C. Cells infected with lentivirus for shRNA expression were cultured in medium supplemented with 0.5 ug ml<sup>-1</sup> puromycin (BD Bioscience, Palo Alto, CA, USA). Successfully infected cells were then maintained using 0.2 µg ml<sup>-1</sup> puromycin and knock-down of Copine III was confirmed by western blotting.

### *Wound healing assay*

Wound healing capability was analyzed using scratch assays. Cells were grown to confluency and starved for 8h in phenol red-free DMEM + 0.1 % FBS. Monolayers were scratched and stimulated with 1 nM HRG. Wound healing was monitored using a Widefield TILL5, LONG RUN, Axiovert 200M (5 % CO<sub>2</sub> and 37 °C chamber). Time-lapse images were digitally captured every 20 min with a CCD camera over 12 h. The area recovered by the migrating cells was calculated using ImageJ and plotted in Excel. For IF, cells were stimulated, scratched and allowed to migrate for 1.5 h, afterwards cells were treated as described previously (Meira *et al.*, 2009).

### *Tissue microarray (TMA) design and immunohistochemistry analysis*

Cancer specific TMAs were prepared (Kononen *et al.*, 1998) and analyzed as described (Capra *et al.*, 2006; Confalonieri *et al.*, 2009). 2 µm sections of the TMA block were cut, mounted on glass slides and processed for immunohistochemistry (IHC). Immunostaining for Copine III was performed using mouse monoclonal antibody (1:600 dilution) followed by detection with the



EnVision Plus/HRP detection system (DAKO, Glostrup, Denmark). A semiquantitative approach was used to evaluate Copine III expression, which was scored as follows: 0, negative staining; 1, weak; 2, moderate; 3, intense. Samples showing IHC scores  $\geq 1.0$  were assigned to the Copine III-positive expression group (or high expression group), whereas those with IHC scores  $< 1.0$  were considered as Copine III-negative expression group (or low expression group).

## 5.4 Results

### *Identification of Copine III as an ErbB2 binding partner by quantitative mass spectrometry*

To identify proteins that specifically bind to pTyr1248 of ErbB2, we used stable isotope labeling of amino acids in cell culture (SILAC) (Blagoev *et al.*, 2003) in combination with an in-vitro peptide affinity pull-down approach (Schulze and Mann, 2004), followed by relative quantification by mass spectrometry (Figure 5-1a). Endogenous amino acids in the T47D breast cancer cell line were substituted by their light (Lys0 and Arg0) and heavy (Lys6 and Arg10) forms. Extracts from both populations were subjected to an affinity pull-down using peptides (Tyr and pTyr) encompassing Tyr1248 of the C-terminal tail of ErbB2. Bound proteins were eluted, subjected to SDS-polyacrylamide electrophoresis (PAGE), digested with trypsin and identified by LC-MS/MS.

Over 100 proteins were identified in each individual pull-down experiment, however, only proteins identified by  $\geq 2$  peptides and with a Mascot protein score  $\geq 20$  were selected. For quantification, specific transitions for the light and heavy form of each peptide were measured over time using multiple reaction monitoring (MRM). The ratio of the peak area for the heavy form over that of the light form was calculated. The majority of the proteins yielded a quantification ratio of around 1, reflecting equal binding to the Tyr and the pTyr peptide (Figure 5-1b). A protein was considered as a specific binder if the mean ratio of all its quantified peptides was  $\geq 1.5$ . Copine III (acc. AAH07017) was quantified with ratio of 1.8 in three independent experiments (Figure 5-1c).

The selective binding of Copine III was confirmed using western blot analysis with a Copine III specific antibody. Tyr1248 and pTyr1248-containing peptides were incubated with T47D cell lysates and used as affinity reagents. Shc, which has been identified as a pTyr1248-binding protein (Dankort *et al.*, 2001b; Schulze *et al.*, 2005) was also examined as a control. These results confirmed the specific binding of Copine III to the pTyr1248-containing peptide (Figure 5-1d).

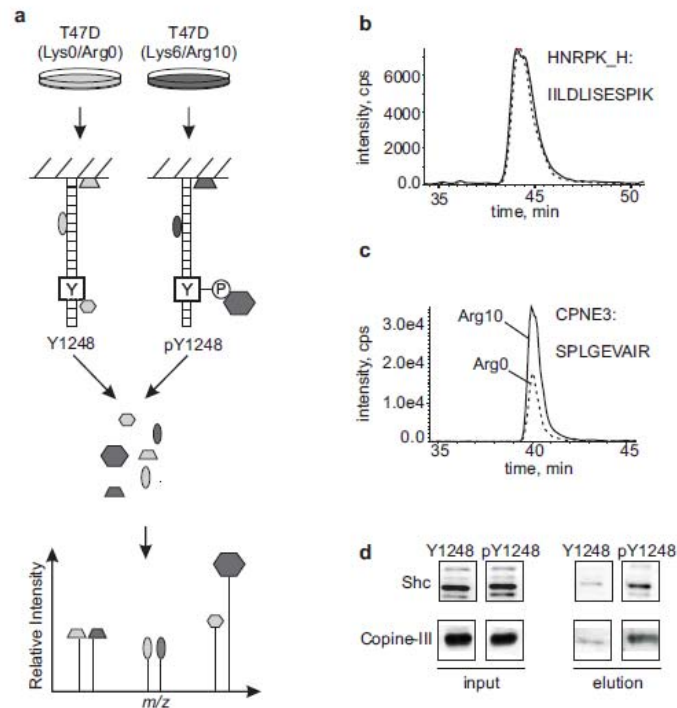


**Figure 5-1 Copine III preferentially binds to pTyr1248 of ErbB2**

(a) Schematic illustration of the peptide affinity method used to identify proteins binding to the pTyr1248 of ErbB2. 15-mer peptides encompassing the Tyr1248 of ErbB2, either phosphorylated or not, were bound to magnetic beads and incubated with protein extract from isotopically lysine (Lys6) and arginine (Arg10) labeled T47D cells (SILAC). Identification and relative quantification of proteins was done by mass spectrometry.

(b and c) Multiple reaction monitoring of single peptide pairs. One transition for each form of a peptide (Lys0/Arg0 and Lys6/Arg10) was measured over time. Peak areas were compared using Analyst 1.4.1 (for details see supplementary Material and Methods) Representative spectra for a peptide pair from a background protein (Heterogeneous nuclear ribonucleoprotein K) and a specific binding protein (Copine III) are shown.

(d) Western blot analysis of Shc and Copine III binding to Tyr/pTyr1248. Peptide pulldowns using HRG stimulated T47D cell extracts were performed and the bound proteins (elution) were monitored by western blot. As a control for equal loading, fractions of the input cell lysate were also loaded on the gel (input).

#### *Copine III is a Ca<sup>2+</sup>-dependent, membrane-binding protein*

Copine III belongs to a family of proteins, which have been shown to be Ca<sup>2+</sup>-dependent, phospholipid binders (Creutz *et al.*, 1998; Tomsig *et al.*, 2003). Copine III is ubiquitously expressed in human tissues (HUGE data base); however, essentially nothing is known about its role in normal or cancer tissue. It was shown that Copine III mRNA and protein are upregulated in response to ErbB2 expression levels and activation (Gharbi *et al.*, 2002; White *et al.*, 2004). Therefore we examined Copine III in more detail using the breast cancer cell lines T47D, with

moderate ErbB2 levels, and SKBr3, which has *ERBB2* amplification and very high levels of the receptor (Lane *et al.*, 2000).

The effect of  $\text{Ca}^{2+}$  on Copine III's cellular location was first assessed by subcellular fractionation experiments. Cells were lysed in buffer containing  $\text{CaCl}_2$  or EGTA and crudely fractionated into cytoplasmic (C) and membrane (M) fractions. In both cell lines Copine III was enriched in the membrane fraction in the presence of  $\text{Ca}^{2+}$  and shifted to the GAPDH-containing cytoplasmic fraction after the addition of EGTA (Figure 5-2a). These results demonstrate that  $\text{Ca}^{2+}$  is required for Copine III localization to membranes. Calnexin, an integral membrane protein of the endoplasmic reticulum (ER), was detected in the crude membrane fraction. Thus, we used immunofluorescence microscopy (IF) to see whether Copine III bound to the ER or to the plasma membrane (PM) in response to  $\text{Ca}^{2+}$ , by treating the cells with the  $\text{Ca}^{2+}$ -ionophore ionomycin. Copine III was detected using a monoclonal antibody directed against its C2B domain. The specificity of the antibody was verified using Copine III knock-down (KD) cells (5-3).

Interestingly, for both cell lines, Copine III was detected in the nucleus upon treatment with ionomycin. However, the role of Copine III in the nucleus was not further pursued in this study. In control DMSO treated cells, Copine III was found mainly in the cytoplasm; treatment with ionomycin caused its re-localization to the PM (Figure 5-2b). In T47D cells, Copine III staining was enriched at cell-cell adhesion membranes (Figure 5-2b left), while in SKBr3 cells Copine III localized to specific regions at the PM (Figure 5-2b, right). Thus, Copine III is a  $\text{Ca}^{2+}$ -dependent membrane-binding protein.

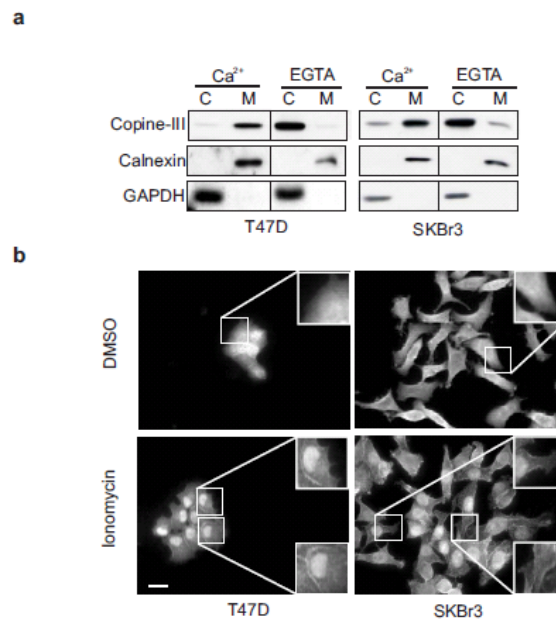


**Figure 5-2 Copine III localizes to membranes in a Ca<sup>2+</sup>-dependent manner**

(a) T47D and SKBr3 cells were incubated in buffer containing either CaCl<sub>2</sub> or EGTA, disrupted by glass-glass homogenization (Dounce) and fractionated into cytoplasmic (C) and membrane (M) fractions. Equal volumes were subjected to SDS-PAGE and subsequent immunoblotting. Calnexin was used as a marker for the membrane and GAPDH for the cytoplasmic fraction.

(b), Immunofluorescence microscopy (IF) of T47D and SKBr3 breast cancer cells. Cells were starved overnight and subsequently treated for 1.5min with 1μM ionomycin or DMSO in control cells. Copine III was visualized with a specific monoclonal antibody. Representative images are shown (scale bar: 20 μm). Inserts show 2x zooms of boxed regions.

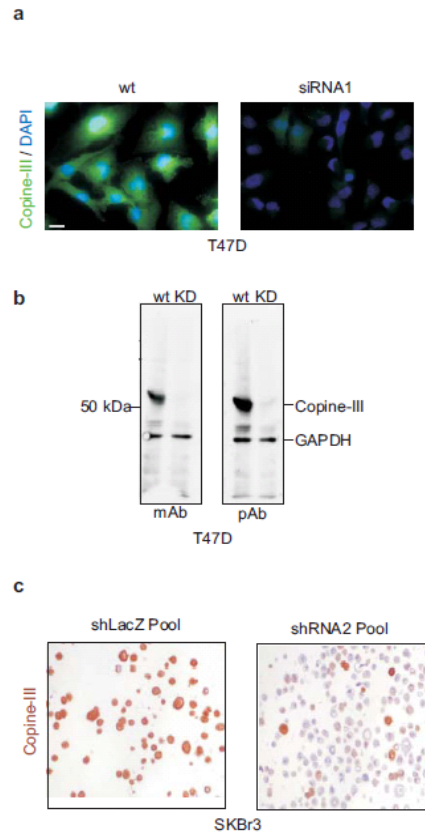


### Figure 5-3 Specificity of the $\alpha$ -Copine III monoclonal antibody

(a) Copine III was visualized with the monoclonal antibody using immunofluorescence microscopy in T47D wt and T47D Copine III KD cells. Excitation time and picture processing was the same for both images (scale bar: 20  $\mu$ m).

(b) T47D wt and Copine III KD cells were subjected to SDS PAGE and levels of Copine III were analyzed using the polyclonal peptide antibody (pAb) and the new monoclonal antibody against the C2B domain of Copine III (mAb).

(c) T47D wt and Copine III KD cells were blotted for expression of Copine III and Copine-I, its closest homolog. Copine-I expression was unaltered in Copine III KD cells.

(d) LacZ transduced and stable Copine III KD SKBr3 cell pools were embedded in paraffin blocks and IHC was performed using the Copine III specific monoclonal antibody.

### *Copine III and ErbB2 co-localize and interact at the PM*

We explored the localization of Copine III and ErbB2 in the breast cancer cell lines using IF. In control T47D cells, Copine III was diffusely distributed throughout the cytoplasm. In response to HRG, Copine III re-localized to the PM, where it co-localized with activated ErbB2 (Figure 5-4a). In control SKBr3 cells, most of Copine III was diffusely distributed throughout the cytoplasm, however, a portion also co-localized with the receptor at the PM. In SKBr3 cells ErbB2 has high levels of pTyr, even in the absence of ligands. HRG treatment caused ErbB2 to distribute along the PM, and increased Copine III at the membrane, where it co-localized with total ErbB2 (Figure 5-4b) and pTyr1248-ErbB2 (Figure 5-5).

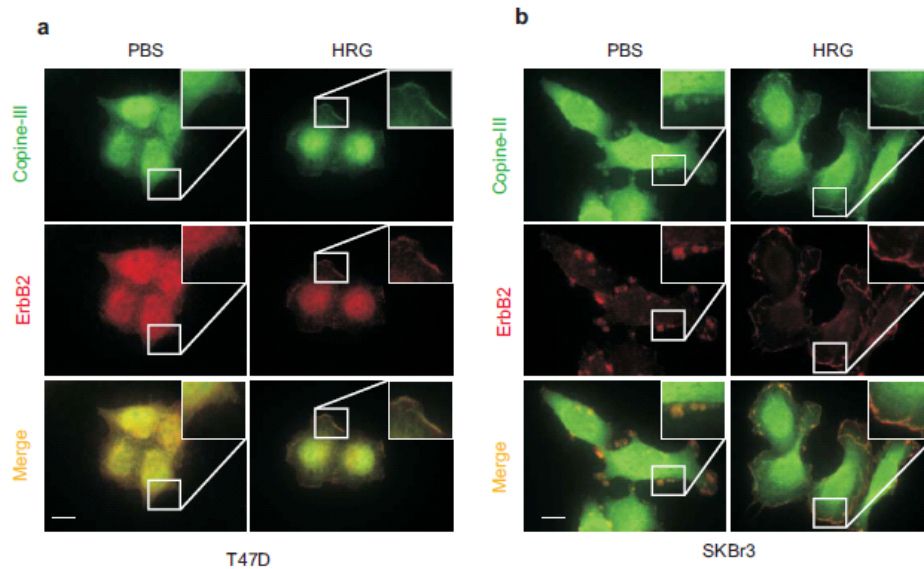


**Figure 5-4 Co-localization of Copine III and ErbB2 at the plasma membrane**

T47D (a) and SKBr3 (b) cells were starved overnight and stimulated with HRG for 20min, control cells were treated with PBS in parallel. Copine III and ErbB2 were visualized with their respective antibodies. The bottom panels are merged images, where yellow represents regions of Copine III and ErbB2 co-localization (scale bar: 10  $\mu$ m). Inserts show 2x zooms of boxed regions showing the co-localization of Copine III and ErbB2 at the plasma membrane.

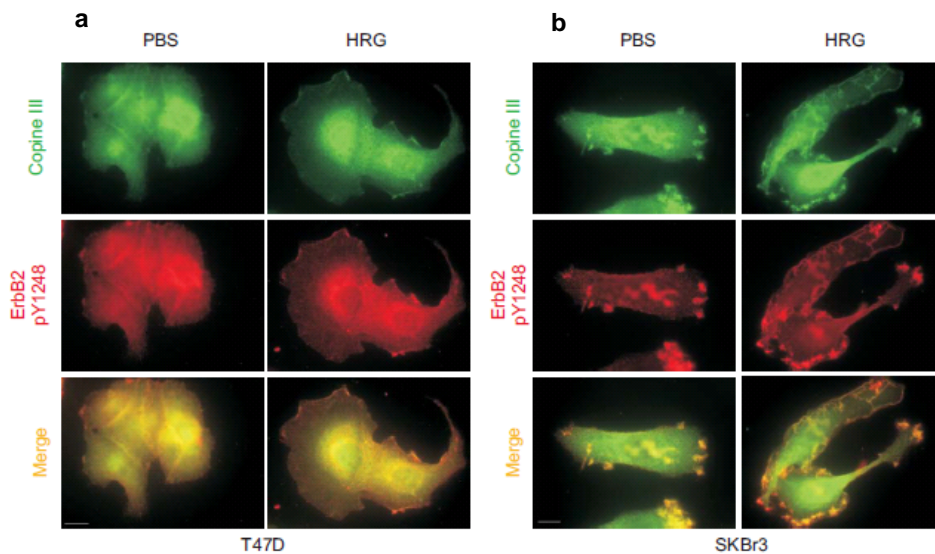


**Figure 5-5 IF staining of Copine III and pTyr1248-ErbB2 in T47D and SKBr3 cells**

T47D (a) and SKBr3 (b) cells were starved overnight and stimulated with HRG for 20min, control cells were treated with PBS in parallel. Copine III and pTyr1248-ErbB2 were visualized with their respective antibodies. The bottom panels are merged images, where yellow represents regions of co-localization of Copine III and pTyr1248-ErbB2 (scale bar: 10  $\mu$ m).

Next we used fluorescence resonance electron transfer (FRET) acceptor photobleaching (Kenworthy, 2001) to examine the interaction of Copine III and ErbB2 in fixed, HRG treated SKBR3 cells. Copine III and ErbB2 were labeled with specific primary antibodies and with a donor (Alexa488) and acceptor (Cy3) fluorophore-conjugated secondary antibody, respectively. Acceptor photobleaching was performed and FRET efficiency was measured at three regions: (1) at the membrane where both proteins co-localize, (2) in the cytoplasm where there is no co-localization and (3) outside the cell to measure background fluorescence (Figure 5-6a). FRET efficiency (E) was calculated by comparing the Alexa488 intensities of region 1, after and before photobleaching of Cy3 (Figure 5-6b). Donor intensities were corrected for background fluorescence (region 3) as well as bleaching due to imaging (region 2).

FRET efficiency was measured between ErbB2 and transferrin receptor (TR) and ErbB2 and Copine III. ErbB2 co-localized with both TR and Copine III at the PM, however, no FRET efficiency was measured between ErbB2 and TR ( $E = 0.6 \pm 1$ ), showing that these receptors co-localize but do not interact (Figure 5-17b, left). Importantly, a significant FRET efficiency was found for ErbB2 and Copine III ( $E = 8.3 \pm 1.3$ ) (Figure 5-6b, middle). As a control, no FRET efficiency was measured for only Alexa488 labeling of Copine III (Figure 5-6b, right). These results suggest that ErbB2 and Copine III interact at the PM in HRG-stimulated SKBr3 cells.

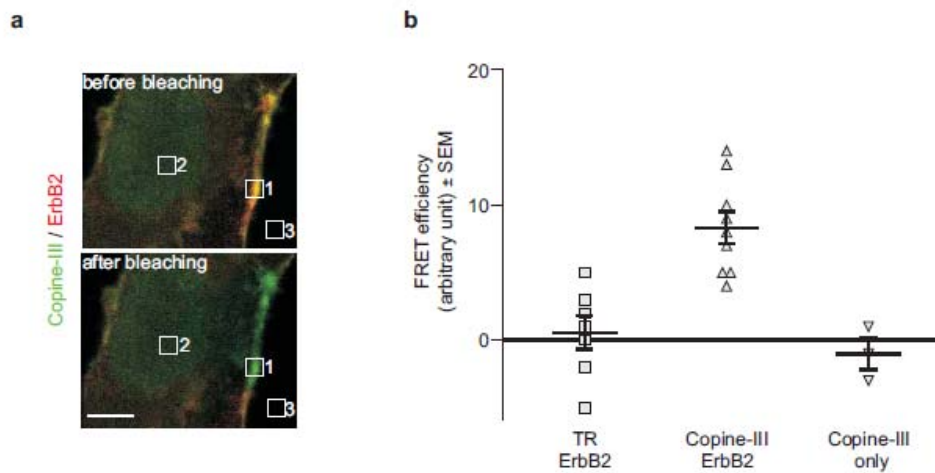


**Figure 5-6 FRET acceptor photobleaching shows the interaction of Copine III and ErbB2 at the plasma membrane**

SKBr3 cells were starved overnight and stimulated with HRG for 20min. Copine III and ErbB2 were labeled with their respective primary antibodies and visualized with an Alexa488-labeled anti-mouse and a Cy3-labeled anti-rabbit secondary antibody, respectively.

(a) Representative images of a single cell before and after acceptor bleaching are shown. Three regions of interest (boxes 1-3) were taken for FRET efficiency calculations (see Materials and Methods) (scale bar: 5  $\mu$ m). (b) Quantification of the FRET acceptor photobleaching experiments (ErbB2/Copine III, middle). In each experiment 4-10 individual cells were measured. As a control transferrin receptor (TR) was visualized with an Alexa488- and ErbB2 with Cy3-labeled secondary antibody and FRET efficiency was measured after acceptor photobleaching (ErbB2/TR, left). As an experimental control, Copine III only was visualized with an Alexa488-labeled secondary antibody and FRET efficiency was measured after photobleaching (Copine III only, right).



*Copine III interacts with the active ErbB2 receptor at the PM*

To test directly if Copine III interacts with active ErbB2, SKBr3 cells were pretreated with the ErbB tyrosine kinase inhibitor (TKI) AEE788 (Traxler *et al.*, 2004) before stimulating with HRG. In TKI-treated cells there was a dramatic decrease in the pTyr content of ErbB2 as shown by immunoprecipitating the receptor and probing the immunoprecipitates (IP) with a pTyr specific antibody (Figure 3-7a, left). Additionally, the activity of the Akt and Erk pathways were also reduced (Figure 3-7a, right). IF revealed that the intense regions of ErbB2-membrane staining in control cells were lost in TKI-treated cells and the receptor re-localized to specific intracellular regions (Figure 3-7b). Strikingly, in AEE788 treated cells there was little or no Copine III at the PM in comparison to control cells, where there was intense membrane staining. Taken together, these results show that Copine III requires active ErbB2 signaling at the PM for its localization there.

We examined complexes of Copine III and ErbB2 using co-IP experiments. ErbB2 was found in IPs of Copine III from lysates of T47D and SKBr3 cells (Figure 5-18c & e). In control cells an association of ErbB2 and Copine III was detected, reflecting autocrine receptor activity in T47D cells (Meira *et al.*, 2009) and ErbB2 overexpression in SKBr3 cells (Lane *et al.*, 2000). In Copine III IPs from lysates of HRG-treated cells there was an increase in complexed, active pTyr-containing ErbB2 (Figure 5-7c & e). Copine III does not possess an SH2- or a PTB-pTyr binding domain. Shc has both domains and has also been found associated with pTyr1248 (Dankort *et al.*, 1997; Schulze *et al.*, 2005) (Figure 5-1). Shc was detected in Copine III IPs from lysates of T47D cells, and Shc levels increased in response to HRG (Figure 5-18d). Together, these data provide evidence that Copine III is found in complexes with ErbB2 and with Shc, the latter perhaps mediating Copine III binding to the receptor.

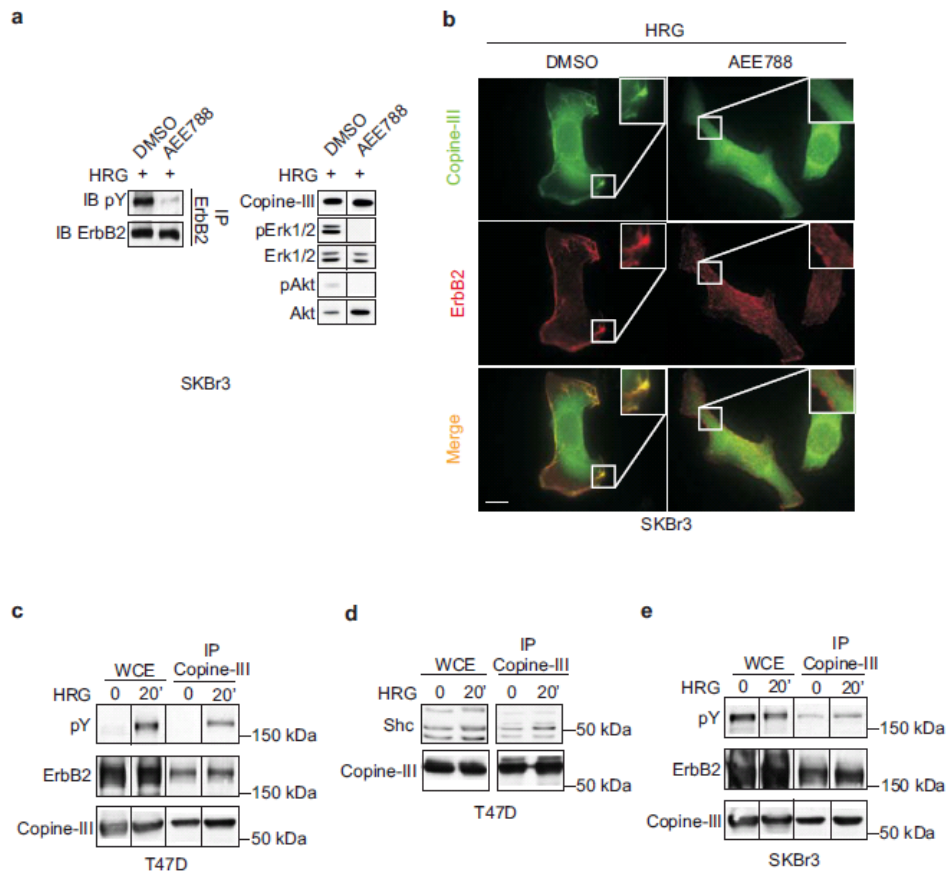


**Figure 5-7 The localization of Copine III depends on activity of the ErbB2 receptor**

SKBr3 cells were starved overnight, treated for 1.5 h with 0.5  $\mu$ M AEE788 or DMSO, for controls, and stimulated for 20 min with HRG or PBS, for controls.

(a) Extracts of control and treated cells were taken for western blot analysis. ErbB2 was immunoprecipitated and its phosphorylation status was monitored using a pTyr-specific antibody (a, left panel). Inhibition of downstream signaling pathways was monitored by western blotting of total lysates for Erk1/2, Akt and their phosphorylated forms.

(b) The localization of Copine III and ErbB2 in HRG treated SKBr3 control- and AEE788 treated cells was visualized by IF using their respective antibodies. Images of representative cells are shown (scale bar: 10 $\mu$ m). Inserts show 2x zooms of boxed regions focusing on the plasma membrane.

(c, d and e) Co-immunoprecipitation of Copine III, ErbB2 and Shc. Copine III was immunoprecipitated from lysates of control and HRG-stimulated T47D (c, d) or SKBr3 (e) cells using a specific monoclonal antibody. The co-IPs were probed for ErbB2 and overall pTyr on ErbB2 (pY in c, e) or for Shc (d). Whole cell extracts (WCE) are shown on the left of each panel.

*Copine III interacts with RACK1 and both proteins complex with ErbB2*

To gain more insight into the role of Copine III in ErbB2-mediated cellular signaling, we sought to identify Copine III binding partners. For this, SKBr3 cells with incorporated light or heavy isotopes of lysine and arginine (SILAC) were transfected with an empty control vector or a Flag-tagged Copine III, respectively. After stimulation with HRG, anti-Flag affinity purification was performed and Copine III binding partners were identified by MRM (Figure 5-8a). The analysis yielded several putative binding partners (Table 5-1), one of these being RACK1, receptor of activated C kinase (Ron *et al.*, 1994)(Figure 5-8a). In an independent experiment we quantified the relative amounts of RACK1 in Copine III IPs from SKBr3 lysates by MRM. We found a 1.5-fold enrichment of RACK1 in Copine III IPs vs. control IPs (data not shown), confirming the interaction. An examination of ErbB2 IPs from SKBr3 and T47D cells showed that ErbB2 is phosphorylated at Tyr1248 and complexed Copine III, Shc and RACK1 (Figure 5-8b and 5-8c).

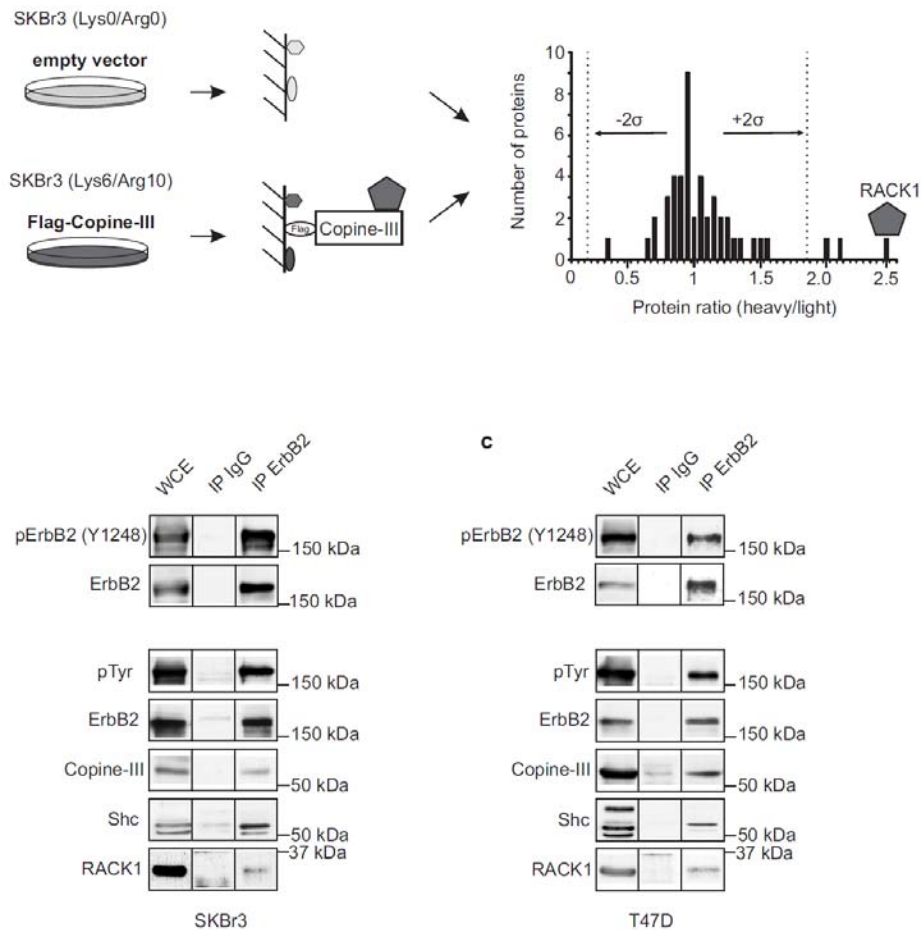


**Figure 5-8 Copine III binds RACK1 and localizes to focal adhesions**

(a) Identification of Copine III binding partners. SKBr3 labeled with SILAC (light (Lys0/Arg0) or heavy (Lys6/Arg10) isoforms) were transiently transfected with an empty vector or a vector expressing Flag-Copine III, respectively. Proteins were extracted and subjected to an affinity purification using anti-Flag columns. Specific binders to Flag-Copine III were identified by LC-MS/MS and quantified using MRM. The protein ratios (heavy/light) of all quantified proteins were plotted. The cut-off for specific binders was determined by assuming a normal distribution and setting the cut-off to  $\pm 2\sigma$  from the mean.

(b + c) Co-IP of Copine III, Shc and RACK1 with ErbB2 in HRG-stimulated cells. In IPs of ErbB2 from HRG-treated SKBR3 (b) and T47D (c) cells ErbB2 Tyr1248 phosphorylation was monitored with a specific antibody. In a further experiment ErbB2 co-IPs were monitored for Shc, Copine III and RACK1 by western blotting. ErbB2 phosphorylation was monitored using a total phospho-tyrosine (pY) antibody. In parallel IgG IPs were probed as controls. Whole cell extracts (WCE) are shown on the left.

*Copine III localizes to focal adhesions and is required for ErbB2-dependent tumor cell migration*

The adaptor protein RACK1 acts as a scaffold in numerous signaling events including cell migration, where it has been shown to localize to nascent focal adhesions (FAs) (Cox *et al.*, 2003). Our finding that Copine III interacts with RACK1 prompted us to examine whether Copine III might also have a role in cell migration. First, we used IF to examine Copine III localization. Copine III and phosphorylated focal adhesion kinase (pTyr397FAK) were both diffusely present in the cytoplasm of control T47D cells and upon HRG treatment co-localized at the PM (Figure 3-9a), suggesting that Copine III is a FA-associated protein.

Next we examined the role of Copine III in cell migration using a KD approach. Two pools of Copine III KD cells and a pool expressing the control (LacZ) vector were generated in T47D cells. Copine III KD was almost complete in pool 2, while it was approximately 50 % in pool 1 (Figure 5-9b, insert). The effect of Copine III KD on migratory ability of T47D cells was examined using a wound healing assay. Wound closure of control and Copine III KD cultures left untreated or stimulated with HRG was monitored over 12h (Figure 5-9b). Basal migration of control cells was low and not affected by Copine III KD. Importantly, compared to control cells, HRG-stimulated Copine III KD cells were significantly impaired in their ability to migrate into the wound ( $p < 0.005$ ) (Figure 5-9b).

The localization of Copine III, pTyr397FAK and ErbB2 was also examined in wounded monolayers. In untreated cells none of these proteins strongly localized to the cell membrane (Figure 5-9c and d, PBS). In contrast, in HRG-treated cultures, Copine III, pTyr397FAK and ErbB2 were each present in membrane protrusions at the edge of the wounded area. Moreover, a high degree of overlap between Copine III and pTyr397FAK staining (Figure 5-9c) and Copine III and ErbB2 staining (Figure 5-9d) was evident. In Copine III KD cells, pTyr397FAK and ErbB2 were localized to membrane protrusions in response to HRG (data not shown), showing that these events are not dependent upon Copine III.

Src and FAK, two proteins with important roles in cell migration were further analyzed. Src, but not FAK, was found in complex with ErbB2 after HRG stimulation (Figure 5-9e).

A western analysis revealed that Src activity increased in control HRG treated cells, as shown by the increase in pTyr418Src levels. In contrast, there was little or no increase in pTyr418Src levels in the two Copine III KD pools (Figure 3-9f). Moreover, the level of pTyr925FAK, a site that has been shown to require Src kinase activity to become phosphorylated (Brunton *et al.*, 2005), also increased in HRG-treated control cultures, while little or no increase was observed in Copine III KD pools (Figure 5-9f), attesting to the decrease in Src activity. In contrast to the effects on Src

kinase activity, activation of the Akt and Erk pathways was similar in response to HRG-treatment in the Copine III KD cultures and the control cells (Figure 5-9f). These findings imply that Copine III might be a component of focal adhesions that is required for Src activity and thus for regulating focal adhesion turnover and ErbB2-mediated migration in response to HRG.

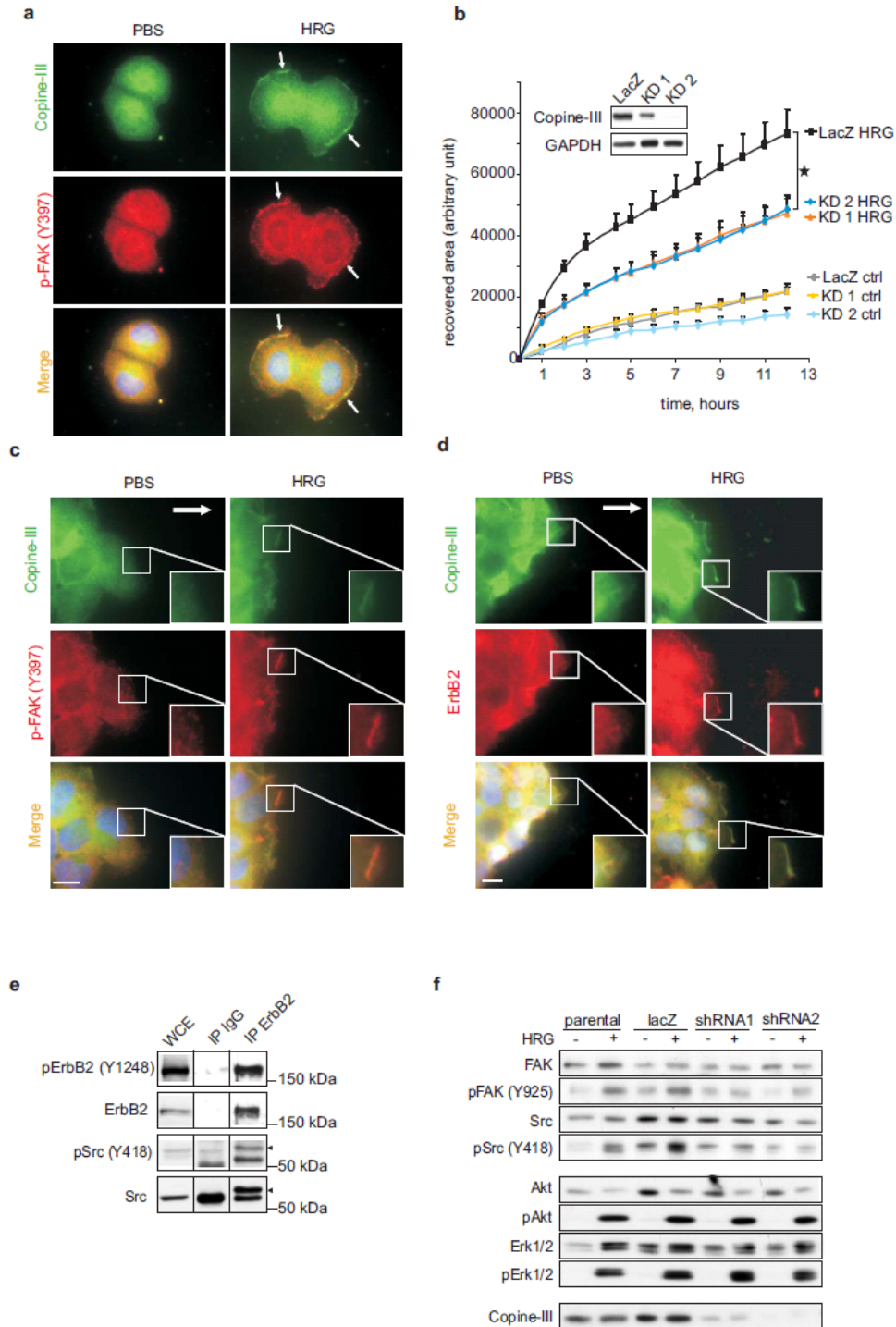


**Figure 5-9 Copine III has a role in HRG-mediated T47D cell migration.**

**Figure 5-9**

(a) Co-localization of Copine III and phosphorylated focal adhesion kinase (pFAK). T47D cells were starved overnight and stimulated with 5 nM HRG for 20min. Control cells were treated with PBS in parallel. Copine III and pTyr397FAK were visualized using their respective antibodies. Merged images in the bottom panel include Hoechst staining for the nucleus in blue (scale bar: 10  $\mu$ m). The arrows indicate areas of co-localization.

(b) Wound healing assay in T47D Copine III KD pools. Two pools of Copine III KD T47D cells were generated with different shRNA targeting vectors (KD1 and 2). A control LacZ pool was also prepared. Expression levels of Copine III in the KD1 and KD2 and the LacZ pools is shown; GAPDH is the loading control (insert). T47D cells were grown to confluency, starved in DMEM for 8 h, then stimulated with 1 nM HRG and subsequently scratched. Cell migration into the wound was monitored for 12 h in 4-6 regions of the scratch. The recovered area of the wound is shown by the mean  $\pm$  SEM. \*  $P < 0.005$

(c and d) Localization of Copine III and pTyr397FAK (c) and Copine III and ErbB2 (d) in migrating T47D cells. Cells were grown to confluency, starved overnight, then stimulated with 5 nM HRG, scratched and allowed to migrate for 1.5 h before they were fixed and stained. Copine III, pTyr397FAK and ErbB2 were visualized by IF using their respective antibodies. The direction of migration into the wound is indicated by the arrow. Merged images in the bottom panel include Hoechst staining for the nucleus in blue (scale bar: 10  $\mu$ m). Inserts show 2x zooms of boxed regions focusing on the leading edge of the migrating monolayer.

(e) Co-IP of Src with ErbB2 in HRG-stimulated T47D cells. IPs of ErbB2 from HRG-treated T47D cells were monitored for Src and pY418 Src by western blotting. ErbB2 was monitored using a total ErbB2 antibody and its phosphorylation was analyzed using a pTyr1248 specific antibody. In parallel IgG IPs were probed as controls. Whole cell extracts (WCE) are shown on the left.

(f) The two pools of Copine III KD T47D cells, the control LacZ pool and the parental cells were treated or not with HRG for 20min. Cell lysates were prepared and western blots were probed for the level of FAK, pTyr925FAK, Src, pTyr481Src, Akt, pAKT, Erk1/2, pErk1/2 and Copine III.

*Copine III expression in human cancer*

We examined Copine III and ErbB2 expression levels in breast tumor cell lines and primary tumors. Copine III was expressed to varying degrees in the breast cancer cells lines, with the highest levels in SKBr3 and BT474, both having *ERBB2* amplification (Figure 5-10a). These data correlate with previous publications showing Copine III upregulation in response to ErbB2 overexpression (Gharbi *et al.*, 2002; White *et al.*, 2004). We also examined Copine III RNA expression in 49 primary breast tumors (Farmer *et al.*, 2005). Plotting log gene expression values of *ERBB2* against expression values for *CPNE3* revealed that high levels of *CPNE3* were significantly correlated with *ERBB2* amplification; 10 of 11 tumors with the highest level of Copine III also possessed the amplicon (Figure 5-10b).

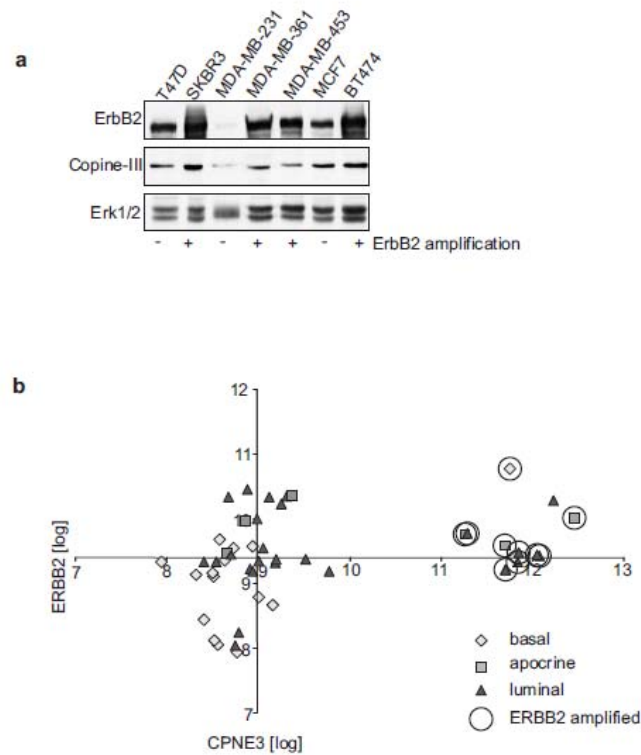


**Figure 5-10 Copine III expression correlates with ErbB2 amplification in breast cancer**

(a) Protein expression levels of Copine III and ErbB2 were analyzed in different breast cancer cell lines by western blotting. WCEs for each cell line were subjected to western blotting and probed for ErbB2, Copine III and Erk1/2 as loading control. The ErbB2 amplification status is indicated by +/-.

(b) Evaluation of *CPNE3* expression values in 49 primary breast tumor samples (Farmer *et al.*, 2005). Log expression of *CPNE3* is plotted on the y-axis and *ERBB2* log expression values on the x-axis. Axes are plotted through the median expression levels of *CPNE3* and *ERBB2*, respectively. The different subtypes of the analyzed breast tumors are denoted: Basal (◇), apocrine (◻) and luminal (▲). *ERBB2* amplified tumors are highlighted with circles.



We also performed an analysis of Copine III expression in different human tumors, initially examining data from published transcriptome studies ([www.oncomine.org](http://www.oncomine.org)) (Rhodes *et al.*, 2004). We found that *CPNE3* expression increased significantly in metastatic prostate cancer in comparison to normal prostate and non-metastatic tumors (data from (Yu *et al.*, 2004)) (Figure 5-11a). Moreover, in comparison to normal ovary, there were significantly higher levels of *CPNE3* in ovarian endometrioid adenocarcinoma (OEA), the second most common type of ovarian cancer (data from (Hendrix *et al.*, 2006)) (Figure 5-11b).

Based on these findings we performed IHC staining of Copine III in breast, prostate and ovarian TMAs. There was a tendency for Copine III to be up-regulated in the epithelial component of cancer tissue compared to normal tissue (Figure 5-11c). Some Copine III staining was evident in normal breast, while normal prostate and ovarian tissues have very low levels of Copine III (Figure 5-11d). Tumors of all three types showed higher Copine III levels. These findings suggest that the up-regulation trend revealed by the Oncomine analysis is retained at the protein level, implying a potential biological function of Copine III in human cancer.

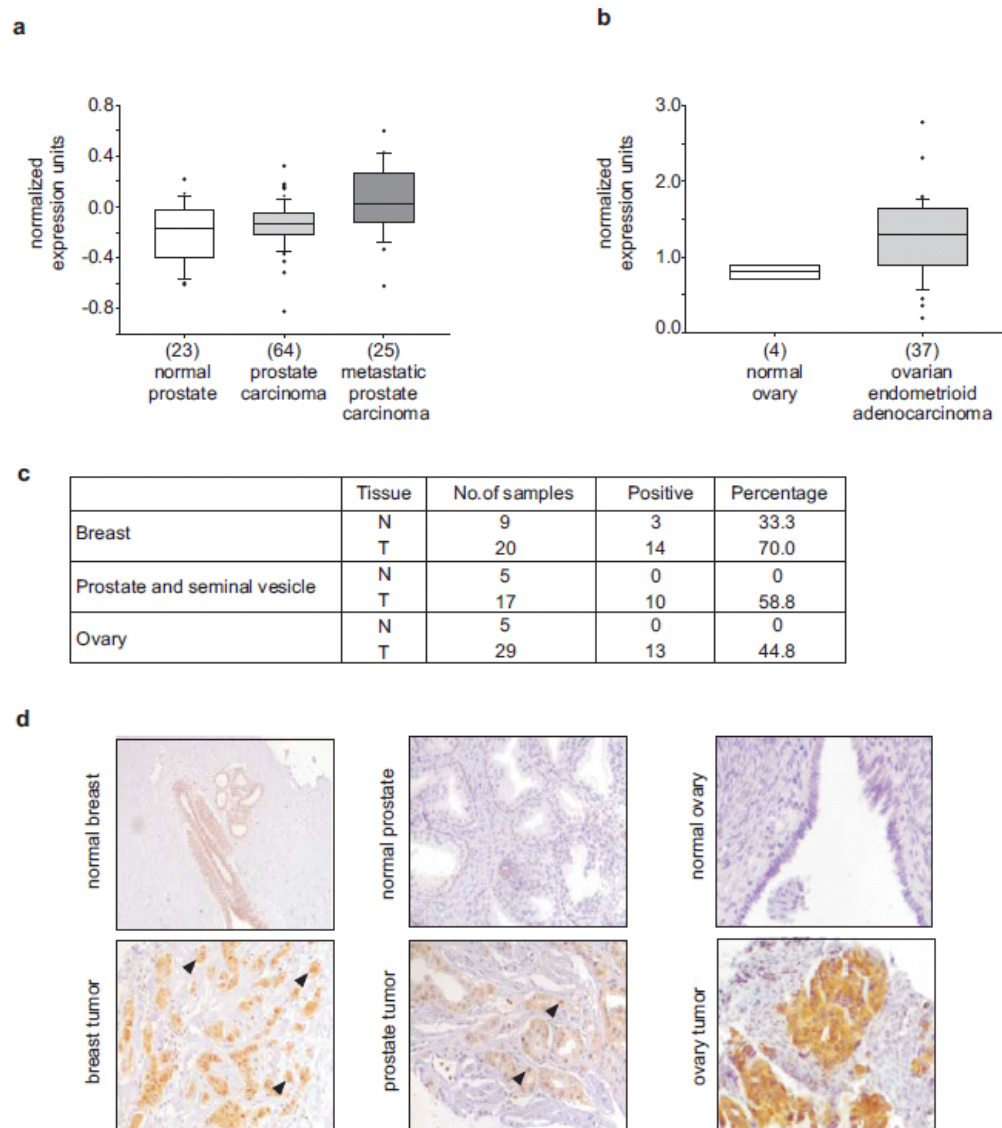


**Figure 5-11 Expression of Copine III in breast, prostate and ovarian cancer samples**

(a and b) *CPNE3* expression analysis in different microarray datasets from the Oncomine database ([www.oncomine.org](http://www.oncomine.org)) (Rhodes *et al.*, 2004). *CPNE3* RNA expression levels in samples from normal prostate tissue, carcinoma and metastatic prostate carcinoma are shown (Yu *et al.*, 2004)(a) as well as in normal ovary and ovarian endometrioid adenocarcinoma samples from the Hendrix *et al.* dataset (Hendrix *et al.*, 2006)(b).

(c) Analysis of Copine III expression in a human breast, prostate and ovarian tissue microarray (TMA). The table shows the number of samples analyzed for normal (N) and tumor tissue (T) for the respective cancer type. The number of Copine III positive samples is annotated as well as their percentage from all analyzed samples using a cut-off of > 1.0 for breast and  $\geq 1.0$  for prostate and ovarian tissue samples.

(d) Examples of IHC staining for Copine III using the monoclonal antibody in breast, prostate and ovarian normal and cancer tissue samples. The magnification is 20x. The arrow heads indicate nuclear Copine III staining.

## 5.5 Discussion

ErbB2 has been shown to play a pivotal role in various types of human cancer. In breast cancer, ErbB2 overexpression correlates with aggressive disease and a metastatic phenotype (Hynes and Lane, 2005). In search of novel ErbB2 effector proteins, we identified Copine III via its ability to specifically bind an ErbB2 pTyr1248-containing peptide. Our results show that Copine III interacts with ErbB2 at the plasma membrane of breast tumor cells in response to HRG treatment. Moreover, we show that Copine III binds the focal adhesion-associated protein RACK1 and is also present in focal adhesions in cells with active ErbB2. Importantly, KD of Copine III in T47D breast tumor cells causes a decrease in HRG-induced migration. Our results suggest that Copine III is a novel ErbB2-interacting protein that might link ErbB2 to focal adhesions, thereby contributing to HRG induced cell motility.

Copines are a conserved family of ubiquitously expressed proteins found in many eukaryotic organisms (Tomsig and Creutz, 2002). Copines possess two C2 domains (C2D-A and C2D-B) and an A domain; C2Ds are responsible for Ca<sup>2+</sup>-dependent membrane-binding properties and A domains bind proteins (Tomsig *et al.*, 2003). Copine family members from various organisms have been shown to bind membranes (Church and Lambie, 2003; Gottschalk *et al.*, 2005; Hua *et al.*, 2001). Bioinformatic analysis showed that aspartate residues required for Ca<sup>2+</sup>-binding are conserved in both Copine III C2Ds. Additionally, between the C2D-B and the A domain of Copine III there is a Lys-rich cluster, which, in PKCs, has been shown to bind phosphatidylinositol(4,5)P<sub>2</sub> thereby strengthening membrane affinity (Guerrero-Valero *et al.*, 2007). Using IF we show that Copine III and ErbB2 co-localize to the PM after HRG stimulation. Moreover, in FRET acceptor photobleaching experiments we measured a FRET efficiency of 8 ± 3 between ErbB2 and Copine III, which agrees well with the FRET efficiency of 14 ± 3 between ErbB2 receptors (Nagy *et al.*, 1998). Taken together, our analysis of Copine III suggests that it is a Ca<sup>2+</sup>-dependent membrane-binding copine that responds to ErbB2 activation and localizes to the PM in close proximity to the receptor.

How does Copine III interact with ErbB2? C2Ds have been classified as Type I and Type II (Nalefski and Falke, 1996) and the Type II C2D of PKCδ has been shown to directly bind specific pTyr-containing peptides (Benes *et al.*, 2005). However, we consider it unlikely that Copine III directly binds ErbB2 since a bioinformatic analysis suggested that Copine III's C2Ds are both likely to be Type I. Moreover, the residues in PKCδ that have been shown to be essential for pTyr binding are not conserved in Copine III. We favor the hypothesis that Shc, which possesses both an SH2 and a PTB domain, mediates Copine III's interaction with ErbB2. Indeed,

complexed Shc was identified in Copine III co-IPs (Figure 5-7d). Although copines have been linked to other membrane receptors, including the nicotinic acetylcholine receptor in *C. elegans* and the TNF $\alpha$  receptor in HEKs (Gottschalk *et al.*, 2005; Tomsig *et al.*, 2004), this is the first description of a copine interaction with ErbB2 or any other RTK.

Copine A domains have been shown to selectively bind various proteins (Tomsig *et al.*, 2003), which suggests that different copines respond to Ca<sup>2+</sup> signals by transporting selectively bound proteins to phospholipid-containing membranes, where they influence activity of signaling pathways. Using mass spectrometry we identified seven Copine III interacting proteins, RACK1 (Figure 5-8) and six other cytoplasmic and nuclear proteins (Table 5-1). This is interesting since we also observed enhanced Copine III nuclear staining following Ca<sup>2+</sup> stimulation or HRG treatment (Figure 3-13b and 3-15) and Copine III nuclear staining was observed on breast and prostate TMAs (Figure 3-11d, arrows). However, this was not pursued further in our studies, which were focused on the Copine III binding partner RACK1.

Candidates	Acc. Number	Protein Name	Ratio (heavy/light)
GBLP_HUMAN	P63244	Guanine nucleotide-binding protein subunit beta-2-like 1, RACK1	3.29
THOC4_HUMAN	Q86V81	THO complex subunit 4	3.12
NUCL_HUMAN	P19338	Nucleolin	21.32
TOP1_HUMAN	P11387	DNA topoisomerase 1	13.44
ILF2_HUMAN	Q12905	Interleukin enhancer-binding factor 2	7.67
YBOX1_HUMAN	P67809	Nuclease-sensitive element-binding protein 1	7.25

**Table 5-1 Putative Copine III binding partners**

Candidates found to specifically bind to Flag-Copine III are listed with their accession number, protein name and ratio of quantification. For the ratio peak areas for the "heavy" stable isotopes (Lys6/Arg10) were divided by peak areas for the "light" stable isotopes (Lys0/Arg0).

The adaptor protein RACK1 acts as a scaffold in numerous signaling events including cell migration, where it has been shown to localize to nascent focal adhesions (FAs) (Cox *et al.*, 2003). RACK1 was recently shown to associate with, and be required for FAK activation (Kiely *et al.*, 2009). We provide evidence that Copine III binds RACK1 and co-localizes with pFAK at focal adhesions in the migrating front of breast cancer cells. Moreover, in Copine III KD cells we observe decreased Src-activity and decreased FAK-phosphorylation at the Src site (pY925). Phosphorylation of Tyr925FAK by Src is required for proper focal adhesion turnover and cell migration (Brunton *et al.*, 2005). A RACK1-Src association has been described (Miller *et al.*, 2004). Thus, we postulate that Copine III is a ErbB2- and Ca<sup>2+</sup>-dependent membrane binding protein that functions at focal adhesions, where it contributes to Src activity and tumor cell migration. The exact mechanism by which Copine III influences cell migration still remains to be

elucidated in future studies. Since other cellular read-outs, such as proliferation and anchorage-independent growth were unaltered in Copine III KD T47D cells, Copine III's influence in response to HRG appears to be specific to migration (Figure 5-12).

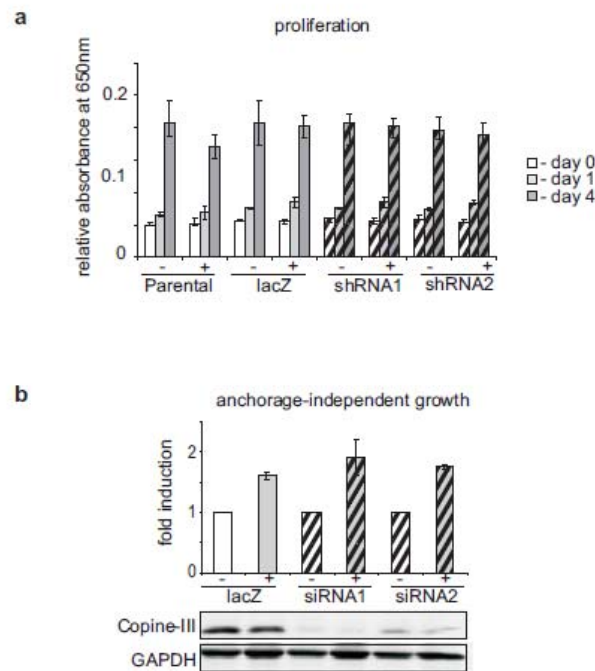


#### Figure 5-12 Analysis of Copine III KD cells

(a) The relative proliferation of control and Copine III KD T47D cell pools was monitored using the methylene blue assay as shown previously (Boulay *et al.*, 2008). Cell proliferation was measured in DMEM + 10 % FBS for 4 days. The relative proliferation is shown by the absorbance at 650nm.

(b) The potential for anchorage-independent growth was measured in T47D control and Copine III KD (siRNA) cells. Cells were plated on polyhema-coated plates and allowed to grow without and in the presence of HRG (Boulay *et al.*, 2008). The fold induction of growth compared to the unstimulated cells is shown. The KD of Copine III was verified by western blotting at the end of the experiment.

By performing pull-down assays with ErbB2 pTyr-containing peptides we have identified multiple proteins with roles in migration (Marone *et al.*, 2004). PLC $\gamma$ 1 and Memo were shown to interact with pTyr1996 and 1222, respectively, and cells with KD of either protein were impaired in HRG-induced directional migration (Meira *et al.*, 2009). Using a KD approach, we show here that Copine III is also required for HRG-induced T47D cell migration. It is tempting to speculate that in cells with low Copine III, ErbB2 loses its ability to couple to proteins and pathways involved in motility. Considering these and other proteins that interact with ErbB2, we propose the following model: In response to ligand activation, ErbB2 binds and activates PLC $\gamma$ 1 (Meira *et al.*, 2009), which causes an increase in diacylglycerol (DAG) levels and initiates

$\text{Ca}^{2+}$  influx from the ER and through store-operated channels into the cytoplasm (Kheifets and Mochly-Rosen, 2007); (Patterson *et al.*, 2005). Interestingly, specific residues that have been mapped in the C2D of PKC $\alpha$  as being essential for RACK1 binding (McCahill *et al.*, 2002), are conserved in Copine III C2D-B. Therefore, it might be possible that RACK1, which is thought to direct PKCs to specific membrane locations (Kheifets and Mochly-Rosen, 2007), might also direct Copine III to the plasma membrane in close proximity to ErbB2. This enables Copine III to interact with the receptor and influence Src activity and cell migration (Figure 5-13).

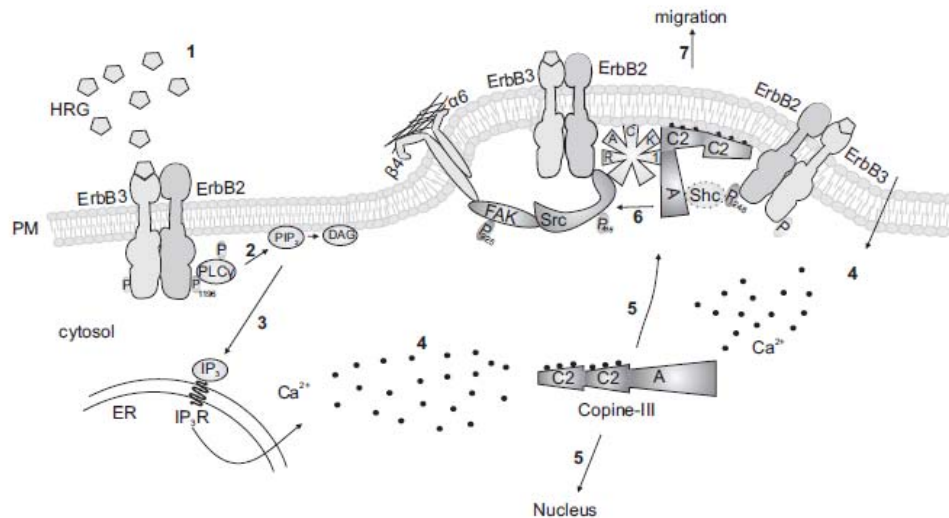


**Figure 5-13 Hypothetical model for the role of Copine III in ErbB2-dependent cell migration.**

Upon stimulation of ErbB2/ErbB3 heterodimers with HRG (1), PLC $\gamma$ 1 binds pTyr1996 of ErbB2 and, once activated, cleaves PIP $_2$  into DAG and IP $_3$  (2), which binds IP $_3$ R (3) leading to the release of Ca $^{2+}$  from intracellular stores and through store-operated channels (4). Ca $^{2+}$  influx allows Copine III to re-locate to the nucleus or the plasma membrane (5). The elucidation of a putative role for Copine III in the nucleus awaits further investigation. At the PM, RACK1 directs it to a specific membrane location in close proximity to ErbB2. It is possible that Copine III interacts with RACK1 via a conserved motif in the C2D domain (McCahill *et al.*, 2002). Copine III associates with pTyr1248, very likely via Shc, and influences Src activation (6), thereby influencing ErbB2-induced cell migration (7). We have seen a direct interaction of Src with ErbB2 in our experiments, which we have shown here. We have drawn a direct Shc-Copine III interaction, however, as indicated by the dots, it is possible that another protein mediates the interaction.

In primary human tumors there was some evidence for a functional relationship between Copine III and ErbB2, since Copine III mRNA and protein levels were shown to correlate with ErbB2 expression (Gharbi *et al.*, 2002; White *et al.*, 2004). We have extended these studies by examining a panel of 49 breast tumors (Farmer *et al.*, 2005) and showing that there is a significant correlation between CPNE3 RNA levels, and ERBB2 gene amplification and

expression,. Furthermore, data mining (Oncomine) and data from our own TMAs provide evidence that Copine III levels are increased in prostate and ovarian tumors. Taken together, these results suggest that Copine III function might be important in multiple cancer types. Our results implicate Copine III as an important player in ErbB2-mediated cancer cell motility making Copine III an interesting target in ErbB2-mediated cancers.

## 5.6 Acknowledgements

We would like to thank Elizabeth A. Grimm for the polyclonal Copine III antibody, Martin Spiess for the Transferrin receptor antibody, Susanne Schenk for help in generating the Copine III monoclonal antibody, Laurent Gelman for help with FRET, Michael Rebhan for some bioinformatic analyses and Gwen MacDonald and Julien Dey for helpful discussions. We would also like to thank Daniel Hess and Florence Dalvai for help with establishing the “MRM buddy”. The work of CH, MV and MB was partially supported by TRANSFOG FP6 IP funding (LSHC-CT-2004-503438). The laboratories of NEH and JH are supported by the Novartis Research Foundation.





## 6 COPINE III *IN VIVO*

### 6.1 Introduction

In the previous section we showed how Copine III was identified as an ErbB2-interactor and illustrated its role in cell migration. Cell migration is a key trait of both unicellular as well as multicellular organisms. Cells are required to migrate during embryogenesis and in the adult, for example during wound healing. In cancer, cell migration plays a pivotal role, since cancer cell migration is an initial step of tumor metastasis. Tumor cells migrate from the initial tumor to invade the surrounding tissue and the lymphatic or blood vasculature, which they subsequently leave again to form metastasis. In breast cancer, metastatic tumors often spread to the brain, which correlates with a very poor prognosis for the patients. Therefore, it is important to elucidate the mechanisms underlying cancer cell migration.

Since we detected a migration phenotype (scratch assay, section 5.3) for Copine III KD cells, we wanted to follow-up on this studying the effect of a Copine III KD *in vivo*. The idea was to first assess the *in vivo* tumor growth of Copine III KD cells and later on analyze their metastasis potential. However, in this section only the *in vivo* tumor growth assays will be discussed, as the metastasis analysis has not been performed up to date.

### 6.2 Materials and Methods

#### *Generation of Copine III rescue cell pools*

For each rescue construct three synonymous (silent) mutations were introduced into the DNA sequence of Copine III in such a way that the shRNA can no longer recognize the mRNA. Thus Copine III will be expressed and not silenced in cells expression these constructs. Furthermore, due to the silent mutations introduced the amino acid sequence of Copine III will stay intact. These rescue constructs were cloned into pLNCX2, a plasmid carrying a CMV promoter and a Hygromycin resistance that is often used for retroviral infections.

Two days after seeding the packaging cell line HEK293 was transfected by adding 15  $\mu$ l Fugene directly to 185  $\mu$ l Optimem. Six  $\mu$ l DNA were added to this mix and incubated for 30 min at RT. The mixture was added dropwise to the cells. One day after transfection the medium was changed to fresh and after another it was harvested. The medium was filtered through a 0.45  $\mu$ m cellulose acetate filter, 30  $\mu$ l of 4 mg/ml polybrene were added and the mixture was used to infect the Copine III KD cells. Fresh medium was added to the packaging cell line, and

virus harvested 24 h later for a second infection. Two days after the initial infection the selection was started using 500 µg/ml Hygromycin B. After selection the cells were maintained in 200 µg/ml Hygromycin B.

*Proliferation assay –methylene blue*

Cells (2500/well) were seeded in 100 µl DMEM + 10 % FCS into a 96-well plate and allowed to attach for 24 h. At day 0 the cells were treated or not with 1 nM HRG. Cells were analyzed at day 0, 2 and 4. For this the cells were fixed by adding 25 µl 20 % glutaraldehyde solution to the medium for 10 min. Afterwards, the cells were washed 3x in H<sub>2</sub>O and stained with 50 µl 0.05 % methylene blue for 10 min. Again, the cells were washed 3x with H<sub>2</sub>O and then lysed in 3 % HCl for 30 min. The absorbance was read at 650nm and plotted as a measure for the relative proliferation of the cells.

*PolyHema assay*

Six cm plates were coated with poly(2-hydroxyethylmethacrylate) (PolyHema) to prevent cells from attaching to the surface. Cells (1x10<sup>6</sup>) were seeded at day 0 and stimulated or not with 1 nM HRG. Cells were left to grow for 4 days and afterwards counted. The total viable cell number was plotted as a read-out for the ability of the cells to grow in anchorage-independent conditions.

*Migration assay – Boyden chamber*

The ability of the cells to migrate in a ligand gradient was assayed in Boyden chambers. The bottom membrane was coated with 25 µl/ml collagen I. Cells were starved overnight in DMEM + 0.1 % FCS, harvested and counted. Cells (1x10<sup>5</sup>) were seeded in serum-free medium in the upper chamber. 600 µl medium with or without 1 nM HRG were put into the lower chamber. The cells were allowed to migrate through the membrane in a ligand gradient for 3 h. Afterwards the non-migrating cells were removed with a cotton swab and the migrated cells were fixed with 4 % paraformaldehyde for 30 min. The nuclei were stained with Hoechst and the number of migrated cells was counted.

*Adhesion assay*

Nunclon Surface plates were coated with collagen (10 µg/ml), laminin (10 µg/ml) or fibronectin (10 µg/ml). After that the wells were blocked with 10 µl 10 mg/ml BSA for 1 h at RT. Cells (1.5x10<sup>5</sup> / ml) were seeded in 10 µl in triplicate per condition +/- 1 nM HRG and allowed to adhere for 1 or 2 h. Then the plate was flooded with PBS to remove non-adherent cells. Adherent cells were fixed in 4 % paraformaldehyde and stained using crystal violet. Cells were counted and the mean of the triplicate +/- SD was plotted.

*Injection of cells into the mammary fat pad and tumor measurements*

Cells ( $1 \times 10^6$ ) were injected into the 4<sup>th</sup> mammary fat pad of 4-6 week old nude mice.

Tumor growth *in vivo* was measured twice a week following the injections. Mice were sacrificed once tumors reached a size close to 2 cm<sup>3</sup>. Tumor length and width was determined and the

total volume was calculated according to:  $V = \left(\frac{w}{2}\right)^2 \times \pi \times l$  (cm<sup>3</sup>).

*Dissection of tumors, preservation and cutting*

Tumors were excised and their final weight measured. The tumor was fixed in freshly prepared 4 % paraformaldehyde in PBS. Half of the material was stored in 70 % ethanol until embedding in paraffin. The other half was put into 30 % sucrose and frozen embedded into O.C.T.. Additionally, two very small tumor sections were snap frozen in liquid nitrogen for protein and RNA extraction.

*Immunohistochemical stainings*

Stainings were carried out with the Discovery XT Staining Module (Ventana Medical Systems). Images were acquired with a Leica DFC420 camera on a Nikon Eclipse E600 microscope using Plan Fluor 10x/0.3 and 20x/0.5 lenses.

Sections were stained for KI-67 (proliferating cells), cleaved caspase 3 (apoptotic cells), CD31 (vessels) and Copine III.

*Protein and RNA extraction*

Snap frozen tumors were resuspended in 500-1000  $\mu$ l lysis buffer and homogenized using a tissue homogenizer. Extracts were spun at 13200 rpm for 30 min to remove debris. Total protein content in the supernatant was measured using Bradford.

RNA was extracted using TRIzol reagent and washed using the RNeasy Mini kit according to the manufacturer's instructions.

*Microarray*

Total RNA was isolated from 3 individual tumors per group (Parental, Copine-III shRNA1, Copine-III shRNA-2). All RNAs were individually amplified and labeled using the Ambion MessageAMP III RNA amplification kit. Biotinylated, fragmented cRNA was hybridized to Affymetrix U133 plus 2.0 human GeneChips™ (Affymetrix). Expression values were estimated using the GC-RMA implementation found in Gendata's Refiner 4.5 software.

The data analysis and gene filtering was performed using R/Bioconductor (Gentleman, 2004 #58). Signal condensation was performed using only the RMA from the Bioconductor Affy package. Differentially expressed genes were identified using the empirical Bayes method (F-test) implemented in the LIMMA package and adjusted with the False Discovery Rate (FDR) method (Wettenhall, 2004 #59). Hierarchical clustering and visualization was performed in R. Gene lists from the resulting contrasts were further classified into regulatory networks and pathways with Ingenuity Pathways Analysis (Ingenuity® Systems). A data set containing gene identifiers and corresponding expression values was uploaded into in the application.

Each gene identifier was mapped to its corresponding gene object in the Ingenuity Pathways Knowledge Base. These genes, called focus genes, were overlaid into a global molecular network developed from information contained in the Ingenuity Pathways Knowledge Base. Networks of these focus genes were then algorithmically generated based on their connectivity. Functional analyses associated with biological functions and/or diseases in the Ingenuity Pathways Knowledge Base were considered and Fischer's exact test was used to calculate a p-value determining the probability that each biological function and/or disease assigned to that data set is due to chance and chance alone. The networks/pathways shown depict a graphical representation of the molecular relationships between genes/gene products.

### 6.3 Results

#### *Stable downregulation of Copine III in MDA-MB-231 cells*

For these experiments we used the MDA-MB-231 breast cancer cell line, which is regularly used to monitor tumor growth and tumor metastasis *in vivo*. Using the same shRNA sequences as described in Section 5.3, the protein expression of Copine-III was stably downregulated in these cells. In parallel, control cells were transduced with a LacZ-shRNA construct. After selection of cell pools carrying the shRNA-vectors, KD levels of Copine III were assessed by western blotting with specific antibodies. Furthermore, the cell pools were screened for differences in their ability to activate several signaling pathways downstream of ErbB2 as well as in their proliferation, adhesion and transformation potential.

Western blots of cell extracts from control cells and cells that were treated with 1 nM HRG for 10 minutes showed that there was a clear downregulation of Copine III in the KD cell pools. However, the major signaling pathways downstream of the ErbB2 receptor, such as the MAPK or PI3K pathways (data not shown), were not affected from the KD of Copine III (Figure 6-1).

It is important to mention, that the MDA-MB-231 cell line is not dependent on ErbB2 signaling. It has an activating Ras mutation and an autocrine loop of HRG production. Therefore, stimulation with HRG is not expected to show changes as it would do in ErbB2-dependent cell lines, such as the T47D cell line.

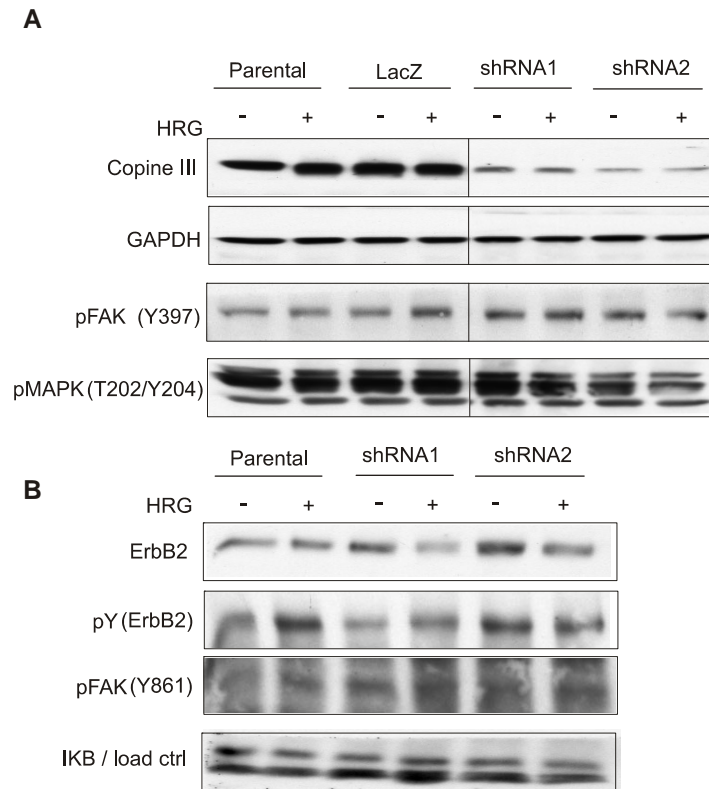


**Figure 6-1 Analysis of major signaling pathways in Copine III MDA-MB-231 KD cells**

MDA-MB-231 cells were starved in DMEM + 0.1 % FCS overnight and stimulated with 1nM HRG for 10 minutes. 10 µg WCE were used for the analysis. Protein expression levels of Copine III, pFAK (Y397), pFAK (Y861), pMAPK (T202/Y204), pTyr (ErbB2) and GAPDH as loading control were assessed.

#### *Analysis of Copine III KD MDA-MB-231 cells*

After confirming that the KD of Copine III was efficient in these cell pools we analyzed them in several assays prior to the *in vivo* experiment. First we assessed their proliferation potential using the methylene blue assay for various stable pools of cells resulting from different infections. No significant difference in rate of proliferation upon the KD of Copine III was observed (Figure 6-2).

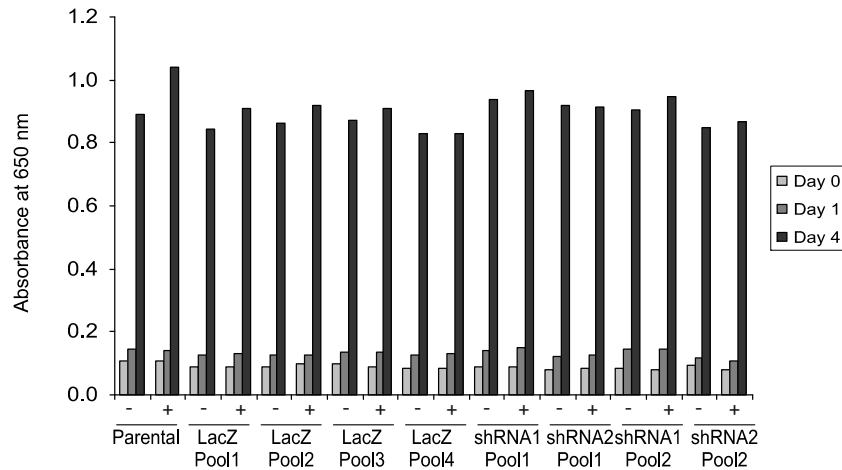


**Figure 6-2 Proliferation of MDA-MB-231 Copine III wt and KD cells**

The relative proliferation of the cells was measured using the methylene blue assay. Cells were treated or not with 1 nM HRG for the entire duration of the assay (-/+). The relative proliferation is plotted as the absorbance at 650 nm.

In addition, the migration of the MDA-MB-231 Copine III KD pools was assessed using the Boyden chamber assay (Figure 6-3). The first observation in this assay was that there was no difference between starved and HRG-stimulated cells for any cell line. The cells of the shRNA1 pool seemed to migrate a lot more than all the other cells. But then again the 2<sup>nd</sup> KD pool was similar in its migration rate to the wt and LacZ pool arguing for no difference in Boyden chamber migration upon KD of Copine III in these cells (Figure 6-3). However, at this point no conclusion can be drawn from this experiment.

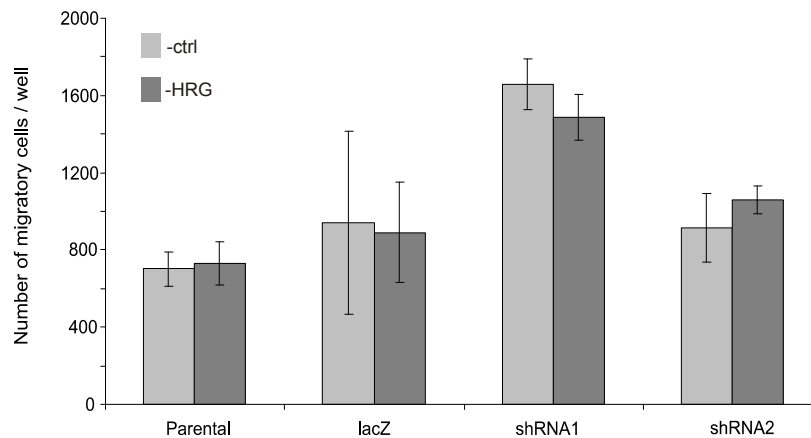


**Figure 6-3 Migration assay (Boyden chamber) of MDA-MB-231 Copine III wt and KD cells**

Parental and KD cell pools of MDA-MB-231 cells were seeded in Boyden chambers and allowed to migrate in a gradient of PBS (ctrl) or HRG for 3 h. Afterwards the nuclei of the migrated cells were stained with Hoechst and the number of migrated cells was counted. The average number of cells from triplicate is plotted as the mean and standard deviation of the mean.

To find out whether Copine III plays a role in cell adhesion we assessed the adhesive properties of wt and Copine III KD MDA-MB-231 cells on different coatings. For this, plates were coated with fibronectin, collagen or laminin. Each of these is a component of the extracellular matrix that surrounds the cells and binds to specific integrins. It has been shown that the ErbB2 receptor can cross-talk with integrins to initiate downstream signaling. Therefore, we wanted to identify whether Copine III, as a interactor of ErbB2 has an effect on cell adhesion. Furthermore, we found in previous experiments (see section 5.3) that Copine III associates with and influences components of focal adhesions, such as focal adhesion kinase, which are important mediators of cell adhesion to a substrate. However, all previous experiments were performed in ErbB2-dependent cell lines and the cell lines used in this experiments, MDA-MB-231, carries other mutations making it a transformed cell line (e.g. constitutively active Ras) and is therefore not dependent of ErbB2 signaling.

We found that a KD of Copine III had no effect on cell adhesion on either substrate (Figure 6-4).

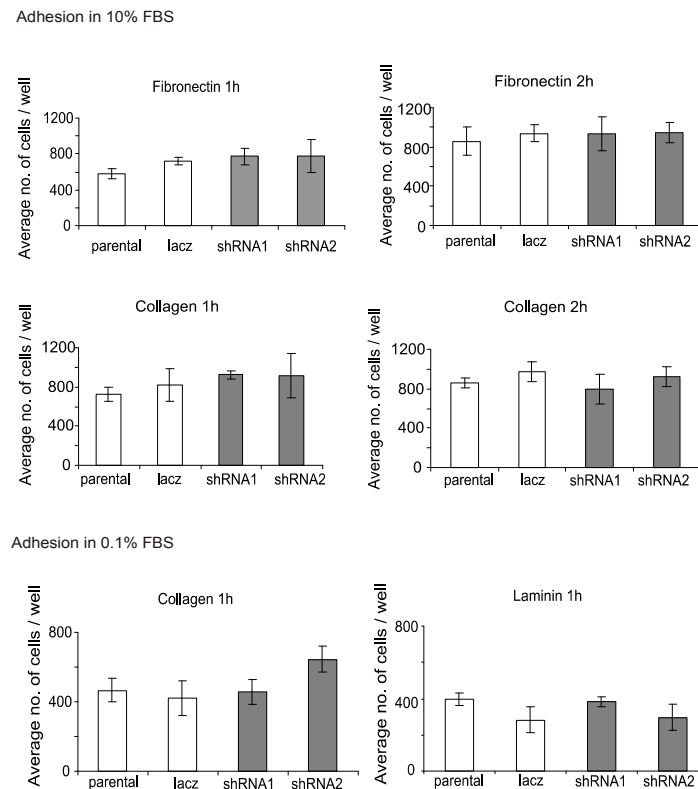


**Figure 6-4 Adhesion of MDA-MB-231 Copine III wt and KD cells to fibronectin and collagen**

Wt, LacZ and Copine III KD cell pools were plated on plates coated with fibronectin, collagen or laminin and allowed to adhere for 1 h or 2 h, respectively. The cells were plated either in medium containing 10 % FCS or containing 0.1 % FCS. Non-adherent cells were washed off the plates and the remaining cells were fixed, stained with crystal violet and counted. Plotted is the mean of adherent cells from three wells with the standard deviation of the mean.

In summary, we successfully reduced the protein expression levels of Copine III in MDA-MB-231 cell. Yet, *in vitro*, this did not have an effect on the tested phenotypes, such as proliferation, migration (Boyden chamber), anchorage-independent growth or adhesion.

Considering the fact that we saw a strong reduction in migration in T47D cells (section 5.3), the next step clearly was to analyze migration of MDA-MB-231 cells in wound healing. Therefore, scratch assays were performed using wt, LacZ ctrl and Copine III KD cell pools (Figure 6-5).

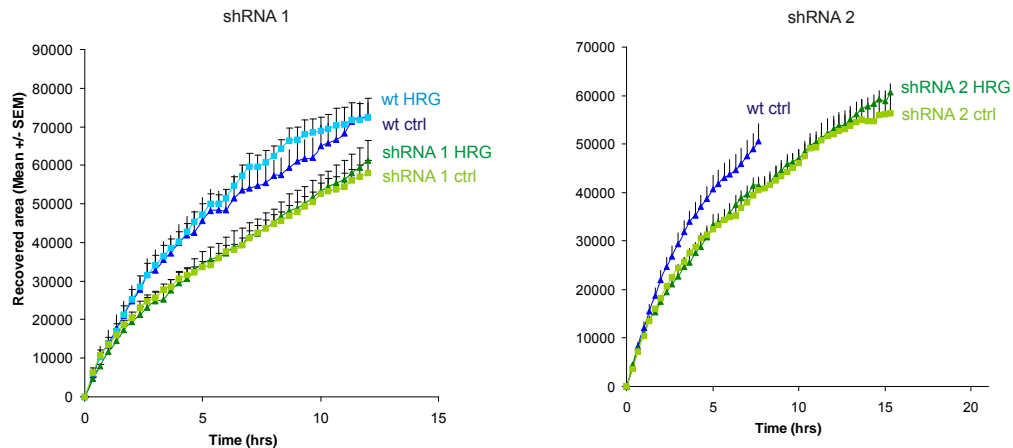


**Figure 6-5 Migration assay (scratch) of wt and Copine III KD MDA-MB-231 cells**

MDA-MB-231 wt, LacZ and KD cells were seeded in medium containing 10 % FCS and grown to confluency. Then the cells were stimulated, or not, with HRG and scratched. Migration into the wound was measured and plotted as the area recovered by the cells as the mean of 6 to 8 specific points of the scratch. The standard error of the mean is also plotted.

Both Copine III KD cell pools were analyzed in separate experiments and compared to wt MDA-MB-231 cells. Both wt and KD cells did not show an increase in migration upon stimulation with HRG. Yet, for both shRNA1 and shRNA2 we saw a significant reduction in wound healing compared to wt cells. For shRNA2 a problem occurred with the wt ctrl and HRG cells and the values could only be measured for the ctrl cells up to 8 hours into the experiment. Already in this timeframe a clear reduction of migration in Copine III KD cells compared to wt cells was observed.

In summary, given the role of Copine III in tumor cell migration, this suggests that Copine III most probably might play a role in tumor metastasis. Further experiments exploring this possibility are necessary to evaluate Copine III as a potential new candidate in ErbB2-driven cancer metastasis. However, prior to this, we investigated the role of Copine III in *in vivo* tumor growth.



*Copine III KD in in vivo tumor growth*

Therefore, we planned to inject these cells into the mammary fat pad of nude mice to analyze their potential in xenograft tumor growth. In a later stage we also planned to analyze their potential in metastasis both from the primary tumor and when injecting the cells directly into the blood stream of the mice (tail vein injection). In this thesis, only the primary tumor growth experiments will be discussed.

MDA-MB-231 cells are a well studied model for assessing *in vivo* tumor growth (Matsuda *et al.*, 2009). Cells ( $1 \times 10^6$ ) of each Parental (wt), LacZ, shRNA1 KD and shRNA2 KD were injected into the 4<sup>th</sup> mammary fat pad of 4-6 week old female nude mice. Eight mice were injected per group. Tumor growth was monitored twice a week and tumors were allowed to grow to a maximum size of 2 cm<sup>3</sup>. Then the mice were sacrificed and the tumors were excised and weighted. Samples of each tumor were taken for protein and RNA extraction and immunohistochemistry (IHC) stainings. The tumor volume was calculated as the area of a cylinder. Cells that did not grow into solid tumors were incorporated with a value of 0 into the calculations of average tumor volumes. These calculated volumes were plotted versus the time of the measurement to evaluate the growth rate of the different cell pools. Furthermore the endpoint tumor weight was measured, after the tumor was excised and an average of all tumors from one group was determined (Figure 6-6).

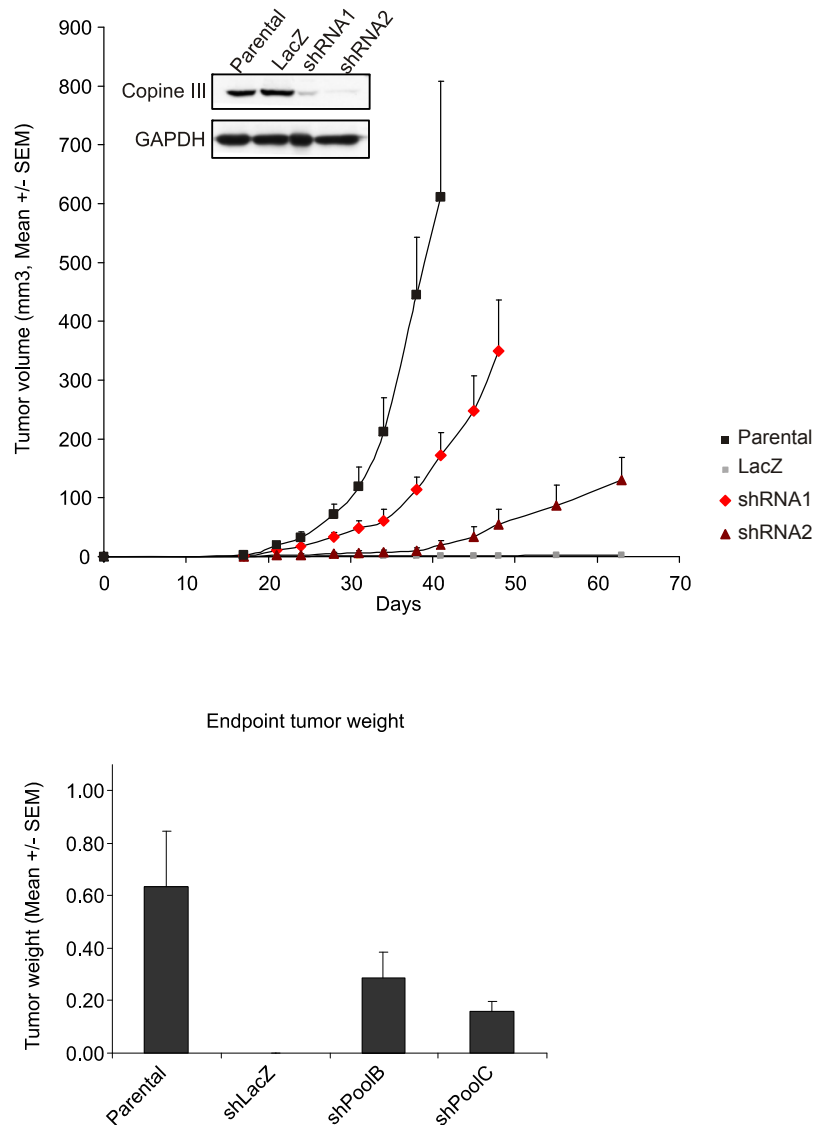


**Figure 6-6 *In vivo* tumor growth of MDA-MB-231 Copine III wt and KD cells**

Cells ( $1 \times 10^6$ ) of each wt, LacZ, shRNA1 KD and shRNA2 KD were injected into female nude mice. The cells were injected into the 4<sup>th</sup> mammary fat pad of 4-6 week old mice. Eight mice were injected per group. The tumor size was measured twice week until tumors reached a maximum size of 2 cm<sup>3</sup>. Either when the tumors reached the maximum size or after 65 days the mice were scarified and the tumors were excised.

Right after the injection the remaining cells were lysed and analyzed for the protein expression levels of Copine III by western blotting (insert in Figure 6-6). This confirmed that the KD of Copine III was efficient in both KD cell pools compared to the wt and LacZ cells. The measurement of the *in vivo* tumor growth showed, that both KD cells pools tend to have a reduced growth rate compared to the wt MDA-MB-231 cells. Yet, a major problem of this particular experiment was, that the control LacZ infected cells did not give rise to any tumors at all. This meant missing a very important control, since the effects seen with the shRNA cell

pools could still come from the treatment and selection process the cells went through after the infection. Interestingly, the reduction of tumor growth correlated with the level of KD of Copine III: shRNA2 infected cells, which show a stronger KD efficiency as the cells infected with shRNA1, also showed a greater reduction in tumor growth (Figure 6-6). This observation strongly suggests that the growth reduction observed was actually due to the KD of Copine III rather than the selection process of the cells.

Similarly, the endpoint tumor weights measured for the two KD cell pools were smaller than those measured for the tumors coming from wt MDA-MB-231 cells. Yet, due to mice in each group, which did not take tumors and were therefore counted as 0, these differences were not statistically significant.

#### *Analysis of signaling pathways in Copine III wild-type and KD tumors*

To further confirm that a KD of Copine III was the cause of the growth reduction, we extracted proteins from all tumor samples and analyzed them by western blotting for Copine III expression levels and other downstream signaling pathways of ErbB2. These analyses confirmed, that after several weeks of *in vivo* growth, Copine III protein levels were still reduced in tumors from the KD cell pools (Figure 6-7)

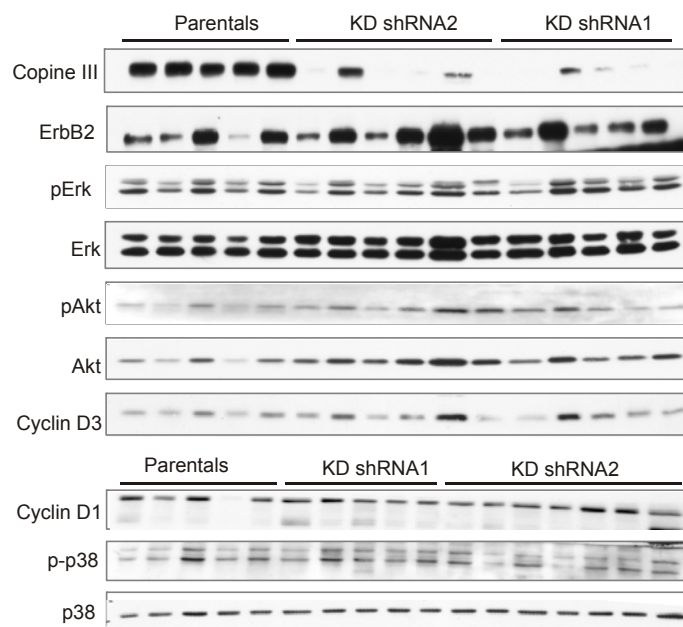


#### **Figure 6-7 Western blot analysis of tumor lysates**

Proteins were extracted from snap frozen tumor samples using a cell homogenizer (Polytron). Total protein concentrations as determined by Bradford and 50  $\mu$ g of total protein were loaded per lane. Proteins were separated by SDS PAGE and transferred onto PVDF membrane. Extract were monitored for protein levels of Copine III, ErbB2 (total), pErk, Erk, pAkt, Akt, Cyclin D1, Cyclin D3, p-p38 and p38.

When we analyzed signaling activity of the tumor cells, such as pErk, p38 or pAkt, we saw that, as for the *in vitro* results, there was no change in the activation of these signaling pathways upon KD of Copine III. Furthermore, cell cycle checkpoint protein, like Cyclin D1 and Cyclin D3, were also unchanged, indicating that Copine III does not influence cell cycle progression. Thus, from this analysis, we concluded that the decreased tumor growth rates seen in Copine III KD cells are neither due to changes in major ErbB2 downstream signaling pathways (Erk, PI3K), nor to changes in cell cycle progression (Cyclins).

*Analysis of proliferation, apoptosis and vascularization in Copine III wild-type and KD tumors*

Other properties that could be the cause for the growth delay seen in Copine III KDs were analyzed by IHC stainings of tumor sections. We found that cell proliferation (Ki-67) and apoptosis (cleaved caspase 3) were both unchanged between wt and Copine III KD cells. IHC stainings for Copine III confirmed the western blot analysis showing a clear reduction of Copine III protein levels in sections from Copine III KD tumors (Figure 6-8).

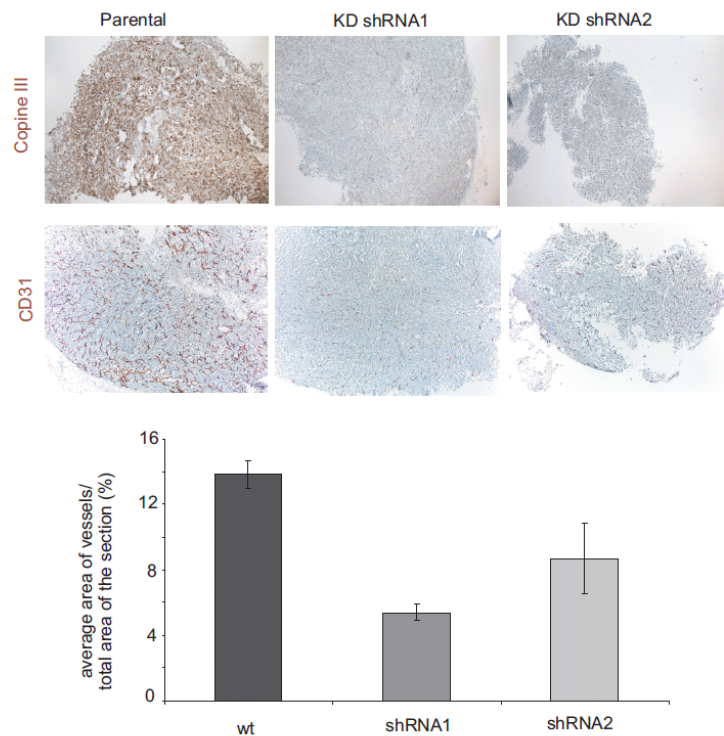


**Figure 6-8 Immunohistochemistry analysis of tumor sections**

Paraffin embedded (for Copine III) and fixed frozen (for CD31) tumors were cut and stained for human Copine III (pAb) and mouse CD31. For the quantification of the CD31 staining pictures of the complete section were taken and analyzed. The ratio of the area covered with vessels (CD31 staining) over the total area of the section was calculated for each tumor. The mean of all these analysis for one group of tumors is plotted as a percentage with the standard error of the mean.

Interestingly, when we stained the sections for CD31, a marker for blood vessels, we found that the vessel density was clearly reduced in Copine III KD tumors. A growing tumor needs blood vessels to secure its supply for oxygen and nutrients. Therefore, a reduction in blood vessel density could well be the reason for the reduction of tumor growth observed. In order to quantify these initial observations pictures from whole tumor sections were analyzed and the area covered by blood vessels as a percentage of the total area of each section was calculated (Figure 6-8).

In this experiment it was important to correlate the area covered by vessels to the total area of the section, since some tumors were much smaller than others. For example, all tumors from the shRNA2 cells were smaller than those from the wt cells. Small tumors are usually densely vascularized, however, once they grow bigger, more oxygen supply is required. Therefore, factors initiating new vessel formation (angiogenesis), such as VEGFs, are secreted from the tumor cells to the surrounding tissue to supply them with new blood vessels. This means, that in very small tumors, one might still see full vascularization, because this vascularization is not due to a new-formation of vessels. Only in larger tumors the difference between a tumor that can initiate vascularization and one that cannot will become obvious.

In the analyzed tumor samples we found that the area covered by vessels was much smaller in the Copine III KD tumors than in the tumors originating from wt MDA-MB-231 cells. This was more striking for tumors originating from shRNA1 than those originating from shRNA2. This might mainly be due to the fact, that nearly all tumors excised from shRNA1 injected mice were larger than those from shRNA2 injected mice. We tried to analyze this by classifying the tumors as larger or smaller than 0.2 cm<sup>3</sup>. From the shRNA1 tumors one was smaller than 0.2 cm<sup>3</sup> and already showed less vascularization than wt tumors of this size. However, for the shRNA2 tumors, two fell into that category and these two showed a high vessel density similar to that of wt tumors. The vessel density in these tumors decreased rapidly in larger tumors that fell into the second category (> 0.2 cm<sup>3</sup>). These results explain the large error bar seen for the shRNA2 KD tumors (Figure 6-8).

Altogether, the analysis of the tumors from Copine III wt and KD cells lead to the conclusion, that Copine III is most likely required for *in vivo* tumor growth. The reduction in tumor growth seen in Copine III KD cells is derived from a lack in the recruitment of new blood vessels to the tumor.

#### *Microarray analysis of Copine III wild-type versus Copine III KD tumors*

To further elucidate the underlying mechanisms in the reduced tumor growth upon Copine III KD, we extracted total RNA from the tumor samples and analyzed changes in the tumor RNA using microarrays. Design and evaluation of microarrays was done as described in Materials

and Methods (section 6.2). From triplicate analysis of tumors from each wt, shRNA1 and shRNA2 tumors, we selected those probe sets with a Log2 average contrast signal of at least 5, an adjusted p-value < 0.05 and an absolute Log2 fold change of > 0.585 (1.5-fold in linear space).

Figure 6-9 shows the Venn diagram for all genes that were found to be differentially regulated, either decreased or increased, in between the different groups. We compared each KD to the wt tumor RNA and the two KD to one another. For comparing the two KD samples to one another we compared the stronger KD, shRNA2, to the less effective KD, shRNA1.

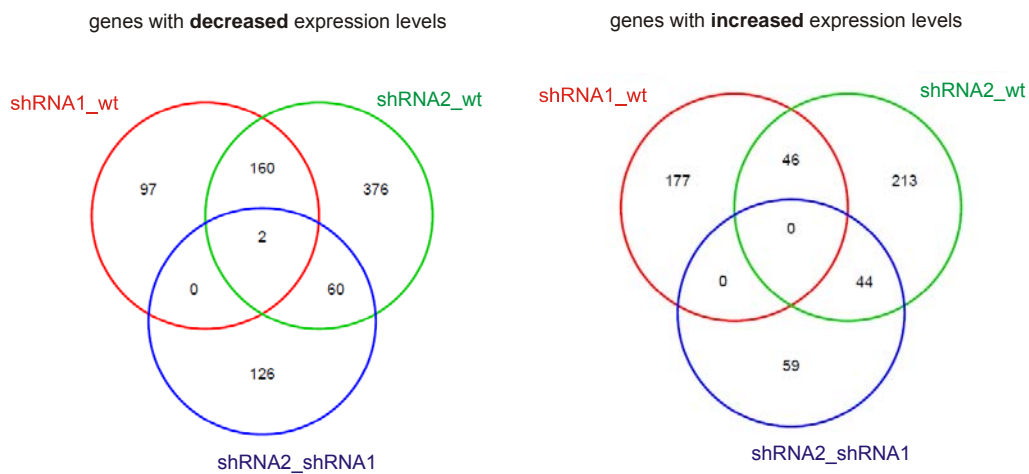


**Figure 6-9 Number of genes changed between the tumor samples analyzed by microarray**

We found that many genes were changed within the analyzed groups and therefore we tried to further group them. For this we used the software ingenuity pathways, which groups the differentially regulated genes into signaling pathways and networks. To confirm our hypothesis, we determined that the major pathways these genes could be grouped into were associated with cancer and the top hit included cellular movement.

When analyzing the list of the top 10 up or downregulated genes, we found that most of the genes upregulated were genes coding for proteins that are components of the extracellular matrix (ECM), like Teneurin-3, Testican-1 or Elastin. On the other hand, most of the top 10 downregulated genes encoded for proteins involved in the degradation of the ECM, like secreted serine proteases (Table 6-1).

**A- top ten upregulated genes**

<b>Molecule</b>	<b>Name</b>	<b>Cellular localization</b>	<b>Function</b>	<b>Expression value</b>
CDON	cell adhesion molecule-related / down-regulated by oncogenes	membrane, trans	cell-cell interaction	2.476
ODZ3	Teneurin-3; Tenascin M3	membrane	cellular signal transducer	2.424
SPOCK1	Testican-1	secreted	cell-cell interaction	2.418
LRRC17	Leucin-rich repeat containing protein 17			2.263
MYLK	Myosin light chain kinase		regulation of endothelial and vascular permeability	2.192
MMP2	Matrix metalloproteinase 2			2.092
KIAA1199		secreted		2.026
DCLK1	Serine/threonine-protein kinase DCLK1		Ca <sup>2+</sup> signaling	1.985
ELN	Elastin	secreted		1.941
TFCP2L1	Transcription factor CP2-lik protein 2	nucleus	transcriptional sipressor, may supress UBP-1 mediated transcriptional activation	1.794

**B- top ten downregulated genes**

<b>Molecule</b>	<b>Name</b>	<b>Cellular localization</b>	<b>Function</b>	<b>Expression value</b>
PRSS2	Serine protease 2 isoform B	secreted	Serine protease, peptidase	-4.196
AGR2	Anterior gradient protein 2 homolog	secreted		-3.713
TFPI2	Tissue factor pathways inhibitor 2	secreted	regulation of plasmin-mediated matrix remodeling	-3.481
TCN1	Transcobalamin-1	secreted	Vitamin B12-binding protein. Transports cobalamin into cells	-2.924
SLC7A11	Cystein 7 Glutamate transporter / solute carrier family 7 member 1	Membrane, trans	Sodium-independent, high-affinity exchange of anionic amino acids	-2.754
ENPP3	Ectonucleotide pTyrroosphatase / phosphodiesterase family member 3	secreted		-2.707
PRSS1	Serine protease 1 (Trypsin-19)	secreted	Proteolytic activity	-2.645
QPCT	Glutaminyl-peptide cyclotransferase			-2.524
TM4SF18	Transmembrane 426 family member 18	membrane, multi-pass		-2.293
SPINT2	Kunitz type protease inhibitor 2	membrane	Inhibitor of HGF activator	-2.285

**Table 6-1 Top ten upregulated and downregulated genes**

Interestingly, there were two genes that were downregulated in all groups and none that were commonly unregulated in all groups (Figure 6-9). These two downregulated genes are fermitin family homolog 1 (FERMT1), a protein claimed to be involved in cell adhesion, possibly via its interaction with integrins that may mediate TGF $\beta$  1 signaling in tumor progression and insulin-like growth factor 2 mRNA binding protein 3 (IGF2BP3), RNA-binding protein that acts as a regulator of mRNA translation and stability and that is found in lamellipodia of the leading edge, in the perinuclear region, and beneath the plasma membrane. This is intriguing since both proteins that these genes code for are expressed in regions of the cells where Copine III is supposed to be active (for example the plasma membrane). Furthermore, fermitin is involved in mediating integrin signaling and we have shown in section 0 that Copine III also plays a part in integrin signaling, since it influences Src and focal adhesion kinase, which are also influenced by integrin signaling.

However, how a KD of Copine III influences the regulation of these genes or how the proteins might work together remains to be speculative.

### *In vivo tumor growth of Copine III rescue cell lines*

Yet, before analyzing the data from this first *in vivo* experiment in too much detail, we wanted to ascertain that the changes in tumor growth were really due to a KD of Copine III. Rescue cell lines re-expressing Copine III in the Copine III shRNA KD background, were generated and tested *in vivo* (Figure 3-35 insert). The experiment was carried out in the same manner as the first *in vivo* experiment. Similarly, the proliferation of the cells was tested *in vitro* prior to starting the *in vivo* experiment. As seen in Figure 6-11, the proliferation rate of the cell pools did not change upon deletion or rescue of Copine III expression.



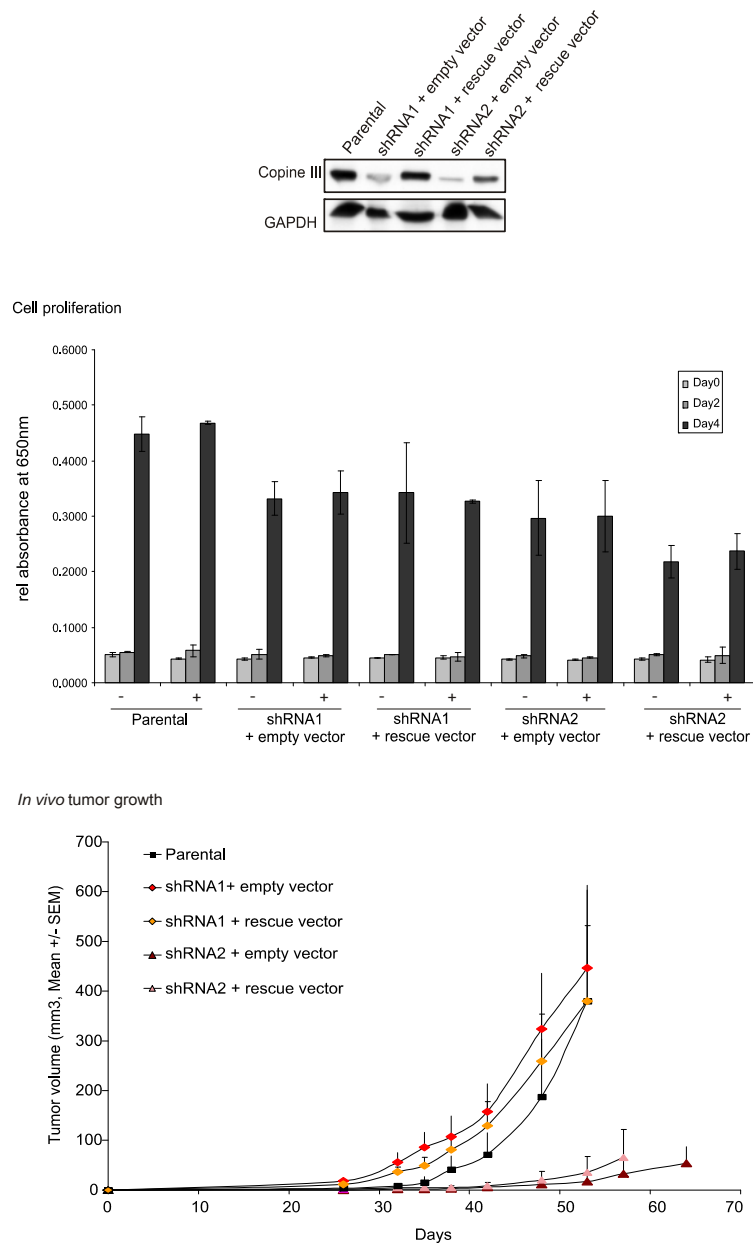


**Figure 6-10 Copine III rescue cell lines- expression, proliferation and *in vivo* tumor growth analysis**

Parental, shRNA1 KD + empty vector, shRNA1 + rescue vector, shRNA2 KD + empty vector and shRNA2 + rescue vector cell pools were analyzed for Copine III protein expression levels (upper panel) and their proliferation potential by methylene blue (middle panel).

Cells ( $1 \times 10^6$ ) of each cell pool were injected into female nude mice. The cells were injected into the 4<sup>th</sup> mammary fat pad of 4-6 week old mice. Eight mice were injected per group. The tumor size was measured twice week until tumors reached a maximum size of 2 cm<sup>3</sup>. The last mice were scarified and the tumors were excised either when the tumors reached the maximum size or after 65 days.

The first observation from this experiment was that similar as before, the shRNA2 + empty vector cells gave rise to much slower growing tumors than any of the other cells (Figure 6-11

light pink triangles). However, apart from that, the results from this experiment were quite different to those seen in the first experiment. The main observation was that the parental cells did not give rise to the fast growing tumors seen in the first experiment. Hence, there was no difference in tumor growth between the parental tumors and the shRNA1+ empty vector tumors. Additionally, both rescue cell pools did not yield tumors growing faster than the KD tumors. Therefore, this second experiment makes the interpretation of the role of Copine III in *in vivo* tumor growth very difficult.

## 6.4 Outlook

Overall, the interpretation of the results obtained from the *in vivo* experiments is difficult. On the one hand, both experiments taken together suggest that Copine III is not involved in tumor growth and the effects that were seen in the first experiment were plainly due to the selection of the cell pools and the treatment prior to the experiment. On the other hand, one could argue that, in the second experiment, due to various reasons, the rescue constructs just were not able to compensate for the functional loss of Copine III and therefore these cell pools should have no influence on the conclusion drawn. Moreover, the parental cells yielded much slower growing tumors in the second experiment, compared to the first experiment. The growth kinetics of parental MDA-MB-231 cell injected into the fat pad of nude mice is well known and well studied (for example see Matsuda *et al.*, 2009). If one would superimpose the growth curve of the parental tumors in experiment one onto experiment two, the tendency of the experiment would remain: both Copine III KD cell pools yield tumors with slower growth kinetics than the parental cells. Moreover, the stronger KD leads to a stronger decrease on tumor growth. Therefore, the argument for a role of Copine III could be that the parental cells did just not grow into tumors as well as in the first experiment. In summary, no clear conclusion can be drawn from these experiments.

To validate the role of Copine III in *in vivo* tumor growth the experiment needs to be repeated thoroughly. First, the rescue cell pools need to be tested as the KD cell pools were initially (activation of signaling pathways, migration, anchorage-independent-growth, etc), to rule out any impairment in these cell pools, which could have led to the results seen in the second tumor growth experiment. Secondly, one has to make sure, that a large enough group of animals is taken for the experiment to be statistically significant and, even more importantly, the cells have to be in the growth phase to ensure proper growth. One major change to improve the outcome of the experiment could be to inject the cells into the 2<sup>nd</sup> and 3<sup>rd</sup> mammary fad pads instead of the 4<sup>th</sup>, as experiments from our laboratory suggest that this site is more conducive to tumor growth and metastasis.

## 7 DISCUSSION AND OUTLOOK

The ErbB receptor signaling network plays a pivotal role in breast cancer development and progression. Up to 25% of all breast cancer patients show an overexpression of the ErbB2 receptor; this is correlated with a more aggressive disease and a poor prognosis. Therefore, the ErbB receptor signaling network is one of the most extensively studied areas in signal transduction. Our knowledge about this system, especially ErbB2, and its role in breast cancer, has continuously increased in the past years. However, in spite of extensive research, many questions, about the signaling cascades initiated by ErbB2 and their downstream effects, remain. One of these is the determination of the individual roles of ErbB2 binding partners in breast cancer. Several proteins binding to specific tyrosine residues in the C-terminal regulatory region of the receptor have been identified and, to some extent, associated with downstream effects. One of these is Memo, mediator of ErbB2-dependent cell migration that binds to pTyr1222 and is important for tumor cell migration (Marone *et al.*, 2004; Meira *et al.*, 2009).

In this study we identified Copine III as a novel binding partner of pTyr1248 of ErbB2. We showed that Copine III interacts with the active ErbB2 receptor at the plasma membrane of breast cancer cells upon receptor stimulation. Moreover, Copine III localizes to focal adhesions and binds to the focal adhesion-associated protein RACK1. Copine III is required for tumor cell migration and influences Src activity. Therefore Copine III might provide a link between ErbB2 and focal adhesions thereby mediating cell migration.

### *The interaction of Copine III and ErbB2 through Shc*

Copine III belongs to a conserved family of Ca<sup>2+</sup>-dependent phospholipid binding proteins. All human Copines contain two C2 domains (C2A and C2B) followed by a Copine-specific A domain at the C-terminus. Furthermore, they have a conserved lysine-rich cluster within their C2B domain. C2 domains are Ca<sup>2+</sup>- and membrane-binding domains that are found in various intracellular proteins (e.g. members of the PKC or synaptotagmin family). It was shown recently that the C2 domain of PKC $\delta$  is able to bind pTyr (Benes *et al.*, 2005). C2 domains can be subdivided into two groups depending on the arrangement of the  $\beta$ -strands in their secondary structure. The order of the 1<sup>st</sup> and the 8<sup>th</sup>  $\beta$ -strand determines whether the domain is classified as type I or type II topology. Most type I C2 domains bind Ca<sup>2+</sup> whereas the majority of the type II C2Ds is Ca<sup>2+</sup>-independent. The C2 domain described by Benes *et al.* is classified as type II topology and does not bind Ca<sup>2+</sup>. Using bioinformatic tools we modeled the secondary structure of the Copine III C2 domains and came to the conclusion that both domains should be classified as type I topology. Both Copine III C2 domains carry 6 conserved aspartate

residues that should mediate Ca<sup>2+</sup>-binding. To further support this *in silico* evidence, we experimentally showed that Copine III is Ca<sup>2+</sup>-dependent in the cell (section 5.3). Therefore, these findings lead to the conclusion that Copine III does, most probably, not bind pTyr through its C2 domains. We therefore propose that Copine III might bind to pTyr1248 via Shc. We and others have shown that Shc binds to this site in a HRG-dependent manner (Dankort *et al.*, 2001a; Schulze *et al.*, 2005).

An interesting follow-up on these results would be to analyze the binding of Copine III to ErbB2 in Shc KD cells. Furthermore, it could be interesting to investigate to which Shc isoforms Copine III binds. Shc encodes three widely expressed isoforms: p46shc, p52shc and p66shc that occur due to differential transcription and alternative splicing (Ravichandran, 2001). These isoforms differ in their tissue specificity, cellular localization and function. The shorter isoforms, p46shc, and p52shc are constitutively and ubiquitously expressed, whereas p66Shc expression is tissue specific. p52Shc is found in the cytosol and acts as adaptor in pathways triggered by surface receptors controlling proliferation, chemotaxis, and survival. p46Shc localizes to mitochondria. Its function is not known. p66Shc is expressed in the cytosol and in mitochondria. It has both antimitogenic and proapoptotic functions and inhibits the activation of the Ras/MAPK pathway by competing with p52Shc (Finetti *et al.*, 2008). As the functions of the three Shc isoforms are quite diverse it would be of great interest to find out whether Copine III binds to one of them preferentially. This finding could either imply a different function of Copine III apart from its role in migration or it could help to further elucidate its role in cellular migration in more detail.

### *Copine III domain architecture- implications for a function?*

Another way to analyze the interaction of Copine III with Shc or with ErbB2 is by studying which domain of Copine III is involved in binding. As mentioned, both C2 domains do probably not interact with pTyr. Copine III additionally carries an A domain that is known to be involved in protein-protein binding in other human Copines and could therefore mediate receptor- or Shc-binding.

We have made deletion mutations of Copine III in order to express individual domains or combinations of different domains. All constructs carry a Flag-tag and can be expressed in mammalian cells (Figure 7-1).

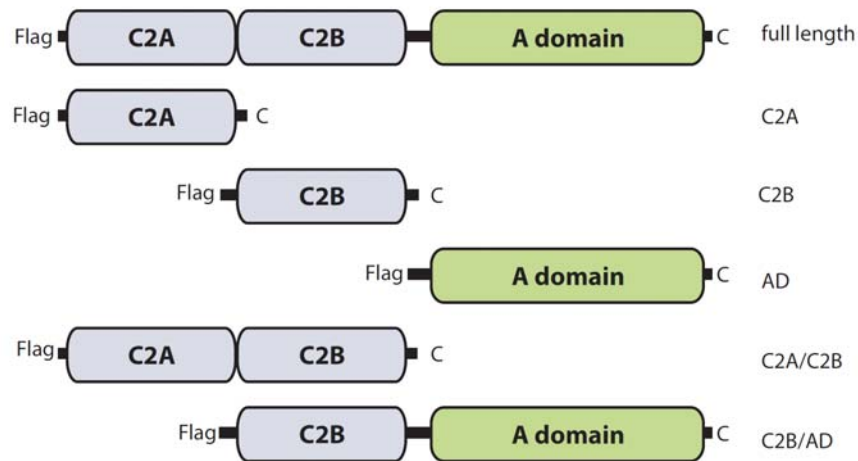


**Figure 7-1 Schematic outline for domain expression of Copine III in mammalian cells**

These constructs have been cloned into a mammalian expression vector and are ready to be used in upcoming experiments.

These constructs could be used to determine, which domain (or domains) of Copine III are required for receptor binding. Such experiments should be performed in both wt and Shc KD cells to verify once more if the domain required for binding, binds the receptor via Shc.

Furthermore, these constructs could be utilized to monitor other specific functions of the individual Copine III domains. It has been suggested that one or both C2 domains mediate membrane binding in a  $\text{Ca}^{2+}$ -dependent manner. We have shown in our study that stimulation of  $\text{Ca}^{2+}$  influx by ionomycin leads to a translocation of full-length (fl) Copine III to the plasma membrane and the nucleus. Additionally, a stimulation of ErbB2 through HRG also leads to membrane localization of Copine III. Which domains mediate this translocation and membrane binding? T47D and SKBr3 breast cancer cell could be transfected with the individual domain constructs and their localization could be tested via immunofluorescence (IF) microscopy after  $\text{Ca}^{2+}$ - or HRG-stimulation. One interesting aspect concerning membrane localization of Copine III is the Lysine-rich cluster (LRC) found within the C2B domain of Copine III. It is well-known that other proteins also carry such LRCs and it has been postulated that these domains stabilize membrane association by binding to  $\text{PIP}_2$ . Through deletion of the complete LRC or mutation of the conserved Lysine residues to Alanines, one could investigate its function in Copine III membrane localization.

What seems to be of even greater interest is the involvement of the individual Copine III domains in its function. Which domain (or domains) is sufficient to restore proper wound healing in Copine III KD cells? Our analysis showed that a KD of Copine III in T47D, but also in SKBr3 (data not shown) and MDA-MB-231 breast cancer cells, leads to a defect in cell migration. Migration into the wound is slower after HRG stimulation in Copine III KD cells compared to control LacZ cells. It would be intriguing to connect this function of Copine III to its individual domains.

### *A putative role for Copine III in the nucleus*

When analyzing the list of putative Copine III binding partners (Table 5-1) we found that out of the six proteins, three can shuttle between the nucleus and the cytoplasm and three are nuclear proteins. Moreover, we have shown in our studies that Copine III localizes to the nucleus in a  $\text{Ca}^{2+}$ - and HRG-dependent manner. The first question to address in this context is whether Copine III truly can be found in the nucleus or whether it localizes to the nuclear membrane. When we analyzed the amino acid (AA) sequence of Copine III no nuclear localization signal (NLS) was found using bioinformatic prediction tools. Usually NLS consist of bipartite basic AA stretch separated by roughly 10 AAs. Copine III contains a basic AA stretch in the LRC. However, again this sequence is not predicted to be an NLS. Experimentally, this could be analyzed by performing confocal microscopy on ionomycin- or HRG-treated cells. However, the pictures already obtained by immunofluorescence (IF) microscopy and the data from putative Copine III binding partners strongly argue that Copine III can reside in the nucleus. Another way to approach the localization of Copine III would be to extract nuclei from starved and stimulated cells and analyze them for Copine III. Furthermore, it would be very interesting to determine the function of Copine III in the nucleus. One way to address this question is to look closer at the functions of the nuclear Copine III binding proteins. Out of these, nucleolin seems to be of special interest, since it has been identified as an ErbB receptor interacting protein (Di Segni *et al.*, 2008). Could this imply that Copine III also interacts with ErbB2 in the nucleus? Another hypothesis could be that Copine III is shuttling between the nucleus and the cytoplasm/plasma membrane and that it transports other proteins back and forth. However, so far, we have found no evidence that directly supports this hypothesis. Therefore, concerning Copine III and the nucleus many open questions remain and it would be a worthwhile challenge to solve them.

### *The interaction of Copine III and RACK1 - functional aspects*

We demonstrated in this study that a KD of Copine III leads to a decrease in Src activity, monitored by phosphorylation of pTyr418, as well as a subsequent decrease of pTyr925 FAK phosphorylation. How does Copine III achieve this? We identified several putative binding

partners of Copine III, one of them being RACK1, receptor of activated C kinase 1. RACK1 has been shown to localize to nascent focal adhesions and to mediate chemotactic cell migration. It was shown, that RACK1 regulates chemotactic migration through binding to Src (Cox *et al.*, 2003). RACK1 deficient cells show increased Src activity and Paxillin phosphorylation, suggesting that RACK1 is a negative regulator of Src activity (Doan and Huttenlocher, 2007). However, there are other reports showing that an overexpression of RACK1 leads to reduced cell migration arguing for a biphasic effect of RACK1 on cell migration (Buensuceso *et al.*, 2001; Doan and Huttenlocher, 2007). With respect to these findings, it is possible, that in our set-up RACK1 acts as a negative regulator of Src activity. Copine III then blocks this activity of RACK1 when it interacts with RACK1 in HRG-stimulated cells. Therefore, in this case, we see an increase of Src phosphorylation upon stimulation. When Copine III is depleted from the cells (Copine III KD), it cannot interact and thus inhibit RACK1 anymore and therefore RACK1 can exert its negative regulation upon Src. This becomes obvious in that there is no increase of Src phosphorylation in Copine III KD cells upon HRG stimulation (Figure 5-9).

Interestingly, RACK1 also binds to PKC and the integrin  $\beta$  subunit. It has been postulated that RACK1 directs "cross-pathway-control" by integrating communication from different signaling pathways (McCahill *et al.*, 2002). Since we also see an effect of Copine III on FAK, a protein that has been shown to interact with integrins, it is well possible that Copine III interacts with RACK1 to mediate inter-pathways crosstalk, e.g. between integrin and RTK signaling in focal adhesions to control cell migration.

#### *A putative role for Copine III in mediating local translation*

Another interesting, but far more speculative, idea about the function of Copine III together with RACK1 is that these two proteins together mediate local translation at focal adhesions. Mass spectrometry studies have demonstrated the association of RACK1 with the small subunit of eukaryotic ribosomes (Sengupta *et al.*, 2004). Cryo-electron microscopy studies showed that RACK1 localizes to the head region of the 40S subunit in the vicinity of the messenger RNA (mRNA) exit channel (Nilsson *et al.*, 2004). Furthermore, RACK1 acts as a linker between signal-transduction and local translation by recruiting PKC to the ribosomes, which leads to the initiation of translation through the phosphorylation of initiation factor 6 (Nilsson *et al.*, 2004). The notion that Copine III, together with RACK1, could play a role in mediating local transcription was underlined by the fact that many ribosomal and ribosome-associated proteins were purified together with RACK1. However, since ribosomal proteins are very abundant within the cell we excluded these proteins from the final protein quantification assuming they were mostly background contamination. Retrospectively, and with the evidence given by studies on RACK1, it is possible that Copine III indeed recruits ribosomes to sites of

local translation and therefore these proteins were true interactors rather than background contaminating proteins. Interestingly, RACK1, through its negative regulation of Src, stimulates the translation of hnRNP-bound RNAs. Thus, by recruiting RACK1 and/or ribosomes to focal adhesions Copine III could directly influence local RNA translation.

To test this hypothesis a first experiment to do would be to check whether Copine III itself (or through its interaction partner RACK1) can bind RNAs. For this, Copine III should be immunoprecipitated (IPed) from cell extracts and RNAs should be extracted. If any RNAs are associated with Copine III these can then be extracted from the gel and analyzed on an array or by deep sequencing to determine their identity. In this way, one could identify the target RNAs of Copine III and then look at their translation specifically in wt versus Copine III KD cells or in starved versus stimulated cells.

Another approach to solving this question would be to analyze a polysome profile of focal adhesion-associated polysomes from wt and Copine III KD cells. The problem of this approach is to specifically separate only membrane-associated polysomes. However, if this is successful, one should be able to determine whether Copine III is involved in local translation initiation.

### *Copine III in the context of other ErbB2 interacting proteins*

Interestingly, Copine III is not the only ErbB2-interacting protein that has been associated with cellular migration. Memo, a recently identified interactor of pTyr1222, is required for tumor cell migration (Marone *et al.*, 2004; Meira *et al.*, 2009). Intriguingly, it has recently been shown that Memo reduces Src activity and subsequent FAK phosphorylation. Moreover, Memo links to another ErbB2 binder, namely PLC $\gamma$ , which interacts with pTyr1196 of ErbB2. Memo KD cells show a difference in PLC $\gamma$  phosphorylation kinetics compared to control cells.

All three of these ErbB2 interacting proteins are interconnected in one or the other way: PLC $\gamma$  activates intracellular Ca<sup>2+</sup>-influx from ER stores and can, in this way, be linked to the activation of Copine III through Ca<sup>2+</sup>. Yet, it seems that PLC $\gamma$  activity itself is regulated by Memo. Memo and Copine III display similar functions in the cells: both act on Src and influence cell migration. Thus, the immediate questions to answer in this respect are: What is the nature of the spatial and temporal binding of these three proteins to ErbB2? Do they influence each other in their binding and/or release from the receptor? Do they influence the activity of one another?

The hypothetical model in Figure 7-2 shows the binding of PLC $\gamma$ , Memo and Copine III to the respective pTyr sites of ErbB2 and the role of Copine III in promoting cell migration.



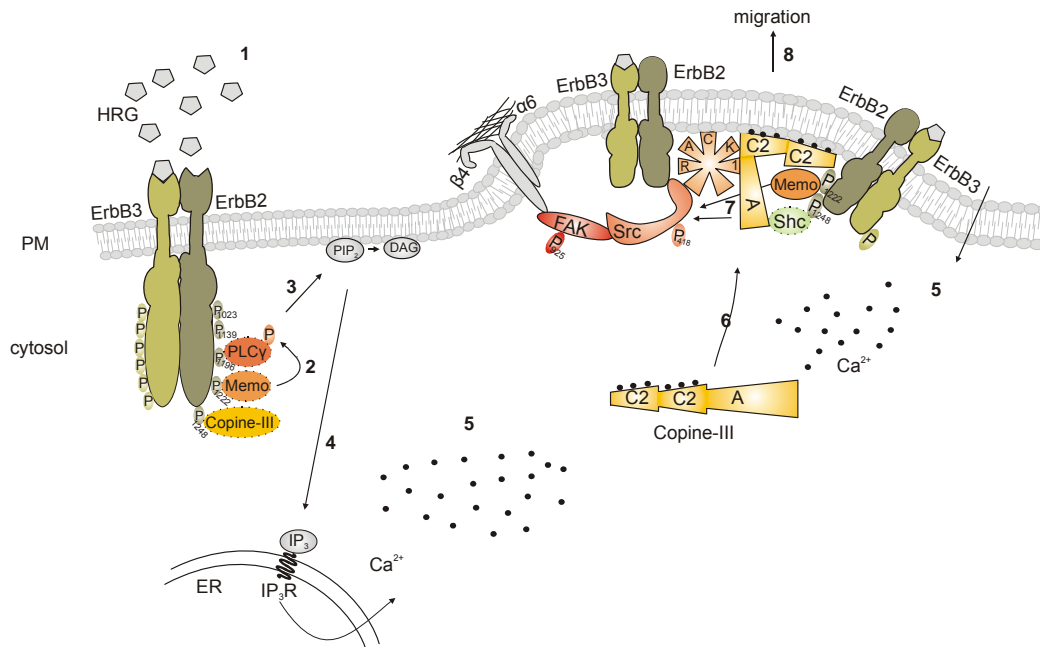


**Figure 7-2 Hypothetical model for the function of Copine III in ErbB2- dependent cell migration including Memo and PLCγ**

Upon stimulation of ErbB2/ErbB3 heterodimers with HRG (1), PLCγ1 binds pTyr1996, Memo pTyr1222 and Copine pTyr1248 of ErbB2. Since we do not know whether all three proteins bind the receptor simultaneously, we have drawn the binding with dotted lines. Memo exerts a function on PLCγ phosphorylation kinetics (2). PLCγ cleaves PIP<sub>2</sub> into DAG and IP<sub>3</sub> (3), which binds IP<sub>3</sub>R (4) leading to the release of Ca<sup>2+</sup> from intracellular stores and through store-operated channels following the replenishment of intracellular Ca<sup>2+</sup> by influx through the plasma membrane (5). Ca<sup>2+</sup> influx allows Copine-III to re-locate to the plasma membrane (6). At the PM, RACK1 directs it to a specific membrane location in close proximity to ErbB2, presumably in spreading initiation centers. It is possible that Copine-III interacts with RACK1 via a conserved motif in the C2D domain (McCahill *et al.*, 2002). Copine-III associates with pTyr1248, very likely via Shc. We have seen a direct interaction of Src with ErbB2 in our experiments, which we have shown here. We have drawn a direct Shc-Copine-III interaction; however, as indicated by the dots, it is possible that another protein mediates the interaction. Memo is also found in spreading initiation centers and might be bound to ErbB2 there. Both Copine III and Memo influences Src activation (7), thereby influencing ErbB2-induced cell migration (8).

To answer at least some of these questions we are planning to analyze whether Copine III, Memo and PLCγ can be found in one complex. This can be done in a first attempt by immunoprecipitations. Another approach to analyze whether Copine III, Memo and PLCγ influence the binding of each other to ErbB2 is FRET acceptor photobleaching experiments with different protein pairs in various cellular backgrounds: one could study the interaction of Copine III and Memo or Copine III and ErbB2 in Memo or PLCγ KD cells, Memo and ErbB2 in Copine III KD cells, PLCγ and ErbB2 in Copine III KD, Memo KD or Copine III and Memo double KD cells.

Such double KD cells, with reduced protein levels of Copine III and Memo could provide the basis for further analysis. Since maybe both proteins act synergistically, the migration potential of these cells might be further reduced when both proteins are missing. Moreover, the effect of a double KD on Src activity and subsequent FAK phosphorylation should be tested.

Memo has been shown to localize to spreading initiation centers. As the name implies these structures only exist during the early stages of cell spreading. They precede the formation of focal adhesions and are characterized by the fact that they contain RACK1. We have identified RACK1 as a binding partner of Copine III and have shown that Copine III co-localizes with focal adhesions. Since Memo KD cells have been shown to have less short lived focal adhesions at the migratory front of the cell (Zaoui *et al.*, 2008), a phenomenon that is associated with the migration phenotype of these cells, it would be of great interest to study these sites in Copine III/Memo double KD cells. There are indications that Copine III might be present in these structures as well, as Copine III interacts with RACK1, a protein that has been identified as a component of nascent focal adhesions (Figure 7-2). An approach to test whether Copine III and Memo both play a role in nascent focal adhesions would be to perform live cell imaging of cells expressing GFP-Copine III or GFP-Memo (or a combination of both with different fluorophores). In this way one could follow the localization of both molecules over time in migrating cells. Subsequently, the localization of each molecule in a background of a KD of the other could be visualized. Since both Copine III and Memo bind to ErbB2 and seem to exhibit a similar function on the cell, it might well be possible that they can compensate the loss of the other in single KD cells.

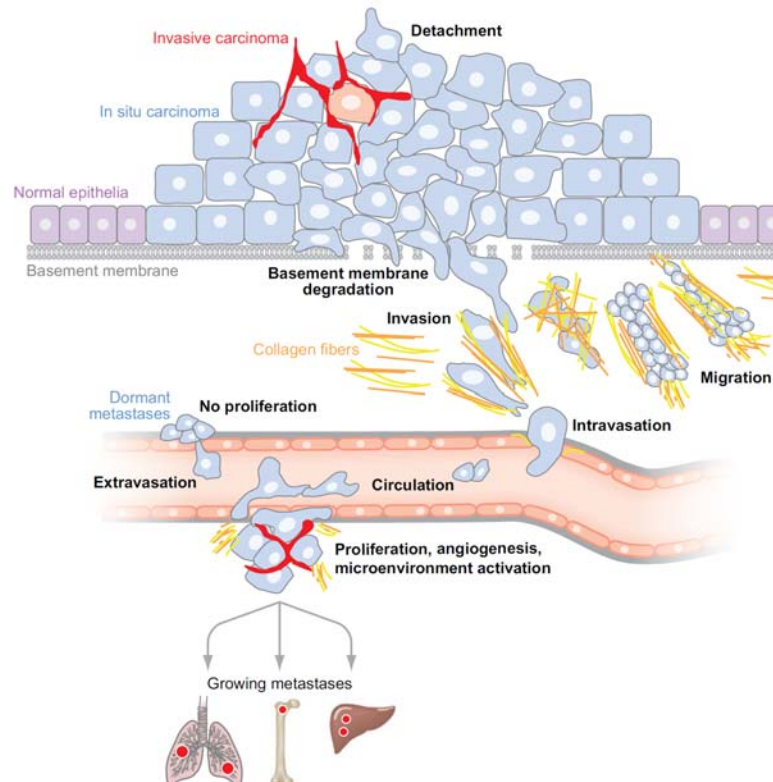
### *Could Copine III be important in tumor metastasis?*

The process of metastasis requires a series of biological events that enables tumor cells to move from the primary neoplasm to a distant location (Figure 7-3). Tumor cells must first invade into the tissue surrounding the primary tumor, then enter into and survive in either the lymphatic system or bloodstream where they eventually arrest and extravasate into a tissue and proliferate at the new site (Steeg, 2006).

The contribution of ErbB2 overexpression to the increased metastatic potential of cancer cells is evident from a number of studies. In fact, a correlation between the number of lymph node metastases and the degree of ErbB2 overexpression has been established in ErbB2 positive breast cancer patients (Slamon *et al.*, 1987).

We have shown that Copine III plays an important role downstream of ErbB2 in tumor migration *in vitro*. Therefore, it would be of great interest to examine whether Copine III is also

required for specific steps of tumor metastasis using other *in vitro* techniques and *in vivo* methods.



(Bacac and Stamenkovic, 2008)

### Figure 7-3 Principal steps in metastasis

Transformation of normal epithelial cells leads to carcinoma in situ, which, as a result of loss of adherens junctions, evolves toward the invasive carcinoma stage. Following basement membrane degradation, tumor cells invade the surrounding stroma, migrate and intravasate into blood or lymph vessels, and become transported until they arrest in the capillaries of a distant organ.

We could increase our understanding of the contribution of Copine III to the process of invasion during metastasis by performing *in vitro* matrigel invasion assays and transendothelial migration assays with our control and Copine III KD cells. In the former, cells must first degrade and then move through a layer of matrigel in a ligand gradient. Such an experiment would provide insight into the role of Copine III in ECM degradation and invasion. In the latter experiment, fibronectin is added to the top compartment of a Boyden chamber and then overlaid with a layer of fluorescently-labeled endothelial cells. The tumor cells are then plated on top of this layer and left to migrate for 24h. This assay allows one to determine the number of cells that can “extravasate” and further allows one to visualize the changes brought about to the endothelial cell layer.

In addition, *in vivo* metastasis assays could be performed: either by monitoring the metastases originating from the primary tumor at a specific site, e.g. the lungs, or by injecting tumor cells directly into the bloodstream of the mice through the tail vein. By using control and Copine III KD cells, these experiments could clearly elucidate the function of Copine III in *in vivo* metastasis.

Tumor metastasis is the major cause of mortality in cancer patients. Many primary site neoplasms are effectively controlled by surgery and radiation therapy. Most metastatic lesions are not treated by surgery, but rather by chemotherapy, hormonal therapy, targeted therapies or radiation, all of which can lead to a significant extension in survival time. However, the fact remains that progression to metastatic disease still correlates with a poor prognosis, thus elucidating the underlying mechanisms of metastasis, including the possible role of Copine III, may have a direct impact on patient survival.

### *Copine III in cancer*

Finally, we showed in this study that Copine III might play a more general role in cancer. In a set of 49 breast tumor samples, 10 of 11 tumors with *ERBB2* amplification showed high levels of Copine III. Furthermore, in a panel of breast cancer cell lines we saw a tendency that the protein expression level of Copine III correlates with ErbB2 amplification. Perhaps most importantly, in tissue microarrays from breast, prostate and ovarian tumor samples we found higher expression levels of Copine III in the tumor samples as compared to the healthy tissues. Furthermore, published transcriptome data also showed that the levels of Copine III are higher in prostate and ovarian tumor samples as compared to normal tissue.

Although descriptive, these data are very intriguing, since they imply a general role for Copine III in cancer progression. If increased sample analysis would statistically confirm these data, it would strengthen the argument for Copine III as a new prognostic or diagnostic factor in cancer. This would further justify studies to uncover the underlying mechanism of the function of Copine III. Future experiments will have to shed light on its function in the development and progression of this disease. Given that Copine III influences cell migration, it would be of great interest to investigate its role in tumor metastasis, which is the major cause of cancer-related deaths. This would certainly clarify whether Copine III is a suitable therapeutic target.

In summary, herein we present evidence that supports the conclusion that Copine III is an important and interesting subject for cancer research, worthy of further investigations.

## 8 APPENDIX

### 8.1 Abbreviations

AA	amino acid	Mg <sup>2+</sup>	Magnesium
AD	A domain	MIDAS	metal ion-dependent adhesion site
ADAM	a disintegrin and metalloproteinase	MMP	matrix metalloproteinase
AQUA	absolute quantification of proteins	Mn <sup>2+</sup>	Manganese
AR	Amphiregulin	MRM	multiple reaction monitoring
ATP	adenosin triphosphate	mRNA	messenger RNA
BON	bonzai	MS	mass spectrometry
BSA	bovine serum albumin	nAChR	nicotinic achetylcholine receptor
BTC	betacellulin	NCCLC	non-small cell lung cancer
C2D	C2 domain	NFκB	nuclear factor kappa-light-chain-enhancer of activated B-cells
Ca <sup>2+</sup>	Calcium	NRG	neuregulin
Cbl	E3 ubiquitin ligase	OCT	optimal cutting temperature
CR	cysteine rich	p	phosphorylated
DAG	diacylglycerol	PA	phosphatidic acid
DMEM	dulbeccos modified eagles medium	PAGE	polyacrylamide gel electrophoresis
DN	dominant negative	Pak	p21-activated kinase
E2	estradiol	PBS	phosphate buffered saline
ECM	extracellular matrix	PG	phosphatidylglycerol
EDTA	ethylenediaminetetraacetic acid	PI	phosphatidylinositide
EGF	epidermal growth factor	PI3K	phosphatidylinositol-3-kinase
EPI	epiregulin	PIP	phosphatidylinositolphosphate
ER	estrogen receptor	PKC	protein kinase C
ERK	extracellular signal-regulated kinase	PLC	phospholipase C
ESI	electrospray ionization	PS	phosphatidylserine
FAK	focal adhesion kinase	PTB	phosphotyrosine-binding domain
FCS	fetal calf serum	PTEN	phosphatase and tensin homolog deleted on chromosome ten
FT	Fourier transformation	PUFA	polyunsaturated fatty acid
Gap	GTPase-activating protein	RNA	ribonucleic acid
Gem	Gon extragenic modifier	RNAi	RNA interference
GFP	green fluorescent protein	RT	room temperature
Gon	gonadogenesis	RTK	receptor tyrosine kinase
GPCR	G-protein coupled receptor	SCCHN	squamous cell carcinomas of head and neck
Grb	growth factor receptor-bound protein	SDS	sodium dodecylsulfate
GTP	guanidine triphosphate	SH2	Src homology 2
HB-EGF	heparin binding EGF	shRNA	short hairpin RNA
HRG	heregulin β-1	SILAC	stable isotope labeling by amino acids in cell culture
ICAT	isotope-coded affinity tags	STAT	signal transducer and activator of transcription
IGF	insulin growth factor	TGF	transforming growth factor
IR	insulin receptor	TIC	total ion chromatogram
IHC	immunohistochemistry	TKI	tyrosine kinase inhibitor
IP <sub>3</sub>	inositoltriphosphate	TOF	time of flight
IP <sub>3</sub> R	inositoltriphosphate receptor	VEGF	vascular endothelial growth factor
iTRAQ	isotope tags for rel. and abs. quant.	VPC	vulval precursor cell
Jak	Janus tyrosine kinase	VWA	von Willebrand A
KD	knockdown	WCE	whole cell extract
LC	liquid chromatography	YTH	yeast two hybrid
<i>m/z</i>	mass to charge ratio		
mAb	monoclonal antibody		
MALDI	matrix assisted laser desorption/ionization		
MAPK	mitogen-activated protein kinase		
Memo	mediator of ErbB2-driven cell motility		

## 8.2 List of figures and tables

### FIGURES

#### Chapter 1

Figure 1-1 Acquired traits of cancer .....	1
Figure 1-2 Human receptor tyrosine kinases.....	2
Figure 1-3 Activation of ADAMs, ectodomain-shedding of EGF ligands and receptor activation .....	6
Figure 1-4 Schematic illustration of ligand-induced conformational changes in sEGFR .....	8
Figure 1-5 The human ErbB receptor/ligand family .....	9
Figure 1-6 The ErbB signaling network.....	11
Figure 1-7 Crosstalk between the ErbB network and other signaling pathways .....	13
Figure 1-8 Targeting the ErbB signaling network in cancer .....	19
Figure 1-9 Domain architecture of Copine family members .....	24
Figure 1-10 Two structurally different topologies of C2 domains.....	25
Figure 1-11 Model of the membrane docked C2 domain of PKC $\alpha$ .....	26
Figure 1-12 Structure of an integrin A domain .....	28
Figure 1-13 Dendrogram showing the relationship of seven human Copines.....	34

#### Chapter 3

Figure 3-1 Common quantitative mass spectrometry workflows.....	43
Figure 3-2 Generic mass spectrometry-based proteomics experiment.....	46
Figure 3-3 Peptide and Protein identification on the 4000QTrap.....	47
Figure 3-4 Identification of binding partners of pTyr1248 of ErbB2.....	50
Figure 3-5 Example of an MRM run for one sample.....	51
Figure 3-6 Peak integration in Analyst 1.4 .....	52
Figure 3-7 Distribution of all quantified protein ratios from one experiment.....	53

#### Chapter 4

Figure 4-1 Sequence alignment of nine human Copine proteins .....	59
Figure 4-2 Alignment of the Copine IIC2B domain to C2 domains of PKC $\delta$ and other Copines .....	60
Figure 4-3 Alignment of Copine III to other Copine family members.....	61

#### Chapter 5

Figure 5-1 Copine III preferentially binds to pTyr1248 of ErbB2 .....	72
Figure 5-2 Copine III localizes to membranes in a Ca <sup>2+</sup> -dependent manner .....	74
Figure 5-3 Specificity of the $\alpha$ -Copine III monoclonal antibody.....	75
Figure 5-4 Co-localization of Copine III and ErbB2 at the plasma membrane .....	76
Figure 5-5 IF staining of Copine III and pTyr1248-ErbB2 in T47D and SKBr3 cells .....	76
Figure 5-6 FRET acceptor photobleaching shows the interaction of Copine III and ErbB2 at the plasma membrane .....	78
Figure 5-7 The localization of Copine III depends on activity of the ErbB2 receptor .....	80
Figure 5-8 Copine III binds RACK1 and localizes to focal adhesions .....	82
Figure 5-9 Copine III has a role in HRG-mediated T47D cell migration. ....	84
Figure 5-10 Copine III expression correlates with ErbB2 amplification in breast cancer.....	86
Figure 5-11 Expression of Copine III in breast, prostate and ovarian cancer samples.....	88
Figure 5-12 Analysis of Copine III KD cells .....	91
Figure 5-13 Hypothetical model for the role of Copine III in ErbB2-dependent cell migration.....	92

#### Chapter 6

Figure 6-1 Analysis of major signaling pathways in Copine III MDA-MB-231 KD cells .....	99
Figure 6-2 Proliferation of MDA-MB-231 Copine III wt and KD cells.....	100
Figure 6-3 Migration assay (Boyden chamber) of MDA-MB-231 Copine III wt and KD cells .....	100
Figure 6-4 Adhesion of MDA-MB-231 Copine III wt and KD cells to fibronectin and collagen .....	101
Figure 6-5 Migration assay (scratch) of wt and Copine III KD MDA-MB-231 cells.....	102

---

Figure 6-6 <i>In vivo</i> tumor growth of MDA-MB-231 Copine III wt and KD cells.....	104
Figure 6-7 Western blot analysis of tumor lysates.....	105
Figure 6-8 Immunohistochemistry analysis of tumor sections.....	106
Figure 6-9 Number of genes changed between the tumor samples analyzed by microarray.....	108
Figure 6-10 Copine III rescue cell lines- expression, proliferation and <i>in vivo</i> tumor growth analysis .....	111

### **Chapter 7**

Figure 7-1 Schematic outline for domain expression of Copine III in mammalian cells.....	115
Figure 7-2 Hypothetical model for the function of Copine III in ErbB2- dependent cell migration including Memo and PLC $\gamma$ .....	119
Figure 7-3 Principal steps in metastasis.....	121

## **TABLES**

### **Chapter 5**

Table 5-1 Putative Copine-III binding partners.....	90
---	----

### **Chapter 6**

Table 6-1 Top ten upregulated and downregulated genes.....	109
--	-----





---

## 9 REFERENCES

- Aebersold R, Mann M (2003). Mass spectrometry-based proteomics. *Nature* **422**: 198-207.
- Agus DB, Akita RW, Fox WD, Lewis GD, Higgins B, Pisacane PI *et al* (2002). Targeting ligand-activated ErbB2 signaling inhibits breast and prostate tumor growth. *Cancer Cell* **2**: 127-37.
- Akiyama T, Matsuda S, Namba Y, Saito T, Toyoshima K, Yamamoto T (1991). The transforming potential of the c-erbB-2 protein is regulated by its autophosphorylation at the carboxyl-terminal domain. *Mol Cell Biol* **11**: 833-42.
- Aroian RV, Sternberg PW (1991). Multiple functions of let-23, a *Caenorhabditis elegans* receptor tyrosine kinase gene required for vulval induction. *Genetics* **128**: 251-67.
- Bacac M, Stamenkovic I (2008). Metastatic cancer cell. *Annu Rev Pathol* **3**: 221-47.
- Bantscheff M, Schirle M, Sweetman G, Rick J, Kuster B (2007). Quantitative mass spectrometry in proteomics: a critical review. *Anal Bioanal Chem* **389**: 1017-31.
- Baselga J (2001). The EGFR as a target for anticancer therapy--focus on cetuximab. *Eur J Cancer* **37 Suppl 4**: S16-22.
- Baselga J, Rischin D, Ranson M, Calvert H, Raymond E, Kieback DG *et al* (2002). Phase I safety, pharmacokinetic, and pharmacodynamic trial of ZD1839, a selective oral epidermal growth factor receptor tyrosine kinase inhibitor, in patients with five selected solid tumor types. *J Clin Oncol* **20**: 4292-302.
- Beerli RR, Hynes NE (1996). Epidermal growth factor-related peptides activate distinct subsets of ErbB receptors and differ in their biological activities. *J Biol Chem* **271**: 6071-6.
- Benes CH, Wu N, Elia AE, Dharia T, Cantley LC, Soltoff SP (2005). The C2 domain of PKCdelta is a phosphotyrosine binding domain. *Cell* **121**: 271-80.
- Biscardi JS, Maa MC, Tice DA, Cox ME, Leu TH, Parsons SJ (1999). c-Src-mediated phosphorylation of the epidermal growth factor receptor on Tyr845 and Tyr1101 is associated with modulation of receptor function. *J Biol Chem* **274**: 8335-43.
- Blagoev B, Kratchmarova I, Ong SE, Nielsen M, Foster LJ, Mann M (2003). A proteomics strategy to elucidate functional protein-protein interactions applied to EGF signaling. *Nat Biotechnol* **21**: 315-8.
- Blume-Jensen P, Hunter T (2001). Oncogenic kinase signalling. *Nature* **411**: 355-65.
- Boulay A, Breuleux M, Stephan C, Fux C, Brisken C, Fiche M *et al* (2008). The Ret receptor tyrosine kinase pathway functionally interacts with the ERalpha pathway in breast cancer. *Cancer Res* **68**: 3743-51.
- Brunton VG, Avizienyte E, Fincham VJ, Serrels B, Metcalf CA, 3rd, Sawyer TK *et al* (2005). Identification of Src-specific phosphorylation site on focal adhesion kinase: dissection of the role of Src SH2 and catalytic functions and their consequences for tumor cell behavior. *Cancer Res* **65**: 1335-42.
- Buck E, Eyzaguirre A, Rosenfeld-Franklin M, Thomson S, Mulvihill M, Barr S *et al* (2008). Feedback mechanisms promote cooperativity for small molecule inhibitors of epidermal and insulin-like growth factor receptors. *Cancer Res* **68**: 8322-32.

- Buensuceso CS, Woodside D, Huff JL, Plopper GE, O'Toole TE (2001). The WD protein Rack1 mediates protein kinase C and integrin-dependent cell migration. *J Cell Sci* **114**: 1691-8.
- Burgess AW, Cho HS, Eigenbrot C, Ferguson KM, Garrett TP, Leahy DJ *et al* (2003). An open-and-shut case? Recent insights into the activation of EGF/ErbB receptors. *Mol Cell* **12**: 541-52.
- Capra M, Nuciforo PG, Confalonieri S, Quarto M, Bianchi M, Nebuloni M *et al* (2006). Frequent alterations in the expression of serine/threonine kinases in human cancers. *Cancer Res* **66**: 8147-54.
- Caudell EG, Caudell JJ, Tang CH, Yu TK, Frederick MJ, Grimm EA (2000). Characterization of human copine III as a phosphoprotein with associated kinase activity. *Biochemistry* **39**: 13034-43.
- Cho HS, Mason K, Ramyar KX, Stanley AM, Gabelli SB, Denney DW, Jr. *et al* (2003). Structure of the extracellular region of HER2 alone and in complex with the Herceptin Fab. *Nature* **421**: 756-60.
- Cho W, Stahelin RV (2006). Membrane binding and subcellular targeting of C2 domains. *Biochim Biophys Acta* **1761**: 838-49.
- Church DL, Lambie EJ (2003). The promotion of gonadal cell divisions by the *Caenorhabditis elegans* TRPM cation channel GON-2 is antagonized by GEM-4 copine. *Genetics* **165**: 563-74.
- Citri A, Yarden Y (2006). EGF-ERBB signalling: towards the systems level. *Nat Rev Mol Cell Biol* **7**: 505-16.
- Civenni G, Holbro T, Hynes NE (2003). Wnt1 and Wnt5a induce cyclin D1 expression through ErbB1 transactivation in HC11 mammary epithelial cells. *EMBO Rep* **4**: 166-71.
- Confalonieri S, Quarto M, Goisis G, Nuciforo P, Donzelli M, Jodice G *et al* (2009). Alterations of ubiquitin ligases in human cancer and their association with the natural history of the tumor. *Oncogene*.
- Cox EA, Bennin D, Doan AT, O'Toole T, Huttenlocher A (2003). RACK1 regulates integrin-mediated adhesion, protrusion, and chemotactic cell migration via its Src-binding site. *Mol Biol Cell* **14**: 658-69.
- Creutz CE, Tomsig JL, Snyder SL, Gautier MC, Skouri F, Beisson J *et al* (1998). The copines, a novel class of C2 domain-containing, calcium-dependent, phospholipid-binding proteins conserved from *Paramecium* to humans. *J Biol Chem* **273**: 1393-402.
- Damer CK, Bayeva M, Hahn ES, Rivera J, Socec CI (2005). Copine A, a calcium-dependent membrane-binding protein, transiently localizes to the plasma membrane and intracellular vacuoles in *Dictyostelium*. *BMC Cell Biol* **6**: 46.
- Damer CK, Bayeva M, Kim PS, Ho LK, Eberhardt ES, Socec CI *et al* (2007). Copine A is required for cytokinesis, contractile vacuole function, and development in *Dictyostelium*. *Eukaryot Cell* **6**: 430-42.
- Dankort D, Jeyabalan N, Jones N, Dumont DJ, Muller WJ (2001a). Multiple ErbB-2/Neu Phosphorylation Sites Mediate Transformation through Distinct Effector Proteins. *J Biol Chem* **276**: 38921-8.
- Dankort D, Maslikowski B, Warner N, Kanno N, Kim H, Wang Z *et al* (2001b). Grb2 and Shc adapter proteins play distinct roles in Neu (ErbB-2)-induced mammary tumorigenesis: implications for human breast cancer. *Mol Cell Biol* **21**: 1540-51.
- Dankort DL, Wang Z, Blackmore V, Moran MF, Muller WJ (1997). Distinct tyrosine autophosphorylation sites negatively and positively modulate neu-mediated transformation. *Mol Cell Biol* **17**: 5410-25.

- 
- de Hoog CL, Mann M (2004). Proteomics. *Annu Rev Genomics Hum Genet* **5**: 267-93.
- Di Segni A, Farin K, Pinkas-Kramarski R (2008). Identification of nucleolin as new ErbB receptors-interacting protein. *PLoS One* **3**: e2310.
- Doan AT, Huttenlocher A (2007). RACK1 regulates Src activity and modulates paxillin dynamics during cell migration. *Exp Cell Res* **313**: 2667-79.
- Downward J, Yarden Y, Mayes E, Scrace G, Totty N, Stockwell P *et al* (1984). Close similarity of epidermal growth factor receptor and v-erb-B oncogene protein sequences. *Nature* **307**: 521-7.
- Farmer P, Bonnefoi H, Becette V, Tubiana-Hulin M, Fumoleau P, Larsimont D *et al* (2005). Identification of molecular apocrine breast tumours by microarray analysis. *Oncogene* **24**: 4660-71.
- Ferguson KM, Berger MB, Mendrola JM, Cho HS, Leahy DJ, Lemmon MA (2003). EGF activates its receptor by removing interactions that autoinhibit ectodomain dimerization. *Mol Cell* **11**: 507-17.
- Finetti F, Pellegrini M, Ulivieri C, Savino MT, Paccagnini E, Ginanneschi C *et al* (2008). The proapoptotic and antimitogenic protein p66SHC acts as a negative regulator of lymphocyte activation and autoimmunity. *Blood* **111**: 5017-27.
- Gabos Z, Sinha R, Hanson J, Chauhan N, Hugh J, Mackey JR *et al* (2006). Prognostic significance of human epidermal growth factor receptor positivity for the development of brain metastasis after newly diagnosed breast cancer. *J Clin Oncol* **24**: 5658-63.
- Gassmann M, Casagrande F, Orioli D, Simon H, Lai C, Klein R *et al* (1995). Aberrant neural and cardiac development in mice lacking the ErbB4 neuregulin receptor. *Nature* **378**: 390-4.
- Gharbi S, Gaffney P, Yang A, Zvelebil MJ, Cramer R, Waterfield MD *et al* (2002). Evaluation of two-dimensional differential gel electrophoresis for proteomic expression analysis of a model breast cancer cell system. *Mol Cell Proteomics* **1**: 91-8.
- Gottschalk A, Almedom RB, Schedletsky T, Anderson SD, Yates JR, 3rd, Schafer WR (2005). Identification and characterization of novel nicotinic receptor-associated proteins in *Caenorhabditis elegans*. *Embo J* **24**: 2566-78.
- Graus-Porta D, Beerli RR, Daly JM, Hynes NE (1997). ErbB-2, the preferred heterodimerization partner of all ErbB receptors, is a mediator of lateral signaling. *Embo J* **16**: 1647-55.
- Greene ND, Leung KY, Wait R, Begum S, Dunn MJ, Copp AJ (2002). Differential protein expression at the stage of neural tube closure in the mouse embryo. *J Biol Chem* **277**: 41645-51.
- Guerrero-Valero M, Marin-Vicente C, Gomez-Fernandez JC, Corbalan-Garcia S (2007). The C2 domains of classical PKCs are specific PtdIns(4,5)P2-sensing domains with different affinities for membrane binding. *J Mol Biol* **371**: 608-21.
- Guix M, Faber AC, Wang SE, Olivares MG, Song Y, Qu S *et al* (2008). Acquired resistance to EGFR tyrosine kinase inhibitors in cancer cells is mediated by loss of IGF-binding proteins. *J Clin Invest* **118**: 2609-19.
- Guo W, Giancotti FG (2004). Integrin signalling during tumour progression. *Nat Rev Mol Cell Biol* **5**: 816-26.
- Gygi SP, Rist B, Gerber SA, Turecek F, Gelb MH, Aebersold R (1999). Quantitative analysis of complex protein mixtures using isotope-coded affinity tags. *Nat Biotechnol* **17**: 994-9.

- Haigler HT, McKanna JA, Cohen S (1979). Rapid stimulation of pinocytosis in human carcinoma cells A-431 by epidermal growth factor. *J Cell Biol* **83**: 82-90.
- Hanahan D, Weinberg RA (2000). The hallmarks of cancer. *Cell* **100**: 57-70.
- Hansen KC, Schmitt-Ulms G, Chalkley RJ, Hirsch J, Baldwin MA, Burlingame AL (2003). Mass spectrometric analysis of protein mixtures at low levels using cleavable <sup>13</sup>C-isotope-coded affinity tag and multidimensional chromatography. *Mol Cell Proteomics* **2**: 299-314.
- Harari D, Yarden Y (2000). Molecular mechanisms underlying ErbB2/HER2 action in breast cancer. *Oncogene* **19**: 6102-14.
- Harris RC, Chung E, Coffey RJ (2003). EGF receptor ligands. *Exp Cell Res* **284**: 2-13.
- Hazan R, Margolis B, Dombalagian M, Ullrich A, Zilberstein A, Schlessinger J (1990). Identification of autophosphorylation sites of HER2/neu. *Cell Growth Differ* **1**: 3-7.
- Hendrix ND, Wu R, Kuick R, Schwartz DR, Fearon ER, Cho KR (2006). Fibroblast growth factor 9 has oncogenic activity and is a downstream target of Wnt signaling in ovarian endometrioid adenocarcinomas. *Cancer Res* **66**: 1354-62.
- Higashiyama S, Iwabuki H, Morimoto C, Hieda M, Inoue H, Matsushita N (2008). Membrane-anchored growth factors, the epidermal growth factor family: beyond receptor ligands. *Cancer Sci* **99**: 214-20.
- Higashiyama S, Iwamoto R, Goishi K, Raab G, Taniguchi N, Klagsbrun M *et al* (1995). The membrane protein CD9/DRAP 27 potentiates the juxtacrine growth factor activity of the membrane-anchored heparin-binding EGF-like growth factor. *J Cell Biol* **128**: 929-38.
- Holbro T, Beerli RR, Maurer F, Koziczak M, Barbas CF, 3rd, Hynes NE (2003a). The ErbB2/ErbB3 heterodimer functions as an oncogenic unit: ErbB2 requires ErbB3 to drive breast tumor cell proliferation. *Proc Natl Acad Sci U S A* **100**: 8933-8.
- Holbro T, Civenni G, Hynes NE (2003b). The ErbB receptors and their role in cancer progression. *Exp Cell Res* **284**: 99-110.
- Holbro T, Hynes NE (2004). ErbB receptors: directing key signaling networks throughout life. *Annu Rev Pharmacol Toxicol* **44**: 195-217.
- Hua J, Grisafi P, Cheng SH, Fink GR (2001). Plant growth homeostasis is controlled by the Arabidopsis BON1 and BAP1 genes. *Genes Dev* **15**: 2263-72.
- Hynes NE, Gerber HA, Saurer S, Groner B (1989). Overexpression of the c-erbB-2 protein in human breast tumor cell lines. *J Cell Biochem* **39**: 167-73.
- Hynes NE, Lane HA (2005). ERBB receptors and cancer: the complexity of targeted inhibitors. *Nat Rev Cancer* **5**: 341-54.
- Hynes NE, MacDonald G (2009). ErbB receptors and signaling pathways in cancer. *Curr Opin Cell Biol* **21**: 177-84.
- Hynes NE, Schlang T (2006). Targeting ADAMS and ERBBs in lung cancer. *Cancer Cell* **10**: 7-11.
- Hynes NE, Stern DF (1994). The biology of erbB-2/neu/HER-2 and its role in cancer. *Biochim Biophys Acta* **1198**: 165-84.

- Izumi Y, Hirata M, Hasuwa H, Iwamoto R, Umata T, Miyado K *et al* (1998). A metalloprotease-disintegrin, MDC9/meltrin-gamma/ADAM9 and PKCdelta are involved in TPA-induced ectodomain shedding of membrane-anchored heparin-binding EGF-like growth factor. *Embo J* **17**: 7260-72.
- Jambunathan N, Siani JM, McNellis TW (2001). A humidity-sensitive Arabidopsis copine mutant exhibits precocious cell death and increased disease resistance. *Plant Cell* **13**: 2225-40.
- Jimenez JL, Davletov B (2007). Beta-strand recombination in tricalbin evolution and the origin of synaptotagmin-like C2 domains. *Proteins* **68**: 770-8.
- Jones RB, Gordus A, Krall JA, MacBeath G (2006). A quantitative protein interaction network for the ErbB receptors using protein microarrays. *Nature* **439**: 168-74.
- Jorissen RN, Walker F, Pouliot N, Garrett TP, Ward CW, Burgess AW (2003). Epidermal growth factor receptor: mechanisms of activation and signalling. *Exp Cell Res* **284**: 31-53.
- Junttila TT, Akita RW, Parsons K, Fields C, Lewis Phillips GD, Friedman LS *et al* (2009). Ligand-independent HER2/HER3/PI3K complex is disrupted by trastuzumab and is effectively inhibited by the PI3K inhibitor GDC-0941. *Cancer Cell* **15**: 429-40.
- Karunagaran D, Tzahar E, Beerli RR, Chen X, Graus-Porta D, Ratzkin BJ *et al* (1996). ErbB-2 is a common auxiliary subunit of NDF and EGF receptors: implications for breast cancer. *Embo J* **15**: 254-64.
- Kauraniemi P, Kallioniemi A (2006). Activation of multiple cancer-associated genes at the ERBB2 amplicon in breast cancer. *Endocr Relat Cancer* **13**: 39-49.
- Keely PJ, Westwick JK, Whitehead IP, Der CJ, Parise LV (1997). Cdc42 and Rac1 induce integrin-mediated cell motility and invasiveness through PI(3)K. *Nature* **390**: 632-6.
- Kenworthy AK (2001). Imaging protein-protein interactions using fluorescence resonance energy transfer microscopy. *Methods* **24**: 289-96.
- Kheifets V, Mochly-Rosen D (2007). Insight into intra- and inter-molecular interactions of PKC: design of specific modulators of kinase function. *Pharmacol Res* **55**: 467-76.
- Kiely PA, Baillie GS, Barrett R, Buckley DA, Adams DR, Houslay MD *et al* (2009). Phosphorylation of RACK1 on tyrosine 52 by c-Abl is required for IGF-I-mediated regulation of focal adhesion kinase (FAK). *J Biol Chem*.
- King CR, Kraus MH, Aaronson SA (1985). Amplification of a novel v-erbB-related gene in a human mammary carcinoma. *Science* **229**: 974-6.
- Klein DE, Nappi VM, Reeves GT, Shvartsman SY, Lemmon MA (2004). Argos inhibits epidermal growth factor receptor signalling by ligand sequestration. *Nature* **430**: 1040-4.
- Klein DE, Stayrook SE, Shi F, Narayan K, Lemmon MA (2008). Structural basis for EGFR ligand sequestration by Argos. *Nature* **453**: 1271-5.
- Klemke RL, Cai S, Giannini AL, Gallagher PJ, de Lanerolle P, Cheresch DA (1997). Regulation of cell motility by mitogen-activated protein kinase. *J Cell Biol* **137**: 481-92.
- Kubagawa HM, Watts JL, Corrigan C, Edmonds JW, Sztul E, Browse J *et al* (2006). Oocyte signals derived from polyunsaturated fatty acids control sperm recruitment in vivo. *Nat Cell Biol* **8**: 1143-8.

- Lane HA, Beuvink I, Motoyama AB, Daly JM, Neve RM, Hynes NE (2000). ErbB2 potentiates breast tumor proliferation through modulation of p27(Kip1)-Cdk2 complex formation: receptor overexpression does not determine growth dependency. *Mol Cell Biol* **20**: 3210-23.
- Lee JO, Bankston LA, Arnaout MA, Liddington RC (1995a). Two conformations of the integrin A-domain (I-domain): a pathway for activation? *Structure* **3**: 1333-40.
- Lee JO, Rieu P, Arnaout MA, Liddington R (1995b). Crystal structure of the A domain from the alpha subunit of integrin CR3 (CD11b/CD18). *Cell* **80**: 631-8.
- Lemmon MA (2008). Membrane recognition by phospholipid-binding domains. *Nat Rev Mol Cell Biol* **9**: 99-111.
- Lu Y, Zi X, Zhao Y, Mascarenhas D, Pollak M (2001). Insulin-like growth factor-I receptor signaling and resistance to trastuzumab (Herceptin). *J Natl Cancer Inst* **93**: 1852-7.
- Marone R, Hess D, Dankort D, Muller WJ, Hynes NE, Badache A (2004). Memo mediates ErbB2-driven cell motility. *Nat Cell Biol* **6**: 515-22.
- Matsuda Y, Schlange T, Oakeley EJ, Boulay A, Hynes NE (2009). WNT signaling enhances breast cancer cell motility and blockade of the WNT pathway by sFRP1 suppresses MDA-MB-231 xenograft growth. *Breast Cancer Res* **11**: R32.
- McCahill A, Warwicker J, Bolger GB, Houslay MD, Yarwood SJ (2002). The RACK1 scaffold protein: a dynamic cog in cell response mechanisms. *Mol Pharmacol* **62**: 1261-73.
- Meira M, Masson R, Stagljær I, Lienhard S, Maurer F, Boulay A *et al* (2009). Memo is a cofilin-interacting protein that influences PLCgamma1 and cofilin activities, and is essential for maintaining directionality during ErbB2-induced tumor-cell migration. *J Cell Sci* **122**: 787-97.
- Miller LD, Lee KC, Mochly-Rosen D, Cartwright CA (2004). RACK1 regulates Src-mediated Sam68 and p190RhoGAP signaling. *Oncogene* **23**: 5682-6.
- Moasser MM (2007). The oncogene HER2: its signaling and transforming functions and its role in human cancer pathogenesis. *Oncogene* **26**: 6469-87.
- Muller WJ, Sinn E, Pattengale PK, Wallace R, Leder P (1988). Single-step induction of mammary adenocarcinoma in transgenic mice bearing the activated c-neu oncogene. *Cell* **54**: 105-15.
- Nagy P, Bene L, Balazs M, Hyun WC, Lockett SJ, Chiang NY *et al* (1998). EGF-induced redistribution of erbB2 on breast tumor cells: flow and image cytometric energy transfer measurements. *Cytometry* **32**: 120-31.
- Nakayama T, Yaoi T, Kuwajima G (1999a). Localization and subcellular distribution of N-copine in mouse brain. *J Neurochem* **72**: 373-9.
- Nakayama T, Yaoi T, Kuwajima G, Yoshie O, Sakata T (1999b). Ca<sup>2+</sup>(+)-dependent interaction of N-copine, a member of the two C2 domain protein family, with OS-9, the product of a gene frequently amplified in osteosarcoma. *FEBS Lett* **453**: 77-80.
- Nakayama T, Yaoi T, Yasui M, Kuwajima G (1998). N-copine: a novel two C2-domain-containing protein with neuronal activity-regulated expression. *FEBS Lett* **428**: 80-4.
- Nalefski EA, Falke JJ (1996). The C2 domain calcium-binding motif: structural and functional diversity. *Protein Sci* **5**: 2375-90.
- Nicholson RI, Gee JM, Harper ME (2001). EGFR and cancer prognosis. *Eur J Cancer* **37 Suppl 4**: S9-15.

- 
- Nilsson J, Sengupta J, Frank J, Nissen P (2004). Regulation of eukaryotic translation by the RACK1 protein: a platform for signalling molecules on the ribosome. *EMBO Rep* **5**: 1137-41.
- Oda Y, Huang K, Cross FR, Cowburn D, Chait BT (1999). Accurate quantitation of protein expression and site-specific phosphorylation. *Proc Natl Acad Sci U S A* **96**: 6591-6.
- Ogiso H, Ishitani R, Nureki O, Fukai S, Yamanaka M, Kim JH *et al* (2002). Crystal structure of the complex of human epidermal growth factor and receptor extracellular domains. *Cell* **110**: 775-87.
- Olayioye MA, Neve RM, Lane HA, Hynes NE (2000). The ErbB signaling network: receptor heterodimerization in development and cancer. *Embo J* **19**: 3159-67.
- Ong SE, Blagoev B, Kratchmarova I, Kristensen DB, Steen H, Pandey A *et al* (2002). Stable isotope labeling by amino acids in cell culture, SILAC, as a simple and accurate approach to expression proteomics. *Mol Cell Proteomics* **1**: 376-86.
- Ong SE, Kratchmarova I, Mann M (2003). Properties of <sup>13</sup>C-substituted arginine in stable isotope labeling by amino acids in cell culture (SILAC). *J Proteome Res* **2**: 173-81.
- Orth JD, Krueger EW, Weller SG, McNiven MA (2006). A novel endocytic mechanism of epidermal growth factor receptor sequestration and internalization. *Cancer Res* **66**: 3603-10.
- Park K, Han S, Kim HJ, Kim J, Shin E (2006). HER2 status in pure ductal carcinoma in situ and in the intraductal and invasive components of invasive ductal carcinoma determined by fluorescence in situ hybridization and immunohistochemistry. *Histopathology* **48**: 702-7.
- Pasa-Tolic L, Jensen, P.K., Anderson, G.A., Lipton, M.S., Peden, K.K., Martinovic, S., Tolic, N., Bruce, J.E., Smith, R.D. (1999). High Throughput Proteome-Wide Precision Measurements of Protein Expression Using Mass Spectrometry *J Am Chem Soc* **121**: 7949-7950.
- Patterson RL, van Rossum DB, Nikolaidis N, Gill DL, Snyder SH (2005). Phospholipase C-gamma: diverse roles in receptor-mediated calcium signaling. *Trends Biochem Sci* **30**: 688-97.
- Perkins DN, Pappin DJ, Creasy DM, Cottrell JS (1999). Probability-based protein identification by searching sequence databases using mass spectrometry data. *Electrophoresis* **20**: 3551-67.
- Qu A, Leahy DJ (1995). Crystal structure of the I-domain from the CD11a/CD18 (LFA-1, alpha L beta 2) integrin. *Proc Natl Acad Sci U S A* **92**: 10277-81.
- Ramsey CS, Yeung F, Stoddard PB, Li D, Creutz CE, Mayo MW (2008). Copine-I represses NF-kappaB transcription by endoproteolysis of p65. *Oncogene*.
- Ravichandran KS (2001). Signaling via Shc family adapter proteins. *Oncogene* **20**: 6322-30.
- Razandi M, Pedram A, Park ST, Levin ER (2003). Proximal events in signaling by plasma membrane estrogen receptors. *J Biol Chem* **278**: 2701-12.
- Rhodes DR, Yu J, Shanker K, Deshpande N, Varambally R, Ghosh D *et al* (2004). ONCOMINE: a cancer microarray database and integrated data-mining platform. *Neoplasia* **6**: 1-6.
- Riese DJ, 2nd, Stern DF (1998). Specificity within the EGF family/ErbB receptor family signaling network. *Bioessays* **20**: 41-8.

- Ron D, Chen CH, Caldwell J, Jamieson L, Orr E, Mochly-Rosen D (1994). Cloning of an intracellular receptor for protein kinase C: a homolog of the beta subunit of G proteins. *Proc Natl Acad Sci U S A* **91**: 839-43.
- Ross JS, Fletcher JA (1998). The HER-2/neu oncogene in breast cancer: prognostic factor, predictive factor, and target for therapy. *Stem Cells* **16**: 413-28.
- Ross JS, Fletcher JA, Linette GP, Stec J, Clark E, Ayers M *et al* (2003). The Her-2/neu gene and protein in breast cancer 2003: biomarker and target of therapy. *Oncologist* **8**: 307-25.
- Schade B, Lam SH, Cernea D, Sanguin-Gendreau V, Cardiff RD, Jung BL *et al* (2007). Distinct ErbB-2 coupled signaling pathways promote mammary tumors with unique pathologic and transcriptional profiles. *Cancer Res* **67**: 7579-88.
- Schechter AL, Hung MC, Vaidyanathan L, Weinberg RA, Yang-Feng TL, Francke U *et al* (1985). The neu gene: an erbB-homologous gene distinct from and unlinked to the gene encoding the EGF receptor. *Science* **229**: 976-8.
- Schechter AL, Stern DF, Vaidyanathan L, Decker SJ, Drebin JA, Greene MI *et al* (1984). The neu oncogene: an erb-B-related gene encoding a 185,000-Mr tumour antigen. *Nature* **312**: 513-6.
- Schlange T, Matsuda Y, Lienhard S, Huber A, Hynes NE (2007). Autocrine WNT signaling contributes to breast cancer cell proliferation via the canonical WNT pathway and EGFR transactivation. *Breast Cancer Res* **9**: R63.
- Schlessinger J (2000). Cell signaling by receptor tyrosine kinases. *Cell* **103**: 211-25.
- Schroeder JA, Lee DC (1998). Dynamic expression and activation of ERBB receptors in the developing mouse mammary gland. *Cell Growth Differ* **9**: 451-64.
- Schulze WX, Deng L, Mann M (2005). Phosphotyrosine interactome of the ErbB-receptor kinase family. *Mol Syst Biol* **1**: 2005 0008.
- Schulze WX, Mann M (2004). A novel proteomic screen for peptide-protein interactions. *J Biol Chem* **279**: 10756-64.
- Schweitzer R, Shilo BZ (1997). A thousand and one roles for the Drosophila EGF receptor. *Trends Genet* **13**: 191-6.
- Sengupta J, Nilsson J, Gursky R, Spahn CM, Nissen P, Frank J (2004). Identification of the versatile scaffold protein RACK1 on the eukaryotic ribosome by cryo-EM. *Nat Struct Mol Biol* **11**: 957-62.
- Shattuck DL, Miller JK, Carraway KL, 3rd, Sweeney C (2008). Met receptor contributes to trastuzumab resistance of Her2-overexpressing breast cancer cells. *Cancer Res* **68**: 1471-7.
- Slamon DJ, Clark GM, Wong SG, Levin WJ, Ullrich A, McGuire WL (1987). Human breast cancer: correlation of relapse and survival with amplification of the HER-2/neu oncogene. *Science* **235**: 177-82.
- Sorkin A, Goh LK (2009). Endocytosis and intracellular trafficking of ErbBs. *Exp Cell Res* **315**: 683-96.
- Steeg PS (2006). Tumor metastasis: mechanistic insights and clinical challenges. *Nat Med* **12**: 895-904.
- Stern DF, Kamps MP (1988). EGF-stimulated tyrosine phosphorylation of p185neu: a potential model for receptor interactions. *Embo J* **7**: 995-1001.



- Strome SE, Sausville EA, Mann D (2007). A mechanistic perspective of monoclonal antibodies in cancer therapy beyond target-related effects. *Oncologist* **12**: 1084-95.
- Tomsig JL, Creutz CE (2000). Biochemical characterization of copine: a ubiquitous Ca<sup>2+</sup>-dependent, phospholipid-binding protein. *Biochemistry* **39**: 16163-75.
- Tomsig JL, Creutz CE (2002). Copines: a ubiquitous family of Ca(2+)-dependent phospholipid-binding proteins. *Cell Mol Life Sci* **59**: 1467-77.
- Tomsig JL, Snyder SL, Creutz CE (2003). Identification of targets for calcium signaling through the copine family of proteins. Characterization of a coiled-coil copine-binding motif. *J Biol Chem* **278**: 10048-54.
- Tomsig JL, Sohma H, Creutz CE (2004). Calcium-dependent regulation of tumour necrosis factor- $\alpha$  receptor signalling by copine. *Biochem J* **378**: 1089-94.
- Traxler P, Allegrini PR, Brandt R, Brueggen J, Cozens R, Fabbro D *et al* (2004). AEE788: a dual family epidermal growth factor receptor/ErbB2 and vascular endothelial growth factor receptor tyrosine kinase inhibitor with antitumor and antiangiogenic activity. *Cancer Res* **64**: 4931-41.
- Ward CW, Gough KH, Rashke M, Wan SS, Tribbick G, Wang J (1996). Systematic mapping of potential binding sites for Shc and Grb2 SH2 domains on insulin receptor substrate-1 and the receptors for insulin, epidermal growth factor, platelet-derived growth factor, and fibroblast growth factor. *J Biol Chem* **271**: 5603-9.
- Ward CW, Hoyne PA, Flegg RH (1995). Insulin and epidermal growth factor receptors contain the cysteine repeat motif found in the tumor necrosis factor receptor. *Proteins* **22**: 141-53.
- White SL, Gharbi S, Bertani MF, Chan HL, Waterfield MD, Timms JF (2004). Cellular responses to ErbB-2 overexpression in human mammary luminal epithelial cells: comparison of mRNA and protein expression. *Br J Cancer* **90**: 173-81.
- Whittaker CA, Hynes RO (2002). Distribution and evolution of von Willebrand/integrin A domains: widely dispersed domains with roles in cell adhesion and elsewhere. *Mol Biol Cell* **13**: 3369-87.
- Wu CC, MacCoss MJ, Howell KE, Matthews DE, Yates JR, 3rd (2004). Metabolic labeling of mammalian organisms with stable isotopes for quantitative proteomic analysis. *Anal Chem* **76**: 4951-9.
- Yamauchi T, Ueki K, Tobe K, Tamemoto H, Sekine N, Wada M *et al* (1997). Tyrosine phosphorylation of the EGF receptor by the kinase Jak2 is induced by growth hormone. *Nature* **390**: 91-6.
- Yang S, Yang H, Grisafi P, Sanchatjate S, Fink GR, Sun Q *et al* (2006). The BON/CPN gene family represses cell death and promotes cell growth in Arabidopsis. *Plant J* **45**: 166-79.
- Yarden Y, Sliwkowski MX (2001). Untangling the ErbB signalling network. *Nat Rev Mol Cell Biol* **2**: 127-37.
- Yoon SO, Shin S, Lipscomb EA (2006). A novel mechanism for integrin-mediated ras activation in breast carcinoma cells: the  $\alpha 6 \beta 4$  integrin regulates ErbB2 translation and transactivates epidermal growth factor receptor/ErbB2 signaling. *Cancer Res* **66**: 2732-9.
- Yu YP, Landsittel D, Jing L, Nelson J, Ren B, Liu L *et al* (2004). Gene expression alterations in prostate cancer predicting tumor aggression and preceding development of malignancy. *J Clin Oncol* **22**: 2790-9.

Zaoui K, Honore S, Isnardon D, Braguer D, Badache A (2008). Memo-RhoA-mDia1 signaling controls microtubules, the actin network, and adhesion site formation in migrating cells. *J Cell Biol* **183**: 401-8.

Zhang X, Gureasko J, Shen K, Cole PA, Kuriyan J (2006). An allosteric mechanism for activation of the kinase domain of epidermal growth factor receptor. *Cell* **125**: 1137-49.

Zieske LR (2006). A perspective on the use of iTRAQ reagent technology for protein complex and profiling studies. *J Exp Bot* **57**: 1501-8.

## 10 ACKNOWLEDGEMENTS

I would like to thank my supervisors Jan Hofsteenge and Nancy Hynes for giving me the chance to work on this exciting project. Jan guided me through the first years of my PhD and Nancy offered me the opportunity to complete my PhD in her lab. I am very grateful to both of you.

Since the project was always a collaborative one, I had the great chance to work both in a biochemical and a cell biology environment. I am very thankful to both of you for the broad spectrum of methods I could gain insight into during my time in your labs.

I also want to acknowledge the remaining member of my thesis committee, Gerhard Christofori, for the good discussions and suggestions for my project.

I want to thank all the members of the Hofsteenge lab and the protein analysis facility: Chun-I Chen, Marianne Grob, Daniel Hess, Claudia Keller, Dominique Klein, Jeremy Keusch, Krisztina Keusch, Carsten Krantz, Reto Portmann, Florence Roux, Ragna Sack, and Matthias Schmidt.

Dominique was the good soul of the lab during my time there, always friendly and helpful. Thank you very much for keeping the spirit up. I want to thank Claudia for helping me so much on the project, I am really happy we became such a great team. Without Ragna especially, Daniel and Florence I would never have learned as much about mass spectrometry as I have so far.

I particularly want to thank all the members of the Hynes lab for the warm welcome they all gave me and the great time we spent together: Julien Dey, Bérengère Fayard, Anna Frei, Albana Gattelli, Barbara Hänzi, Amine Issa, Shunya Kondo, Susanne Lienhard, Gwen MacDonald, Francisca Maurer, Ivan Schlatter, and Tina Stölzle. I especially want to thank Susanne for being such a great help and Anne for all the helpful discussions and suggestions.

I am thankful to Manuela Vecchi and Marco Bianchi who performed all the experiments with the tissue microarrays, Laurent Gelman of the FMI FAIM team for help with FRET and Susanne Schenk for help with the production of the Copine III monoclonal antibody.

I am very grateful to all my friends who supported me so much. You always encouraged me to make the best of everything. Without you there were times when it would have been extremely difficult. Thank you.

The same gratitude goes to my family who supported me during this time. I would have never imagined getting this amount of support and encouragement as I experienced from you. You were always there for me when I needed you, thank you all very much.

André, I will never forget in what a great way you always tried to encourage me. Your love, comfort, support and motivation always helped and still help me.



## 11 CURRICULUM VITAE

### *PERSONAL DATA*

---

Name	Constanze Heinrich
Date of birth	14 <sup>th</sup> June 1979
Address	Günterstalstr. 10, D-79100 Freiburg
Phone	+49-761-4296813
Mobile	+49-179-2250692
Email	constanze.heinrich@fmi.ch

### *INDUSTRIAL AND ACADEMIC WORK EXPERIENCE*

---

Jan 2005 – Dec 2009	<b>PhD thesis</b> in the groups of Prof. Dr. Jan Hofsteenge and Prof. Dr. Nancy Hynes, Friedrich Miescher Institute for biomedical research, Basel, Switzerland: <i>Copine III interacts with ErbB2 and promotes tumor cell migration</i>
Mar 2003 – Sep 2004	<b>Master thesis</b> in the group of Dr. Andreas Ladurner at the EMBL (European Molecular Biology Laboratories), Heidelberg: <i>Identification and characterization of a mammalian RITS complex homologue</i>
Sep 2003 – Oct 2003	Practical work experience in the group of Dr. Andreas Ladurner at the EMBL, Heidelberg: <i>Gene Expression – Does a Histone Chaperone Interact with TAF<sub>II</sub>250, a Factor Essential for Transcription?</i>
Oct 2002 – Mar 2003	<b>Bachelor thesis</b> at Syngenta Crop Protection AG, Basel, Switzerland, <i>Evaluation of Methods for Glycoproteome Analysis</i>
Sep 2001 – Feb 2002	Placement at Syngenta Crop Protection AG, Jealott's Hill, England: <i>Novel Protein Discovery and Cloning of Genes for Nematocidal Activity</i>
Aug 1998 – Sep 1999	Voluntary social work (Freiwilliges Soziales Jahr) in a center for the rehabilitation of people suffering from psychiatric illness in Ulm, Germany.

### **EDUCATION**

---

Jan 2005 – Dec 2009	<b>PhD Cell Biology</b> , FMI, Basel, Switzerland
Mar 2003 – Oct 2004	<b>Master of Science (M. Sc.) Biotechnology</b> , grade: 1.3 Hochschule Mannheim (Mannheim University of Applied Sciences), Germany
Oct 1999 – Mar 2003	<b>Bachelor of Science (B.Sc.,hons) Biotechnology</b> , grade: 1.8 Hochschule Mannheim, (Mannheim University of Applied Sciences), Germany
Sep 1989 – Jul 1998	University entrance qualification (allgemeine Hochschulreife); GPA: 2.0. Schelztorgymnasium, Esslingen, Germany

### **OTHER SKILLS**

---

Languages:	German (native tongue), English (very good), French (good)
PC- skills:	MS Office, Programs relevant for DNA analysis (VectorNTI), bioinformatics tools (ClustalW, Blast, etc.), Corel Draw

### **FUNDING**

---

Jan 2005 – Aug 2007	EU Framework 6
---------------------	----------------

### **TEACHING AND TRAINING**

---

Teaching	Supervision of a Master student, 2007/2008  Tutoring of 1 <sup>st</sup> semester biology students, 2006
Further training	LTK module 1 certification Introductory course in Laboratory Animal Science, 2009  Participation in the WIN (women into industry) program of the University of Basel and Novartis, 2007/08

### **ACTIVITIES**

---

Climbing, tennis, squash, flute playing, handcrafting

### **PUBLICATIONS**

---

Heinrich C, Keller C, Boulay A, Vecchi M, Bianchi M, Sack R, Lienhard S, Duss, S, Hofsteenge J and Hynes, NE: Copine III interacts with ErbB2 and promotes tumor cell migration (Oncogene, in press)

Till S, LeJeune E, Thermann R, Bortfeld M, Hothorn M, Enderle D, Heinrich C, Hentze MW, Ladurner AG.: A conserved motif in Argonaute-interacting proteins mediates functional interactions through the Argonaute PIWI domain.  
Nat Struct Mol Biol. 2007 Oct; 14(10):897-903.